THE SYNTHESIS AND ROLE OF OXYLIPIN VOLATILES IN MAIZE INTERACTIONS WITH PATHOGENS AND DARK-INDUCED DEFENSE PRIMING

A Dissertation

by

ZACHARY JAMES GORMAN

Submitted to the Office of Graduate and Professional Studies of
Texas A&M University
in partial fulfillment of the requirements for the degree of

DOCTOR OF PHILOSOPHY

Chair of Committee,	Mikhailo Kolomiets
Committee Members,	Daniel Ebbole
	Leonardo Lombardini
	Jason West
Head of Department,	Leland Pierson III

December 2020

Major Subject: Plant Pathology

Copyright 2020 Zachary James Gorman

ABSTRACT

Lipoxygenases (LOX) are enzymes that produce an array of oxylipins that regulate multiple plant physiological processes. ZmLOX10 is an important LOX isoform that is required for the synthesis of many diverse oxylipins, including its well-known and critical role in green leaf volatile (GLV) synthesis. Transgenic *Arabidopsis* over-expressing ZmLOX6 has also been implicated in synthesis of pentyl leaf volatiles (PLV). By utilizing genetic knockout mutants of *Zea mays* and transgenic over-expressors of *Arabidopsis thaliana*, I show that both ZmLOX6 and ZmLOX10 function in PLV synthesis in maize, and that PLV synthesis is partially dependent on jasmonic acid (JA) signaling. I also establish the biosynthetic order of analysis of PLVs through exogenous treatments with select PLVs, and that popular method of plant tissue volatile analysis, freeze-thawing, is flawed and provides erroneous results.

Compared to PLVs, significantly more is known regarding GLVs, including their well-known ability to induce synthesis of the important phytohormone, JA. JA is a key regulator of defense against both pathogens and insects. JA also shares strong antagonism with another phytohormone, salicylic acid (SA), that regulates defense against biotrophic and hemi-biotrophic pathogens. Studies detailing the impact of GLVs on plant-pathogen interactions have almost exclusively focused on necrotrophic pathogens, which showed that GLVs promote resistance. Utilizing GLV- and JA-deficient knockout mutants of maize and the hemi-biotrophic fungus, *Colletotrichum graminicola*, I show that GLVs induce susceptibility in maize to the anthracnose fungus,

Colletotrichum graminicola. GLV-mediated susceptibility is accomplished by induction of JA, which in turn suppresses synthesis of SA.

In addition to being released in response to a wide variety of stresses, GLVs are also emitted in massive amounts after light-to-dark transitions. The physiological implications of this phenomenon had previously not been investigated. My results show that dark-induced GLV emission causes a brief spike in non-ZmLOX10-derived JA synthesis. I further show that these phenomena prime the plant for increased resistance to the insect herbivore, *Spodoptera frugiperda* (fall armyworm), and that this resistance lasts for at least 24 hours. Lastly, I show that GLVs are potent inducers of stomatal closure in maize, particularly GLV aldehydes.

ACKNOWLEDGEMENTS

Firstly, I would like to thank Mike Kolomiets for his guidance throughout my Ph.D. program, and his willingness and encouragement to explore the science which interested me most. I would also like to thank my committee members Daniel Ebbole, Leonardo Lombardini, and Jason West for their assistance, advice, and review of my work. I would also like to thank the many members of the Department of Plant Pathology and Microbiology who assisted me over the years. In particular, I would like to acknowledge the many lab members with whom I was fortunate enough to have worked with throughout my program. They helped me tremendously with a variety of aspects regarding science and beyond. Lastly, and most importantly, I would like to thank my family, who never stopped supporting me throughout this endeavor. This holds especially true for my wonderful wife, who provided unending and tremendous support and encouragement throughout the duration of my program.

CONTRIBUTORS AND FUNDING SOURCES

Contributors

This work was supervised by a dissertation committee consisting of Professors Michael Kolomiets and Daniel Ebbole of the Department of Plant Pathology and Microbiology, Leonardo Lombardini of the Department of Horticultural Sciences, and Jason West of the Department of Ecosystem Science and Management.

Transgenic and mutant *A. thaliana* lines in Chapter 3 were generated by Jordan Tolley in the lab of Hisashi Koiwa, Department of Horticultural Sciences. Analysis of anthracnose stalk rot in *lox10-3* mutants of the B73 background was performed by Shawn Christensen in the Department of Plant Pathology and Microbiology, as seen in Chapter 4. Analysis of anthracnose stalk rot in *opr7-5opr8-2* mutants in Chapter 4 was performed by Yaunxin Yan, Department of Plant Pathology and Microbiology. Microscopy of LOX10-YFP in Chapter 4 was performed by Jordan Tolley in the lab of Hisashi Koiwa. *opr7-5opr8-2* mutant stalks used in phytohormone analysis of anthracnose stalk rot in Chapter 4 were infected and harvested by Yongming He, Department of Plant Pathology and Microbiology and Jiangxi Key Laboratory of Crop Physiology, Ecology, and Genetic Breeding at Jiangxi Agricultural University. Eli Borrego, Department of Plant Pathology and Microbiology, assisted with phytohormone analysis seen in Chapter 4 and 5. All other work conducted for the dissertation was completed by the student independently.

Funding Sources

The work performed in this study was supported by USDA-NIFA (2017-67013-26524) grant awarded to Michael V. Kolomiets.

NOMENCLATURE

12-OPDA	12-oxo-phytodienoic acid
13*S*-HPOT	13*S*-hydroperoxy octadecadienoic acid
13*S*-HPOD	13*S*-hydroperoxy octadecenoic acid
ADH	Alcohol dehydrogenase
AOC	Allene oxide cyclase
AOS	Allene oxide synthase
ALB	Anthracnose leaf blight
ASR	Anthracnose stalk rot
CHAT	Cis-3-hexenol-acetyl transferase
FAW	Fall Armyworm
GC-MS	Gas chromatography-mass spectrometry
GLV	Green leaf volatile
HPL	Hydroperoxide lyase
JA	Jasmonic acid
JA-Ile	Jasmonyl-isoleucine
C18:2	Linoleic acid
C18:3	Linolenic acid
LOX	Lipoxygenase
LC-MS/MS	Liquid chromatography-mass spectrometry

MeJA	Methyl jasmonate
MeSA	Methyl salicylate
OTD	13-oxo-9(*Z*)-11(*E*)-tridecadienoic acid
PLV	Pentyl leaf volatile
SA	Salicylic acid
VOC	Volatile organic compound

TABLE OF CONTENTS

Page

ABSTRACT ii

ACKNOWLEDGEMENTS iv

CONTRIBUTORS AND FUNDING SOURCES v

NOMENCLATURE vii

TABLE OF CONTENTS ix

LIST OF FIGURES xii

LIST OF TABLES xix

CHAPTER I INTRODUCTION 1

CHAPTER II METHODS 4

- Plant, Fungal, and Insect Materials 4
- Microscopy 5
- Pentyl Leaf Volatile Metabolism Assay 5
- Wound and Freeze-Thaw Analysis 6
- Anthracnose Stalk Rot Assays 6
- Anthracnose Leaf Blight Assays 7
- Dark-Induced Green Leaf Volatile Analysis 8
- Light-to-Dark Transition Hormone Analysis 9
- Fall Armyworm Assays 9
- RNAseq Analysis 10
- qPCR Analysis 12
- Stomata Assays 13
- Volatile Analysis 14
- Hormone Analysis 15

CHAPTER III VOLATILE OXYLIPIN SYNTHESIS IN MAIZE 17

- Introduction 17
  - GLV synthesis 18
  - PLV synthesis 19

Results 22
Metabolism of PLVs 22
ZmLOX10 is critical for efficient synthesis of PLVs 25
ZmLOX6 depends on substrate from a GLV-producing LOX for PLV synthesis 28
The role of JA in PLV and GLV synthesis 30
Freeze-thaw treatment distorts the volatile profile of samples 33
Discussion 38

CHAPTER IV GREEN LEAF VOLATILES AND JASMONIC ACID ENHANCE SUSCEPTIBILITY TO ANTHRACNOSE DISEASES CAUSED BY COLLETOTRICHUM GRAMINICOLA IN MAIZE 49

Introduction 49
Colletotrichum graminicola 49
Jasmonic acid 50
Green leaf volatiles 51
Results 53
GLV- and JA-deficiency results in increased resistance to ASR 53
Increased resistance to ASR correlates with reduced JA and increased SA 54
GLV- and JA-deficiency results in increased resistance to ALB 58
Increased resistance to ALB correlates with reduced JA and increased SA 60
LOX10 localizes to chloroplasts, the site of JA and GLV biosynthesis 63
GLVs mediate susceptibility to *C. graminicola* through induction of JA 65
SA induces defense and JA promotes susceptibility to *C. graminicola* 67
GLVs, but not JA, induce susceptibility after the switch to necrotrophy by *C. graminicola* 69
Discussion 70

CHAPTER V DARK-INDUCED GLV EMISSIONS TRIGGER JASMONIC ACID BIOSYNTHESIS AND ESTABLISH PRIMING AGAINST FALL ARMYWORM, AND FACILITATE STOMATE CLOSURE 78

Introduction 78
Results 84
ZmLOX10-derived GLVs are emitted in response to light-to-dark transitions 84
Jasmonates accumulates in response to light-to-dark transitions 86
GLVs released after light-to-dark transitions increase jasmonates in leaves 90
ZmLOX10 induce JA signaling through ZmLOX8 after light-to-dark transitions 92
Dark-induced GLV emissions result in long-term, cyclic priming to FAW 97
Dark-induced GLV emissions do not regulate circadian rhythm 99
GLVs facilitate closure of stomata 103
Discussion 106

CHAPTER VI SUMMARY 117

REFERENCES 122

LIST OF FIGURES

Page

Figure 1 Structural similarity of green leaf volatiles and pentyl leaf volatiles. 18

Figure 2 Synthesis of primary PLVs and GLVs. Shows difference in the formation of primary GLVs and PLVs (Salch et al., 1995). Names in green font denote the HPL pathway and its products, names in blue font depict the LOX pathway and its products. Adapted from Salch et al. (1995) and Mukhatarova et al. (2018).....20

Figure 3 Metabolism of exogenous PLVs by *A. thaliana*. Intact *A. thaliana* Col-0 were exposed to various PLVs for 20 min before volatiles were collected for an additional 20 min. Four pots (5 plants/pot) were placed in small jars and exposed to 5 µL of 100 mM of various individual PLVs or dichloromethane (control). X-axis shows individual exogenous PLV treatments. Y-axis shows target analytes (nmol/h). Analyte target responses matching the same volatile treatment were omitted (black cells). Blank cells indicate targets that were not detected. (2*Z*)-pentenol (2*Z*-POL), (2*E*)-pentenol (2*E*-POL), (2*E*)-pentenal (2*E*-PAL), pentanol (POL), pentanal (PAL), penten-3-ol (PEOL), 1-penten-3-one (PEON), 3-pentanol (3-POL), 3-pentanone (3-PON). 25

Figure 4 Wound-induced GLV and PLV emissions are greatly diminished in *lox10-3* mutants of maize. Volatiles were collected for 1 h after leaves of two WT inbred lines, B73 and W438 (blue), and *lox10-3* mutants (red) in each respective background, were cut into 1 cm pieces. (a) shows various GLVs and (b) shows various PLVs (mean ± SE, nmol per gram of fresh weight per hour). Student's T-test was performed to determine statistical difference between treatments for each individual inbred genetic background [p<.05 = (*), p<.005 = (**), p<.0005 = (***)] (n=4). 27

Figure 5 ZmLOX6 depends on AtLOX2, the GLV- and PLV-producing LOX, in transgenic ZmLOX6-OE lines of *A. thaliana*. Volatiles were collected for 1 h after leaves of two ZmLOX6-OE transgenic lines (line #44 and line #72), *Atlox2-1* mutants, and *Atlox2-1* ZmLOX6-OE mutant/transgenic lines (line #44 and line #72) in the Col-0 background were cut into 1 cm pieces. Shows various PLVs (mean ± SE, nmol per gram of fresh weight per hour). Dunnett's test was performed to determine statistical difference between Col-0 (control, left bracket) and ZmLOX6-OE transgenic lines treatments, and between *Atlox2-1* mutants (control, right bracket) and *Atlox2-1* ZmLOX6-OE mutant/transgenic lines [p<.05 = (*), p<.005 = (**), p<.0005 = (***)] (n=4). 30

Figure 6 GLV and PLV emissions are diminished in *opr7-5opr8-2* and *lox10-3* mutants of maize. Volatiles were collected for 1 h after leaves of WT, *lox10-3*, and *opr7-5opr8-2* mutants in the B73 genetic background, were cut into 1 cm pieces. (a) shows various GLVs and (b) shows various PLVs (mean ± SE, nmol per gram of fresh weight per hour). Tukey's Test was performed to determine statistical difference between genotypes, where letters denote statistical significance (P<.05) (n=6). 32

Figure 7 Freezing distorts the GLV and PLV profiles of maize. Volatiles were collected for 1 h after leaves of two inbred lines, B73 and W438, and *lox10-3* mutants in each respective background, were either cut into 1 cm pieces (blue) or briefly flash frozen in liquid nitrogen (red). (a) shows various GLVs and (b) shows various PLVs (mean ± SE, nmol per gram of fresh weight per hour). Student's T-test was performed to determine statistical difference between treatments for each individual genotype [p<.05 = (*), p<.005 = (**), p<.0005 = (***)] (n=4). 35

Figure 8 Freezing distorts the GLV and PLV profiles of *A. thaliana*. Volatiles were collected for 1 h after leaves of Col-0 were either cut into 1 cm pieces (blue) or briefly flash frozen in liquid nitrogen (red). (a) shows various GLVs and (b) shows various PLVs (mean ± SE, nmol per gram of fresh weight per hour). Student's T-test was performed to determine statistical difference between treatments for each individual genotype [p<.05 = (*), p<.005 = (**), p<.0005 = (***)] (n=4).....37

Figure 9 Working model of the PLV pathway in maize. (a) shows C18:3-derived and (b) C18:2-derived PLV pathways. Dashed arrows indicate possible reactions. Alcohol dehydrogenase (ADH), acetyl transferase (CHAT), reductase (RED), non-enzymatic (NE), isomerase (ISO). The names of PLVs are blue, the names of potential artificial or trace PLVs are black, and the names of 13-carbon compounds are orange. Adapted from Gardner et al. (1996).....41

Figure 10 Working model of the HPL pathway in maize. (a) shows C18:3-derived and (b) C18:2-derived PLV pathways. Dashed arrows indicate possible reactions. Alcohol dehydrogenase (ADH), acetyl transferase (CHAT), peroxygenase (POX) non-enzymatic (NE), isomerase (ISO). The names of GLVs are green, the names of traumatins are orange. Adapted from Matsui et al. (2012).....42

Figure 11 *lox10* and *opr7-5 opr8-2* mutant stalks are more resistant to *C. gramnicola*. (a) shows representative stalks of WT and *lox10-3* mutants in the W438 genetic background 11 dpi. (b) shows *lox10-2* and (c) shows *lox10-3* mutants and their near-isogenic WTs in the B73 genetic

background 10 dpi. (d) shows stalks of *opr7-5*, *opr8-2*, and *opr7-5 opr8-2* mutants and their respective WTs in the B73 background 10 dpi. Stalks were split and imaged and lesions were quantified from the digital images. [Mean ± SE, (mm^2)]. For (a,b,c) Student's T-test was used to determine statistical significance [p<.005 = (**), p<.0005 = (***)]. Tukey's HSD test was used to determine statistical significance for (d) where different letters denote statistical difference (p<.05) (n=10). 54

Figure 12 Hormone analysis shows jasmonates are low or absent, and SA is high, in *lox10-3* and *opr7-5 opr8-2* mutant stalks after inoculation. The left column shows 12-OPDA (a), JA (b), JA-Ile (c), and SA (d) levels in WT and *lox10-3* mutant stalks in the W438 background 1, 4, and 6 dpi. The right column shows 12-OPDA (e), JA (f), JA-Ile (g), and SA (h) levels in WT and *opr7-5 opr8-2* mutants stalks in the B73 after infection. (n.d. = not detected). Control = mock-treated 1 dpi. (Mean ± SE, pmol per gram of fresh weight). Student's T-test was used to determine statistical difference between genotypes of each timepoint/treatment [p<.05 = (*), p<.005 = (**), p<.0005 = (***)] (n=5). 56

Figure 13 Basal hormone analysis of *lox10-3* and *opr7-5 opr8-2* mutant stalks shows that 12-OPDA is low in *lox10-3* mutants and SA is high in *opr7-5 opr8-2* mutants. The left column of the figure show amounts of 12-OPDA (a), JA (b), JA-Ile (c), and SA (d) levels in untreated WT and *lox10-3* mutant stalks in the W438 background. The right column of the figure shows 12-OPDA (e), JA (f), JA-Ile (g), and SA (h) levels in untreated WT and *opr7-5 opr8-2* mutant stalks in the B73 background. (Mean ± SE, pmol per gram of fresh weight) (n.d. = no detection). Student's T-test was used to determine statistical difference between genotypes [p<.005 = (**)] (n=5). 57

Figure 14 *lox10* and *opr7-5 opr8-2* mutant leaves are resistant to *C. graminicola.* Shows the mean areas of lesion after inoculation of *lox10-2* (b) & (d), *lox10-3* (a) & (b), and *opr7-5 opr8-2* (b) mutants. (a) & (b) show *lox10-2* and *lox10-3* mutants in the W438 background. (c) & (d) shows *lox10-2*, *lox10-3*, and *opr7-5 opr8-2* mutants in the B73 background. Leaves were harvested 5 (a) & (c) or 6 (b) & (d) dpi and scanned to produce digital images from which lesion areas were measured. [Mean ± SE, lesion area (mm^2)]. For (a,b,d), Student's T-test was performed to determine statistical significance of lesion areas [p<.005 = (**), p<.0001 = (***)]. Tukey's HSD test was performed for (c), where different letters denote statistical significance (p<.05) (n=5). 59

Figure 15 Hormone analysis shows jasmonates are low or absent, and that SA is high, in *lox10-3* and *opr7-5 opr8-2* mutant leaves before or throughout

infection. The left column shows 12-OPDA (a), JA (b), JA-Ile (c), and SA (d) levels in WT and *lox10-3* mutants leaves in the W438 background 0, 1, 3, and 5 dpi. The right column shows 12-OPDA (e), JA (f), JA-Ile (g), and SA (h) levels in WT and *opr7-5 opr8-2* mutant leaves in the B73 background 0, 1, 3, and 5 dpi. 0 dpi plants were untreated. (Mean ± SE, pmol per gram of fresh weight). (n.d. = not detected). Student's t-test was used to determine statistical difference between genotypes of each timepoint/treatment [p<.05 = (*), p<.005 = (**), p<.0005 = (***)] (n=6).....62

Figure 16 LOX10-YFP tagged maize lines reveal that ZmLOX10 localizes to chloroplasts of bundle sheath cells. (a-d) show images of untransformed leaves of B73 inbred line and (e-l) show images of transgenic lines in the B73 background expressing YFP-tagged LOX10 (LOX10-YFP) under its native promoter, where (e-h) show images comparable to (a-d) and (i-l) show zoomed-in views of (e-h) detailing LOX10 localization to bundle sheath chloroplast (i-l). Columns in order of left to right show brightfield views, chlorophyll autofluorescence, YFP fluorescence, and a merged view. (Scale bars = 50 μm). 64

Figure 17 GLV exposure rescues *lox10-3* mutant, but not *opr7-5 opr8-2* mutant, susceptibility by increasing JA and JA-Ile. *lox10-3* and *opr7-5 opr8-2* mutants in the W438 (a) or B73 (b) backgrounds were exposed to either an exogenous GLV mixture or triacetin (control) for 1 h, followed by inoculation with *C. graminicola*. Infected leaves were harvested and scanned 4 dpi to produce digital images from which lesions were measured [Mean ± SE, (mm^2)]. 12-OPDA (c), JA (d), and JA-Ile (e) were measured in *lox10-3* mutants after GLV exposure (Mean ± SE, pmol per gram of fresh weight). Tukey's HSD test was used to determine statistical significance in, where different letters denote statistical significance (p<.05) (n=6). 66

Figure 18 Treatment with MeJA rescues susceptibility in *lox10-3* and *opr7-5 opr8-2* mutants while treatment with MeSA increases resistance in WT. WT and *lox10-3* mutant in the W438 genetic background (a) & (b) and WT and *opr7-5 opr8-2* mutants in the B73 genetic background were exposed to either MeSA (a) & (b), MeJA (c) & (d), or ethanol (control) before inoculation with *C. graminicola*. Treatments consisted of exposing plants to 10 μmol MeSA or MeJA dissolved in ethanol, or ethanol (control) for 2 (a,b) or 6 (c,d) h. Leaves were harvested and scanned 4 dpi to produce digital images from which lesions were measured [Mean ± SE, (mm^2)]. Tukey's HSD test was used to determine statistical significance, where different letters denote statistical significance (p<.05) (n=5). 68

Figure 19 GLV treatment during necrotrophy rescues susceptibility in *lox10-3* mutants, but MeJA treatment does not. *lox10-3* and *opr7-5 opr8-2* mutants were inoculated with *C. graminicola* and infection was left to proceed for 3 days before they were exposed to GLVs (a), MeJA (b,c), and their respective control treatments (triacetin and ethanol, respectively). Leaves were harvested and scanned 6 dpi to produce digital images from which lesions were measured [Mean ± SE, (mm^2)]. Tukey's HSD test was used to determine statistical significance, where different letters denote statistical significance. 70

Figure 20 Working model of GLV and JA interactions in maize. Dashed arrows indicate signaling. Hydroperoxide lyase (HPL); allene oxide synthase (AOS); green leaf volatiles (GLVs); 12-oxo-phydienoic acid (12-OPDA); jasmonic acid (JA); jasmonic acid isoleucine (JA-Ile); alcohol dehydrogenase (ADH); cis-3-hexenol acetyl transferase (CHAT). Green names denote HPL-derived metabolites, blue names denote AOS-derived metabolites. Adapted from Acosta et al. (2009), Matsui et al. (2012), Borrego & Kolomiets (2016). 81

Figure 21 GLVs produced by ZmLOX10 are emitted after the onset of dark. Figure shows the mean amount of the GLVs, (3*Z*)-hexenal, (3*Z*)-hexenol, and (3*Z*)-hexenyl acetate emitted 1 h before (blue) or after (red) the onset of darkness. (a) shows the amounts of GLVs emitted after transition after a diurnal transition to dark in WT and *lox10-3* mutants in the W438 background. (b) shows the amount of GLVs released after both diurnal (end of the photophase) and non-diurnal (middle of the photophase) transitions to dark. Analytes are reported in (nmol/h). (a) Student's T-test was used to determine statistical significance between light and dark emissions [$p<.05$ = (*), $p<.005$ = (**)] (n=4). (b) Tukey's Test was used to determine statistical significance of (b), where letters denote statistical significance ($p=.05$) (n=4). 86

Figure 22 ZmLOX10 is required for induction of jasmonates and traumatins after the onset of darkness. Figure shows the amount of (a) 12-OPDA, (b) JA, (c) JA-Ile, (d) TAN, (e) TA and (f) OTD in W438 inbred (blue) or *lox10-3* mutants (red) at various timepoints just before and throughout the night (nmol/g FW). Bars indicate standard error (n=8). White background indicates timepoints during the photophase whereas grey background indicates timepoints during the scotophase. Student's T-test was used to determine statistical difference between the genotypes at every timepoint (* = $p<.05$), (** = $p<.005$), (*** = $p<.0005$). 88

Figure 23 Roots do not experience a sharp increase of jasmonates upon the onset of dark. Figure shows the amount of (a) 12-OPDA, (b) JA, (c) JA-Ile, and

(d) TA in W438 inbred (blue) or *lox10-3* mutants (red) at various timepoints just before darkness and throughout the night (nmol/g FW). Bars indicate standard error (n=8). White background indicates timepoints during the photophase whereas grey background indicates timepoints during the scotophase. Student's t-test was used to determine statistical difference between treatments at timepoint [p<.05 = (*), p<.005 = (**), p<.0005 = (***)] (n=6). 90

Figure 24 Exogenous GLV treatment rescues dark-induced JA accumulation in *lox10-3* mutants. The graphs show the amount of (a) 12-OPDA, (b) JA, (c) JA-Ile in *lox10-3* mutants exposed to either control treatment (ethanol, blue) or a GLV mixture (red) after the onset of darkness. Plants were exposed for 30 min starting at the onset of darkness (0 h) Jasmonates were measured at various timepoints just before and after dark treatment (pmol/g FW). White background indicates timepoints during the photophase whereas grey background indicates timepoints during the scotophase. Student's t-test was used to determine statistical difference between treatments at timepoint [p<.05 = (*), p<.005 = (**), p<.0005 = (***)] (n=6). 92

Figure 25 ZmLOX10-mediated signaling controls expression of multiple genes differentially regulated during light-to-dark transitions. Figure shows heatmap of transcripts levels of WT and *lox10-3* mutant leaves in the W438 background 1 hour before (-1 h) or 1 hour after (+1 h) dark. Heatmap shows differences in gene expression among different genotypes/timepoints using Z-score (blue=low, red=high) of fragments per kilobase million (FPKM). Genes were placed in 6 different groups based on similarity of expression pattern across all timepoints/genotypes. Each genotype/timepoint represents a sample consisting of 4 plants. 94

Figure 26 Transcript accumulation of JA biosynthesis and signaling genes is increased after darkness in a ZmLOX10-dependent manner. Figure shows the relative expression of (a) *ZmLOX10*, (b) *ZmLOX8*, (c) *ZmAOS1c*, (d) *ZmOPR7*, (e) *ZmOPR8*, (f) *Zmbhlh91*, (g) *ZmMYC7*, (h) *ZmJAZ2*, and (i) *ZmJAZ3* after darkness in leaves of WT W438 inbred (blue) and *lox10-3* mutants (red) in the W438 background. Relative expression was calculated by the ΔΔCT method (Livak and Schmittgen, 2001), where all timepoints are compared to the (-1 h) timepoint (the timepoint before the onset of dark). Expression greater than 1 indicates higher expression than at (-1 h), and lower than 1 indicates lesser expression than at (-1 h). All bars represent standard error (n=4). 96

Figure 27 GLV exposure at the onset of dark rescues *lox10-3* susceptibility to FAW and inhibits FAW weight gain. (a) and (b) show the result of a FAW

feeding assay, in which WT and *lox10-3* mutants were exposed to GLVs or triacetin (control) for 30 min after dark, and then a 4th instar FAW was placed on a leaf in a clip cage and allowed to feed for 16 h. Leaves were scanned afterwards and analyzed with ImageJ software to determine the area of leaf eaten. (a) shows representative images of leaves after feeding. (b) shows the mean of area (mm^2) eaten in W438 (blue) and *lox10-3* mutants (red). (c) and (d) shows weights of neonate FAW after feeding for 7 days on WT and *lox10-3* mutants that were exposed to GLVs or triacetin (control) for 30 min every day at the onset of dark. (c) shows representative FAW after 7 days of feeding. (d) shows mean weight of FAW after 7 days of feeding on W438 (blue) or *lox10-3* mutants (blue). Different letters denote statistical significance (Tukey's HSD). 99

Figure 28 Expression of circadian clock oscillators are largely unaffected by ZmLOX10. (a-d) shows the expression of *ZmCCA1* (a), *ZmLHY1* (b), *ZmTOC1* (c), and *ZmTOC2* (d) in *lox10-3* mutants (red) relative to WT (blue) at each timepoint. (e-h) shows the expression of the morning loop oscillators, *ZmCCA1* (e) and *ZmLHY1* (f), and the evening loop oscillators, *ZmTOC1* (g) and *ZmTOC2* (h), at every timepoint in WT and *lox10-3* mutants relative to the ZT 12 (a & b) or ZT 4 (c & d) timepoints. Background color indicates light/dark. Data shown is the mean of the log of ΔΔCT. All bars represent standard error. Student's T-test was used to determine statistical difference between genotypes at every timepoint (* = p<.05), (** = p<.005), (*** = p<.0005). 102

Figure 29 LOX10-YFP tagged maize lines show that LOX10 localizes to chloroplasts of guard cells. (a-d) show images of untransformed leaves of B73 inbred line and (e-l) show images of transgenic lines in the B73 background expressing YFP-tagged LOX10 (LOX10-YFP) under its native promoter. (a-d) shows LOX10-YFP is not present in WT leaves, including in guard cells. (e-h) details localization of LOX10-YFP to chloroplasts of guard cells. Columns in order of left to right show brightfield views, chlorophyll autofluorescence, YFP fluorescence, and a merged view. YFP signal is absent in untransformed lines (c), but abundant in LOX10-YFP lines (g) where it overlaps with chlorophyll autofluorescence (h). Scale bars represent 50 µm. 104

Figure 30 GLVs aid in stomatal closure. Figure shows the difference in stomatal aperture between W438 inbred line and *lox10-3* mutant epidermal peels with no treatment (a) and (b), in response to various GLV treatments 100 µM (c), and in response to dose-dependent treatment with (2*E*)-hexenal (d). Students T-test was used to determine statistical significance for (a) (*** = p<.0001) (n>100). Tukey's test was used for (c) and (d) (p<.05) (n>100), where different letters denote statistical significance. 106

LIST OF TABLES

Page

Table 1 List of genes and primers used in qPCR analysis. 13

CHAPTER I

INTRODUCTION

Lipid signaling is a critical aspect of life for unicellular and multicellular organisms on Earth. Plants, which form the cornerstone of agriculture, are no exception and rely on lipid signaling for regulation of almost every aspect of their lives, including defense against biotic and abiotic stresses. The most well-known lipid-derived signals in plants are oxygenated lipids, or oxylipins, most of which are produced by lipoxygenases (LOXs). Plant LOXs are largely divided into two classes, 9-LOX or 13-LOX, corresponding to the carbon position at which they add molecular oxygen (Andreou & Feussner, 2009). LOXs largely act on either linoleic acid (C18:2) or linolenic acid (C18:3) to produce 9- or 13-hydroperoxides. Through subsequent enzymatic and non-enzymatic action, these hydroperoxides are converted to an estimated 650 diverse metabolites (Feussner and Wasternack, 2002; Borrego & Kolomiets, 2016; He et al., 2020). In humans, about 80% of pharmaceutical drugs approved by the Food and Drug Administration target oxylipin pathways (Borrego and Kolomiets, 2016), yet the vast majority of these metabolites are very poorly characterized. Despite their limited knowledge in humans, oxylipin identity, synthesis, metabolism, and function remain vastly more enigmatic in plants.

Within the family of oxylipins produced by LOXs are important volatile oxylipins. As sessile organisms, volatile-based communication between different plants and distal parts of a plant is crucial in anticipating imminent stresses and readying

defenses against them. The most well-known group of volatile oxylipins are the six-carbon, LOX-derived, green leaf volatiles (GLVs), which are emitted in response to a litany of stresses. GLVs are produced in the hydroperoxide lyase (HPL) branch of the LOX pathway, and are typically produced by a single GLV-specializing LOX (Leon et al., 2002; Allman et al., 2010; Christensen et al., 2013; Shen et al., 2014; Mochizuki et al., 2016). Though GLVs are the most prominent group of oxylipin volatiles, they are not the only group. Like GLVs, pentyl leaf volatiles (PLVs) are also a group of volatile oxylipins, though as their name suggests, they consist of five-carbon volatiles. Much is known regarding the synthesis, metabolism, and function of GLVs, yet other than their synthesis requiring a GLV-producing LOX isoform and their widespread emission to various stresses, little is known about PLVs (Shen et al., 2014; Mochizuki et al., 2016). Given their ubiquitous and widespread emission in plants, PLVs represent an unexplored, yet potentially vital, group of plant-based volatile cues.

GLVs are generally regarded as important signals for direct and immediate induction of defensive metabolism and defense priming. One of the major mechanisms by which they prime plant defense is through induction of the major phytohormone, jasmonic acid (JA). JA is an oxylipin that possesses a well-established role in defense against chewing insects and against necrotrophic pathogens, as well as roles in other physiological processes, including root growth (Ueda and Kato, 1980), seed germination (Yamane, 1981), flower development (Dathe et al., 1981; Barendse et al., 1985; Acosta et al., 2009; Yan et al., 2012), senescence (Ueda & Kato, 1980; He et al., 2002, Reinbothe et al., 2009; Yan et al., 2012), stomatal aperture (Popova et al., 1988; Wang et

al., 1999; Suhita et al., 2004), and shade avoidance (Robson et al., 2010). Though GLVs are regarded as important components of defense against pathogens, studies investigating their role regarding plant-pathogen interactions have almost exclusively used necrotrophic pathogens, with little information regarding their role in plant interactions with either biotrophic or hemi-biotrophic pathogens.

In addition to their emission in response to a variety of stresses, GLVs are also released upon light-to-dark transitions in massive amounts. This phenomenon has only been documented a few times (Fall et al., 1999; Graus et al., 2004; Brilli et al., 2011; Jardine et al., 2012), but no resulting physiological impact on the plant of such emissions has been reported. Furthermore, this has been reported for diverse plant species, suggesting this phenomenon is widespread in the plant kingdom and a basic, integral part of plant life. Given the prominent nature of GLVs as defense signals and inducers of JA, I hypothesized that this phenomenon may prime plant defenses against one or more stresses, and may assist plant adaptation to the dark.

The major objectives of this study were to elucidate biosynthesis of PLVs in maize, to establish the role of GLVs in interactions between maize and the hemi-biotrophic fungal pathogen, *Colletotrichum graminicola*, and to investigate the physiological impact of dark-induced GLV emissions in maize. This study collectively aimed to better elucidate the role of volatile oxylipins in maize so that the knowledge obtained can be applied by breeders to generate more stress tolerant elite genetic germplasm.

CHAPTER II

METHODS

PLANT, FUNGAL, AND INSECT MATERIALS

As previously described, mutant alleles of ZmLOX10, ZmOPR7, and ZmOPR8 were obtained by PCR screening of the Mutator-transposon insertional genetics resource at DuPont-Pioneer, Inc. (http://www.pioneer.com) for insertions in these genes (Christensen et al., 2013; Yan et al., 2012). The *lox10-2, lox10-3, opr7-5,* and *opr8-2* alleles are all confirmed exon-insertional knockout mutants. Original mutants were backcrossed into the B73 (*lox10-2, lox10-3, opr7-5, opr8-2*) and W438 (*lox10-2* and *lox10-3*) backgrounds and genetically advanced to the backcross 5-7 stages. All mutants were genotyped by PCR analysis for confirmation of homozygous mutant status. Transgenic C-terminal YFP-tagged LOX10 were generated as described by Mohanty et al. (2009) and advanced to the BC3 stage in the B73 genetic background. All *C. graminicola* plates used in infection assays were grown from culture stock (*C. graminicola* 1.001 strain) kept in a -80 ^{o}C freezer. Cultures were grown on PDA plates for at least two weeks before conidia were collected for use in plant inoculations. Spore extractions were performed as previously described by Gao et al. (2007) and were used within 2 h of extraction. Fall armyworms (FAW) used in the feeding assay were 4th instar, FAW used in weight gain assay were neonates, approximately 1 day old.

MICROSCOPY

LOX10-YFP plants were grown to the V3 stage in TX-360 Metro Mix soil (Sun Gro Horticulture, Agawam, MA) in a growth chamber under 16 h of light (~600 µmol m^{-2} s^{-1}) at 28 °C and 8 h of dark at 24 °C with 50% humidity. Leaves were harvested and then imaged using a Digital Eclipse C1 confocal microscope (Nikon, Melville, NY) (Tolley et al., 2018).

PENTYL LEAF VOLATILE METABOLISM ASSAY

Four intact *Arabidopsis thaliana*, Col-0, grown in small pots (5 plants/pot) were enclosed in 800-mL jars alongside a cotton ball containing 5 µL of 100 mM of select PLVs dissolved in dichloromethane, 5 µL of dichloromethane (control). Treatments included the use of purified chemical standards of (2*Z*)-pentenol, (2*E*)-pentenol, (2*E*)-pentenal, pentanol, pentanal, 1-penten-3-ol, 1-penten-3-one, 3-pentanol, and 3-pentanone obtained from Sigma-Aldrich (St. Louis, MO). Plants were incubated alongside the PLV treatments for 20 min, and then volatiles were collected onto HaySepQ filters via dynamic airflow (approximately 1 L/min) for an additional 20 min. Volatiles were eluted off the HaySepQ filter traps containing 80-100 mesh (Supelco, Bellefonte, PA) with 250 µL of dichloromethane containing 100 µM of the internal standard, (4*Z*)-hexenol (Sigma-Aldrich, St. Louis, MO). Volatiles were analyzed and quantified via gas chromatography mass spectrometry (GC-MS).

WOUND AND FREEZE-THAW ANALYSIS

For volatile analysis of wounding responses, maize leaves of V4 stage plants were cut into 1-cm pieces, quickly weighed out, and immediately placed into 800-mL small jars. For maize, 4 replicates, 2 plants per replicate were used, except for the analysis of B73, *lox10-3*, and *opr7-5opr8-2* mutants which contained 6 replicates. Wounding analysis of *Arabidopsis* was similar to maize, except that 5-6 plants per replicate were used. Freeze-thawing analysis was performed by quickly weighing out leaf tissue, freezing it in liquid nitrogen, and placing it in small jars. Four biological replicates consisting of either 2 maize plants, or 5-6 *Arabidopsis* plants were used. For wounding experiments that did not also involve freeze-thawing treatment, 3 g of tissue was used. For experiments employing both wounding and freezing treatment, 1.5 g of tissue was used. Volatiles were collected for 1 h as described above.

ANTHRACNOSE STALK ROT ASSAYS

lox10-2 and *lox10-3* mutants and their near isogenic wild-types (WT) or recurrent parent inbred used in anthracnose stalk rot (ASR) lesion size assays were grown to the VT stage outdoors under natural conditions throughout late spring and summer (College Station, TX) in 14 L pots filled with TX-360 Metro Mix soil. Stalks were inoculated as previously described by Gao et al. (2007). For determination of lesion areas in *lox10* mutants, 3 internodes of 10 plants per genotype were infected and harvested 10-11 dpi. Post-harvest, infected internodes were split and photographed to produce digital images that were analyzed by ImageJ software (Schneider et al., 2012). *opr7-5* and *orp8-2*

mutants were grown in 14-L pots filled with sterile TX-360 Metro Mix soil in greenhouses during the summer. Four internodes of four plants per genotype were inoculated, harvested, and analyzed 10 dpi as described above.

For hormone analysis of ASR, plant stalks were inoculated with either *C. graminicola* or sterile distilled water (control) as previously described by Gao et al. (2007). For *lox10-3* mutants, 3 internodes of 5 plants per genotype/timepoint were inoculated and harvested 1, 4, and 6 dpi as described above. For *opr7-5 opr8-2* mutants, 4 internodes of 4 plants per genotype/timepoint were inoculated and harvested after 1, 3, or 5 dpi. All harvested stalks were immediately frozen in liquid nitrogen before being placed in a -80 °C freezer, where they remained until further use.

ANTHRACNOSE LEAF BLIGHT ASSAYS

Plants used in anthracnose leaf blight (ALB) assays were grown as described above to the V4 stage and were inoculated as previously described by Gao et al. (2007) except 6 plants per genotype/treatment were inoculated at 6 different points. *opr7-5opr8-2* mutants and other genotypes compared against them were grown in sterile soil, as they cannot survive in normal soil (Yan et al., 2012). For lesion size determination, plants were left for 4-6 days after inoculation before the infected leaves were excised and scanned to produce digital images. Lesion sizes were determined from digital images using ImageJ software (Schneider et al., 2012). For volatile treatments, plants were exposed to GLVs for 1 h, methyl salicylate (MeSA) for 2 h, or methyl jasmonate (MeJA) for 6 h, before being inoculated 1 h after volatile exposure ended. Six plants of each

genotype/treatment were placed into a 6-L glass container along with a cotton ball containing 100 µL of the chosen volatile(s). GLV treatment consisted of a mix containing 10 nmol of (3*Z*)-hexenal (50% in triacetin), 10 nmol of (3*Z*)-hexenol (>98%), and 10 nmol of (3*Z*)-hexenyl acetate (>98%,) dissolved in triacetin. MeSA (>98%) and MeJA (>98%) treatment consisted of 10 µmol of either chemical dissolved in ethanol. All chemical standards were purchased from Sigma-Aldrich (St. Louis, MO). For GLV and JA treatments during necrotrophy, plants were exposed to the volatile treatments 3 dpi, and leaves were harvested for lesion size determination after 6 dpi.

For analysis of hormones responses to GLV exposure, plants were grown in a growth chamber to the V4 stage and exposed to GLVs as described above. Leaves of the plants were harvested 1 h post exposure. For hormone analysis ALB, shoots were inoculated using an atomizer to spray a mist of 5 mL of 10^6 spores/mL onto each plant (0 h timepoint plants were not treated) before plants were sealed in a humidity chamber as previously described by Gao et al. (2007). Five plants per genotype/timepoint were used. After 1, 3, or 5 dpi, their leaves were harvested. All harvested stalks were immediately frozen in liquid nitrogen before being placed in a -80 °C freezer, where they remained until further use.

DARK-INDUCED GREEN LEAF VOLATILE ANALYSIS

WT W438 inbred line and *lox10-3* mutants in the W438 genetic background were grown to the V4 stage in a growth chamber as described above before being placed into 6-L glass containers, 10 plants per jar/replicate, 4 replicates per genotype/timepoint.

Volatiles were collected as described above for 1 h leading up to the light-to-dark transition, and for 1 h after light-to-dark transition. Two different types of light-to-dark transitions were performed with W438 inbred, a diurnal transition that occurred at the normally entrained time of light-to-dark transition, and a non-diurnal transition which occurred at the middle of the normally entrained photophase.

LIGHT-TO-DARK TRANSITION HORMONE ANALYSIS

WT inbred and *lox10-3* mutants in the W438 genetic background were grown to the V4 stage in a growth chamber as described above. Eight plants per genotype/timepoint were collected 1 h before the normal diurnal light-to-dark transition (-1 h), seconds after the transition (0 h), 30 min after the transition (+ 0.5 h), and 1 (+ 1 h), 2 (+ 2 h), and 3 (+ 3 h) h after the transition. Leaves were collected and instantly placed in liquid nitrogen, whereas roots were washed off and dried, in less than 3 min after leaf harvesting, before being placed in liquid nitrogen. Samples were then processed and analyzed by liquid chromatography tandem mass spectrometry (LC-MS/MS).

FALL ARMYWORM ASSAYS

WT inbred and *lox10-3* mutants in the W438 background were grown to the V4 stage in a growth chamber as described above. For the feeding damage assay, plants were placed in 6 L jars before exposed to either control treatment (triacetin), or a GLV mixture of 100 nmol of (3*Z*)-hexenal, (3*Z*)-hexenol, (3*Z*)-hexenyl acetate as described

above. Exposure began at the light-to-dark transition and lasted for 30 min. In order to insure that there were no direct effects of GLVs on the FAWs, the air from the growth chamber was allowed to diffuse out before a 4th instar FAW was placed on the 3rd leaf of each plant in a clip cage. FAW were allowed to feed for 16 h, after which the leaves were harvested, scanned and analyzed by ImageJ software (Schneider et al., 2012) to determine the area of the leaf consumed.

For the FAW weight gain assay, the V3 stage seedlings were grown in a growth chamber as described above. Plants were enclosed into individual apparatuses along with 3 FAW neonates per a seedling. Plants were exposed to GLVs at the light-to-dark transition or control treatment (triacetin) as described above, except the cotton balls containing the volatile treatments were placed within the individual apparatuses rather than a 6-L glass jar. Treatment continued for 30 min after the onset of darkness. These treatments occurred every day of the experiment at this time, which lasted for 7 days in total. Afterwards FAW were euthanized by placing in a freezer for 1 h. Afterward, the weights of larvae FAW were recorded.

RNASEQ ANALYSIS

WT inbred line and *lox10-3* mutants in the W438 background of maize were grown to the V4 stage in a growth chamber as described above. Leaves of the plants, 4 plants per timepoint per genotype, were collected 1 h before and after the light-to-dark transition and placed in a -80 °C freezer. Under liquid nitrogen, samples were ground into a fine powder using a mortar pestle. Twenty-five mg of ground tissue of each

sample within a timepoint/genotype were combined, 100 mg overall, and 1 mL of TRIzol (Ambion, Austin, TX) was added to each sample. The samples were then vortexed and allowed to incubate at room temperature for 5 min. Two-hundred µL of chloroform was added to each sample, vortexed again, and allowed to incubate at room temperature for 10 min. Afterward, the samples were then centrifuged at 13,500 x g for 15 min at 4 °C and the supernatant was then transferred to new tubes along with 500 µL of isopropanol. The samples were vortexed, allowed to incubate for 10 min at room temperature, and transferred to RNeasy Mini spin columns (Qiagen, Venlo, Netherlands). The samples were then cleaned up according to RNeasy Plant Mini Kit protocol (Qiagen, Venlo, Netherlands). Samples were treated with DNAse I (Thermo Scientific, Waltham, MA) to degrade DNA within the samples. Base-calling, quality checking, and removal of adaptor sequences was performed by the TexasA&M AgriLife Genomic and Bioinformatics Service. Raw, paired end, 50-bp reads were aligned to the B73 reference genome sequence (AGPv4 release 38) with the TopHat2 v2.1.0 pipeline (Kim et al., 2013). Uniquely aligned reads were counted with the HT-Seq 0.6.1 pipeline (Anders et al., 2015) using the Ensembl GCA_000005005.6 Zm-B73-REFERENCEGRAMENE-4.0 for annotation. The fragment per million kilobase (FPKM) values were calculated via the Ballgown (v2.10.0) pipeline (https://ccb.jhu.edu/software.shtml). A heatmap of genes was generated utilizing the heatmap.2 package in RStudio (RStudio: Integrated Development for R. RStudio, PBC, Boston, MA URL http://www.rstudio.com/).

QPCR ANALYSIS

For analysis of circadian clock oscillators, WT inbred line and *lox10-3* mutants in the W438 background of maize were grown to the V4 stage in a growth chamber as described above. Three plants of each genotype were harvested every 2 h for 24 h, immediately frozen in liquid nitrogen, and then stored in a -80 °C freezer. Additional tissue from the light-to-dark transition hormone analysis experiment was used for the analysis of dark-response genes involved in JA-signaling. Under liquid nitrogen, leaf tissue was ground using a mortar and into a fine powder. One hundred mg of sample was weighed out and 1 mL of TRIzol (Ambion, Austin, TX) was added to each sample before vigorous vortexing. After sitting at room temperature for 5 min, 200 µL of chloroform was added and vortexed again. After incubating at room temperature for 10 min, the samples were then centrifuged at 13,500 x g for 15 min at 4 °C. The supernatant was then transferred to new tubes, 500 µL of isopropanol was added, and then vortexed. Samples incubated for 10 min at room temperature before being centrifuged at 13,500 x g for 5 min at 4 °C. Three consecutive washes with diethylpyrocarbonate (DEPC)-treated 70% ethanol were then performed. Nucleic acids were allowed to air dry for 30 min and the samples were dissolved in DEPC-treated sterile water. Samples were incubated at 55 °C for 5 min in a dry heat block. Samples were treated with DNAse I (Thermo Scientific, Waltham, MA) prior use. RT-qPCR analysis of genes listed in Table 1 was performed using the Verso 1-Step RT-qPCR kit from Thermo Scientific (Waltham, MA). Primers for each gene are also found in Table 1. The data collected from qPCR was analyzed by the ΔΔCT method. Circadian clock oscillator data was log

transformed in order to normalize the differences in expression. A full list of gene IDs and primers can be found in Table I.

Gene Name	Gene ID	Forward Primer	Reverse Primer
ZmLOX10	Zm00001d053675	TCATCGACGAGTGCAACAA	GAGGATGGATCAGATGGAGATG
ZmLOX8	Zm00001d003533	CAGTACCGACAGACAGCCAT	GGTCGGACCACCAAATCAA
ZmAOS1c	Zm00001d013185	AAGCTGATCACCAAGTGG	CCGGTCGTAGTCCTTCTT
ZmOPR7	Zm00001d032049	GCACGCATGTGATTTGATTATTAGT	GAGATGACTGCTGATTGCTGTGCA
ZmOPR8	Zm00001d050107	TGTTCGTGTATTGTGGCTTGAGA	CAATCGCGGCATTACCCAGATGT
Zmbhlh91	Zm00001d047017	GAGCTCAACTTCTCGGATTT	GACTCGGGCTTGAAGAAC
ZmMYC7	Zm00001d030028	GTCTGCTTCCCCGTCGGCAC	GCGTCGGCGAGCCATAGCAT
ZmJAZ2	Zm00001d027901	GCCGCTCACCATCTTCTA	CGGGAAGTCGTCGAACA
ZmJAZ3	Zm00001d029448	GAGCGAGGGAGTAGAGTAAA	CAAATCTCCACCGCAACT
ZmCCA1	Zm00001d049543	CGAGGAAACTGTGGTAAAGG	GCCATGCTCTGCCATAAA
ZmLHY1	Zm00001d024546	CTAATGGCAGGTGATGCATCTC	GGGCATCACGGAAGAGATTAAG
ZmTOC1	Zm00001d051114	GAAACAGGCACCTCAAAGC	CGCTCTTCTTGGAGAGGATTT
ZmTOC2	Zm00001d017241	AAACGGGCACCTCAAATCAG	GATGATTGACTGGCATCTAGGG

Table 1 List of genes and primers used in qPCR analysis.

STOMATA ASSAYS

WT inbred line and *lox10-3* mutants in the W438 genetic background were grown under growth lights (~300 µmol m^{-2} s^{-1}) under 16:8 h (light:dark) cycles at room temperature to the V2 genetic stage. Epidermal peels were taken from either the 1st or 2nd leaves and placed in a petri dish containing 25 mL of stomata opening buffer (SOB), which was comprised of 10 mM 2-(N-morpholino)ethanesulfonic acid and 50 mM potassium chloride, adjusted to a pH of 6.2 by potassium hydroxide. Peels were incubated under growth lights in SOB for 1.75 h, with CO_2-free air gently bubbled in, to fully open stomata. Afterwards, peels were moved into new petri dishes containing SOB with 0.001% fluorescein diacetate (FDA) and 100 µM of (3*Z*)-hexenal, (3*Z*)-hexenol, (3*Z*)-hexenyl acetate, (2*E*)-hexenal, abscisic acid, or ethanol (control) and incubated for

1 h in the same conditions as before. Dilution series of (2*E*)-hexenal involved the transfer of peels after opening to SOB with 0.001% FDA and either 0, 10, 25, 50, 100 µM (2*E*)-hexenal. Images of epidermal peels were taken with an Olympus BX60 fluorescence microscope (Olympus, Tokyo, Japan) and analyzed via ImageJ (Schneider et al., 2012) software to determine aperture widths. Only stomata whose chloroplasts fluoresced, which indicated living cells, were measured and included in the analysis.

VOLATILE ANALYSIS

An Agilent 7890B gas chromatograph connected to an Agilent 5977B quadrupole mass spectrometer (Agilent, Santa Clara, CA) was utilized to quantify volatiles. Two µL of liquid sample was injected splitless into a HP-5ms Ultra Inert column (Agilent, Santa Clara, CA). The inlet temperature was set to 240 °C for the duration of the run. The oven temperature was as follows: 40 °C hold – 2 min, 3 °C/min ramp to 160 °C, 15 °C/min ramp to 280 °C, 280 °C/min hold – 2 min. The solvent delay was 2.5 min. Analytes were fragmented by positive EI (230 °C – source, 150 °C – quadrupole, ionization energy – 70eV, scan range – 25-500 amu). Most compounds were identified and quantified based off of retention times and spectra of pure external standards purchased from Sigma-Aldrich (St. Louis, MO). The 4-oxo-(2*E*)-hexenal, (2*Z*)-pentenyl acetate, pentyl acetate, pentanoic acid, and 2-methyl-3-pentanone were identified based off matching of mass spectra and retention index (RI), calculated according to Van Der Dool and Kratz (1963), in the NIST14 library. (2*Z*)-pentenal and (2*Z*)-hexenal were identified by almost identical spectral matching to (2*E*)-pentenal and

(2*E*)-hexenal, respectively, and retention times characteristic of other lipoxygenase-derived volatile (*E*/*Z*)-isomers. All volatiles were quantified based by utilizing internal and external standards.

HORMONE ANALYSIS

A mortar and pestle were used to grind frozen plant material into a fine powder under liquid nitrogen. Hormones were extracted from tissue and quantified by LC-MS/MS. One hundred mg of ground tissue was mixed with 10 µL of 5 µM internal standards of d-JA (2,4,4-d3; acetyl-2,2-d_2 JA (CDN Isotopes, Pointe-Claire, Quebec, Canada), d_6-SA (Sigma-Aldrich, St. Louis, MO), and 500 µL phytohormone extraction buffer (1-propanol/water/HCl [2:1:0.002 vol/vol/vol]). The samples were agitated for 30 min at 4°C under darkness and then 500 µL dichloromethane was added to each sample. The samples were again agitated for 30 min at 4 °C in darkness and then centrifuged at 14,000 rpm for 5 min. The lower organic layer of each sample was transferred to a glass vial for evaporation under nitrogen gas. Samples were resuspended in 150 µL methanol, transferred to a 1.5 mL microcentrifuge tube, and centrifuged at 14,000 rpm for 2 min to separate any debris. Approximately 90 µL of supernatant of each sample was transferred into autosampler vials for LC-MS/MS. The simultaneous detection of several phytohormones utilized methods of Muller et al. (2011) with modifications. An Ascentis Express C-18 Column (3 cm × 2.1 mm, 2.7 µm) (Sigma-Aldrich, St. Louis, MO) connected to an API 3200 LC-MS/MS (Sciex, Framingham, MA) using electrospray ionization with multiple reaction mentoring was used. The injection volume was 10 µL

and had a 450 μL min-1 mobile phase consisting of Solution A (0.2% acetic acid in water) and Solution B (0.2% acetic acid in acetonitrile) with a gradient consisting of (time – %B): 0.5 – 10%, 1.0 – 20%, 21.0 – 70%, 24.6 – 100%, 24.8 – 10%, 29 – stop. All hormones were quantified by comparing against isotopically-labeled internal standards from Sigma-Aldrich (St. Louis, MO) and Cayman Chemical (Ann Arbor, MI).

CHAPTER III

VOLATILE OXYLIPIN SYNTHESIS IN MAIZE

INTRODUCTION

Plants are sessile organisms, and as such, have evolved complex mechanisms that allow them to withstand a variety of different stresses. Volatile-mediated signaling facilitates systemic communication within a plant, plant-to-plant communication, and communication with insects (Matsui et al., 2012; Allman and Baldwin, 2010). This volatile-based communication allows plants to anticipate and pre-emptively prime defenses against a wide range of imminent stresses (Engelberth et al., 2004). There are several key groups of volatile organic compounds (VOC) that are integral to these processes, including green leaf volatiles (GLV), which are a group of six-carbon, lipid-derived, volatile oxylipins synthesized in the hydroperoxide lyase (HPL) branch of the lipoxygenase (LOX) pathway (Matsui, 2006). These volatiles are widely emitted in response to various stresses and are known to induce defense against a variety of stresses, as well as in response to pathogen infection (Ameye et al., 2018). Though GLVs have been well characterized, they are not the only major group of LOX-derived volatile oxylipins, including some jasmonates, such as methyl jasmonate and cis-jasmone, and pentyl leaf volatiles (PLV).

PLV constitute another major, and often underreported, group of LOX-derived volatiles that are often co-emitted with GLVs. As their name suggests, this group of volatiles consists of five-carbon volatiles and their derivatives. Like GLVs, PLVs are

widely emitted in response to a litany of stresses in numerous plant species, including during infection with pathogens (Heiden et al., 2003), wounding (Fall et al., 2001; Mochizuki et al., 2016), and light-to-dark transitions (Jardine et al., 2012). Despite this, there has been little focus on this group of volatiles, with priming of pathogen defense (Song et al., 2015) and weevil attraction (van Tol et al., 2012) the only reported physiological functions of PLVs. This study seeks to better elucidate the synthesis of this enigmatic group of volatile oxylipins in maize.

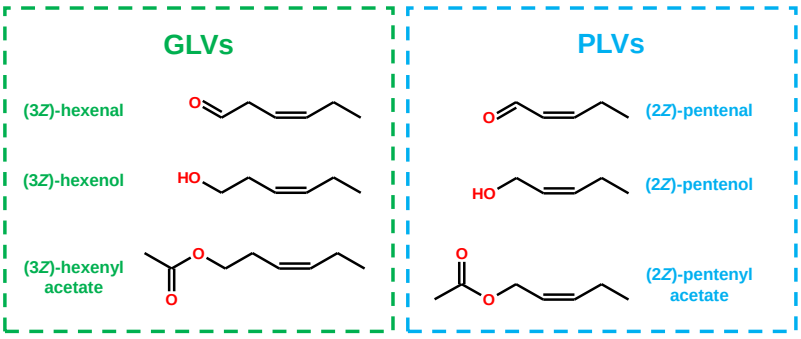

Figure 1 Structural similarity of green leaf volatiles and pentyl leaf volatiles.

GLV synthesis

Despite the structural similarity between various individual PLVs and GLVs (Fig. 1), their synthesis is largely different. GLV synthesis occurs in the HPL branch of the LOX pathway, where either 9- or 13-LOX-derived hydroperoxides, derived from either linoleic acid (C18:2) and *a*-linolenic acid (C18:3), are acted upon by either a 9- or 13-HPL, respectively. For simplicity, we will focus exclusively on 13-LOX-derived GLV synthesis from C18:3. Recently, it was revealed that HPLs cleave their substrate by forming a hemi-acetal that rapidly spontaneously degrades into a 6-carbon aldehyde GLV, (3*Z*)-hexenal, and a non-volatile 12-carbon compound, (9*Z*)-traumatin (Hatanaka,

1993; Mukhtarova et al., 2018) (Fig. 2). (3*Z*)-hexenal can be enzymatically or non-enzymatically isomerized to another aldehyde, (2*E*)-hexenal (Hatanaka, 1993; Kunishima et al., 2016; Spyropoulou et al., 2017). Another aldehyde, (2*Z*)-hexenal also appears to be formed, likely through non-enzymatic generation from (3*Z*)-hexenal.

Both (3*Z*)-hexenal and (2*E*)-hexenal can be enzymatically reduced to their corresponding alcohols, (3Z)-hexenol and (2*E*)-hexenol, by NADH-dependent (Bate et al., 1998; Speirs et al., 1998) and NADPH-dependent alcohol dehydrogenases (ADH) (Tanaka et al., 2018). These alcohols can then be further converted to their respective acetate-conjugates, (3*Z*)-hexenyl acetate and (2*E*)-hexenyl acetate, by acetyl-CoA-dependent acetyl transferases (CHAT) (D'Auria et al., 2007). A variety of additional GLV conjugates have been reported (Moon et al., 1996; Farag et al., 2004; Allman and Baldwin, 2010; Sugimoto et al., 2013; López-Gresa et al., 2018); however, these are not as universally emitted in maize, or across diverse plant species. In some instances, (3*Z*)-hexenal may also be non-enzymatically converted into more reactive GLVs, including 4-hydroxy-(2*E*)-hexenal, 4-oxo-(2*E*)-hexenal (Gardner and Grove, 1998; Matsui et al., 2012), but these are emitted much less than enzymatically generated derivatives of (3*Z*)-hexenal.

PLV synthesis

Unlike GLV synthesis, PLV synthesis originates from the LOX branch of the LOX pathway. This branch can produce a variety of compounds through various reactions, including keto-octadecenoates (Gardner, 1991), epoxy-keto-octadecenoates (Goodfriend et al., 2002), and PLVs (Salch et al., 1995) and their 13-carbon counterparts

(Gao et al., 2008). While GLVs may be synthesized from 9- and 13-hydroperoxides derived from C18:2 and C18:3, only 13-hydroperoxides have been reported to serve as substrate for PLV synthesis, particularly 13*S*-hydroperoxy octadecetrienoic acid (13*S* -HPOT) (Salch et al., 1995). 13-LOX-derived 13*S*-HPOT is converted to a radical by a subsequent secondary 13-LOX reaction, which quickly and spontaneously undergoes a β-scission reaction to form a pentene allylic radical that rapidly forms the isomers, 1-penten-3-ol and (2*Z*)-pentenol (Salch et al., 1995) (Fig. 2). Pentanol may also be produced from 13*S*-HPOD through this reaction. This reaction also generates a 13-carbon compound, 13-oxo-9(*Z*)-11(*E*)-tridecedienoic acid (OTD) (de Groot et al., 1975; Verhagen et al., 1977; Salch et al., 1995; He et al., 2020). As with its GLV-counterpart, traumatin, which is converted into the more stable traumatic acid, OTD may be converted to 9(*Z*)-11(*E*)-tridecedien-1,13-dioic acid (TDD), although this metabolite has only been reported *in vitro* (Gao et al., 2008).

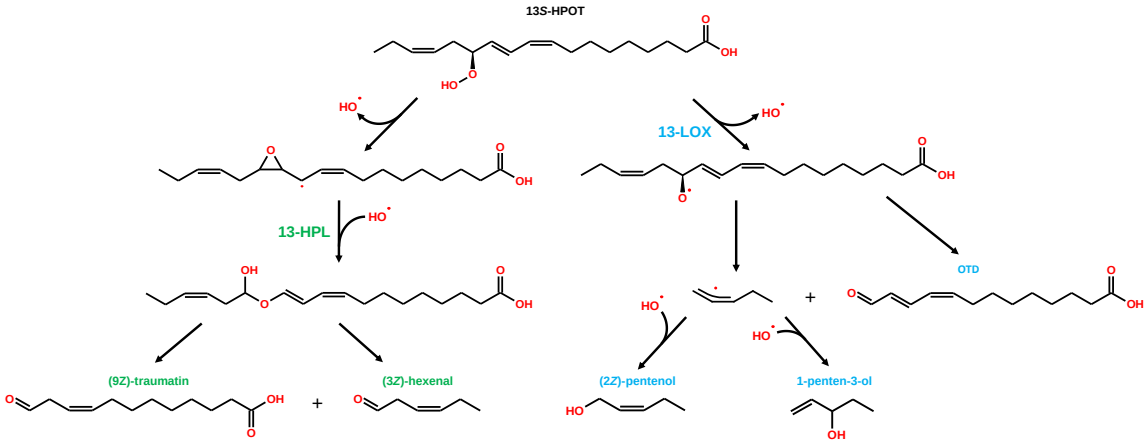

Figure 2 Synthesis of primary PLVs and GLVs. Shows difference in the formation of primary GLVs and PLVs (Salch et al., 1995). Names in green font denote the HPL pathway and its products, names in blue font depict the LOX pathway and its products. Adapted from Salch et al. (1995) and Mukhatarova et al. (2018).

The two primary PLVs may then converted into aldehydes and ketones (Gardner et al., 1996). PLV synthesis is largely derived from 13*S*-HPOT substrate, with LOXs displaying less enzymatic activity toward 13*S*-HPOD (Salch et al., 1995). Anaerobic conditions are reported to drive this reaction, as the ferrous iron ion found in LOXs is oxidized to its ferric state by the hydroperoxide group of 13*S*-HPOT, instead of by free molecular oxygen (Salch et al., 1995). As 13*S*-HPOT is reported to be the major substrate for PLV synthesis, C18:3 is largely required for synthesis of these metabolites, indicating that C18:3-rich organelles, such as plastids, are the likely site of initial PLV and OTD synthesis. This is also true for GLV synthesis, which chiefly relies upon chloroplast-localized LOXs and HPLs (Froehlich et al., 2001; Gorman et al., 2020). Thus, it is not surprising that the major GLV-producing LOX isoforms of various species have also been reported to be the major PLV-producing LOX isoforms (Shen et al., 2014, Mochizuki et al., 2016).

Though GLV-producing LOXs have been reported to be important for PLV synthesis, a small portion of PLVs appear to be synthesized by other LOX isoforms due to the continued, albeit severely depleted, levels of PLVs in mutants of GLV-producing LOXs (Shen et al., 2014; Mochizuki et al., 2016; He et al., 2020). Several 13-LOXs of soybean displayed the ability to generate PLVs *in vitro*, although some displayed greater involvement in PLV synthesis than others (Fisher et al., 2003). A peculiar LOX isoform in maize, ZmLOX6, seems to have evolved to specifically produce PLVs and OTD, as it appears to have lost the ability to form hydroperoxides from polyunsaturated fatty acids (Gao et al., 2008; Tolley, 2020). Orthologs of ZmLOX6 are only found in a handful of

monocot species, suggesting a recent neo-specialization of this LOX. Since ZmLOX10 is the only GLV-producing LOX isoform in maize, this suggests both ZmLOX6 and ZmLOX10 may be important for PLV synthesis in maize. As ZmLOX6 appears to have lost oxygenating activity characteristic of LOXs (Gao et al., 2008), it may depend on the substrate from ZmLOX10 or other 13-LOXs for PLV synthesis. Utilizing mutants of maize and *Arabidopsis thaliana*, as well as transgenic ZmLOX6 over-expressing lines of *A. thaliana* (ZmLOX6-OE), I establish the biosynthetic order of PLVs in the LOX pathway, and provide evidence that despite the similar structure of PLVs and GLVs, they are metabolized differently. I also show that in maize, ZmLOX10 is required for PLV synthesis, and that jasmonic acid (JA) is a key hormone in the regulation of PLV synthesis. Additionally, I show that ZmLOX6 largely requires substrate from GLV-producing LOX10 to generate PLVs, indicating that ZmLOX10 may feed substrate to ZmLOX6 for maize PLV synthesis. Lastly, I provide evidence that freeze-thawing analysis of volatiles, one of the most widely utilized and popular method of volatile analysis, distorts the volatile profiles of plant tissue and represents an inherently flawed method of volatile analysis.

RESULTS

Metabolism of PLVs

Firstly, I wanted to establish the order in which different PLV molecular species are synthesized. Previous publications have postulated the biosynthetic order of the pathway, but did not experimentally test these hypotheses. In order to establish a more

definitive order of the PLV pathway, I treated intact *A. thaliana*, Col-0 accession, with a variety of exogenous PLV standards and measured the output of their volatiles. Intact *A. thaliana* Col-0 were exposed to various PLVs for 20 min before headspace air was dynamically collected over HaySepQ traps for an additional 20 min. Plants were individually exposed to (2*Z*)-pentenol, (2*E*)-pentenol, (2*E*)-pentenal, pentanol, pentanal, 1-penten-3-ol, 1-penten-3-one, 3-pentanol, and 3-pentanone. (2*Z*)-pentenol was converted into the greatest number of compounds (Fig. 3), likely due to its status as one of the two primarily synthesized PLVs. (2*Z*)-pentenol was mostly converted to (2*Z*)-pentenal and (2*Z*)-pentenyl acetate, followed by (2*E*)-pentenal, pentanol, and (2*E*)-pentenol. This suggests that (2*Z*)-pentenol can be converted to (2*Z*)-pentenal by an ADH. Both (2*Z*)-pentenol and (2*E*)-pentenol exposure resulted in the re-emission of (2*E*)-pentenal, indicating that (2*E*)-pentenol may also be acted upon by an ADH (Fig. 3).

Unexpectedly, both (2*Z*)-pentenol and (2*E*)-pentenol exposure resulted in the emission of pentanol, suggesting that these alcohols may undergo enzymatic reduction of their carbon-carbon double bond (Fig. 3). This indicates that pentanol may be derived from both C18:3 and C18:2 substrate. (2*Z*)-pentenol and (2*E*)-pentenol were also reduced to their respective acetate conjugates, (2*Z*)-pentenyl acetate and (2*E*)-pentenyl acetate, indicating that PLVs may also be acted upon by a CHAT (Fig. 3). Pentanol treatment only resulted in the emission of a small amount of pentanal and pentyl acetate, suggesting that while pentanol may also serve as substrate for the ADH(s) and CHAT(s) that act on its alkene counterparts, it is a less effective substrate (Fig. 3). Exposure to pentanal largely resulted in the emission of pentanoic acid, and to a lesser extent,

pentanol. Similarly, (2*E*)-pentenal exposure resulted in the emission of (2*E*)-pentenol and pentanol, although the pentanol was likely derived from (2*E*)-pentenol. This indicates that bi-directional interconversion between alcohol and aldehyde PLVs may occur, and that these reactions are dependent upon different enzymes as well as stoichiometry. This suggests that PLV alkanes may be derived from either LOX-mediated cleavage of 13*S*-HPOD, or from PLV alkenes via unknown reductases.

Treatment of plants with 1-penten-3-ol resulted in the second largest number of derivatives, further suggesting it sits at the top of the PLV pathway. 3-pentanone was the most emitted volatile after 1-penten-3-ol treatment, followed by 1-penten-3-one, and small amounts of 3-pentanol (Fig. 3). 1-penten-3-one treatment also resulted in the emission of similar amounts of 3-pentanol and 3-pentanone, suggesting that the presence of these volatiles after 1-penten-3-ol treatment is owed to its conversion to 1-penten-3-one (Fig. 3). 3-pentanol treatment resulted in the emission of 3-pentanone, but in much greater amounts, indicating its rapid conversion by an ADH (Fig. 3). This suggests that 3-pentanone may be generated by both oxidation of 3-pentanol or reduction of 1-penten-3-one. Treatment of 3-pentanone yielded a small amount of 3-pentanol, likely a result of the high concentrations applied (Fig. 3). Both 3-pentanol and 3-pentanone treatment resulted in relatively minor emissions of a novel PLV, 2-methyl-3-pentanone, that has not previously been previously reported (Fig. 3). This could also be a result of the high exogenous concentrations used in this experiment.

		Treatment									
		Control	(2*Z*)-POL	(2*E*)-POL	(2*E*)-PAL	POL	PAL	PEOL	POEN	3-POL	3-PON
Analytes (nmol/h)	(2*Z*)-pentanol										
	(2*Z*)-pentanal		8.8		0.3						
	(2*Z*)-pentanyl acetate		7.7								
	(2*E*)-pentanol		0.9		23.4						
	(2*E*)-pentanal		3.2	5.7							
	(2*E*)-pentanal acetate			0.7	0.5						
	pentanol		1.5	3.9	5.7		7.7				
	pentanal					0.9					
	pentanoic acid						184.9				
	pentyl acetate			0.2		1.7	0.3				
	1-penten-3-ol										
	1-penten-3-one							22.9			
	3-pentanol							1.0	0.5		1.5
	3-pentenone							65.1	72.8	140.0	
	2-methyl-3-pentanone									5.5	0.1

Figure 3 Metabolism of exogenous PLVs by *A. thaliana*. Intact *A. thaliana* Col-0 were exposed to various PLVs for 20 min before volatiles were collected for an additional 20 min. Four pots (5 plants/pot) were placed in small jars and exposed to 5 µL of 100 mM of various individual PLVs or dichloromethane (control). X-axis shows individual exogenous PLV treatments. Y-axis shows target analytes (nmol/h). Analyte target responses matching the same volatile treatment were omitted (black cells). Blank cells indicate targets that were not detected. (2*Z*)-pentenol (2*Z*-POL), (2*E*)-pentenol (2*E*-POL), (2*E*)-pentenal (2*E*-PAL), pentanol (POL), pentanal (PAL), penten-3-ol (PEOL), 1-penten-3-one (PEON), 3-pentanol (3-POL), 3-pentanone (3-PON).

ZmLOX10 is critical for efficient synthesis of PLVs

With the biosynthetic order of PLVs elucidated, I next wanted to determine the important LOX isoforms for PLV synthesis in maize. As GLV-producing LOXs have been reported to also be major PLV-producing LOXs (Shen et al., 2014, Mochizuki et al., 2016), I started by evaluating the role of the maize GLV-producing LOX isoform, ZmLOX10 (Christensen et al., 2013), in PLV synthesis. To do this, I heavily wounded leaves of wild-type (WT) maize and near-isogenic, 98.5% (BC7) similarity to WT, *lox10-3* knockout mutant lines in two diverse inbred genetic backgrounds, B73 and W438. Volatiles of the leaves were collected onto a HaySepQ trap for 1 h after wounding, and then analyzed by gas chromatography-mass spectrometry (GC-MS). This

analysis revealed that *lox10-3* mutants were deficient in almost all types of PLVs, though there were clear differences in the contribution of ZmLOX10 toward the synthesis of alkane and alkene PLVs, highlighting the different efficiencies of 13*S*-HPOT and 13*S*-HPOD as substrate for PLV synthesis (Salch et al., 1995) (Fig. 4b). Most alkene PLVs were greatly diminished, by at least 90%, in *lox10-3* mutants of either background (Fig. 4b). The only notable exceptions were 3-pentanone and (2*E*)-pentenol, which were not statistically different between *lox10-3* mutants and their respective WTs (Fig. 4b). Other than these two compounds, (2*Z*)-pentenol and 1-penten-3-ol displayed the least amount of difference between *lox10-3* mutants and WT, but were also emitted in the highest amounts (Fig. 4b). This is not surprising as they are the first PLVs synthesized in the C18:3-PLV pathway. 95% or more of all C18:3-derived GLVs were eliminated in *lox10-3* mutants of either background, but only about 50-75% of C18:2-derived GLVs were absent (Fig. 4a). Taken together these results suggest that ZmLOX10 is both the C18:3-derived PLV- and GLV-producing LOX isoform. These results also suggest that ZmLOX10 has an important, but comparatively smaller, role in C18:2-derived GLV synthesis, and an insignificant role in C18:2-derived PLV synthesis.

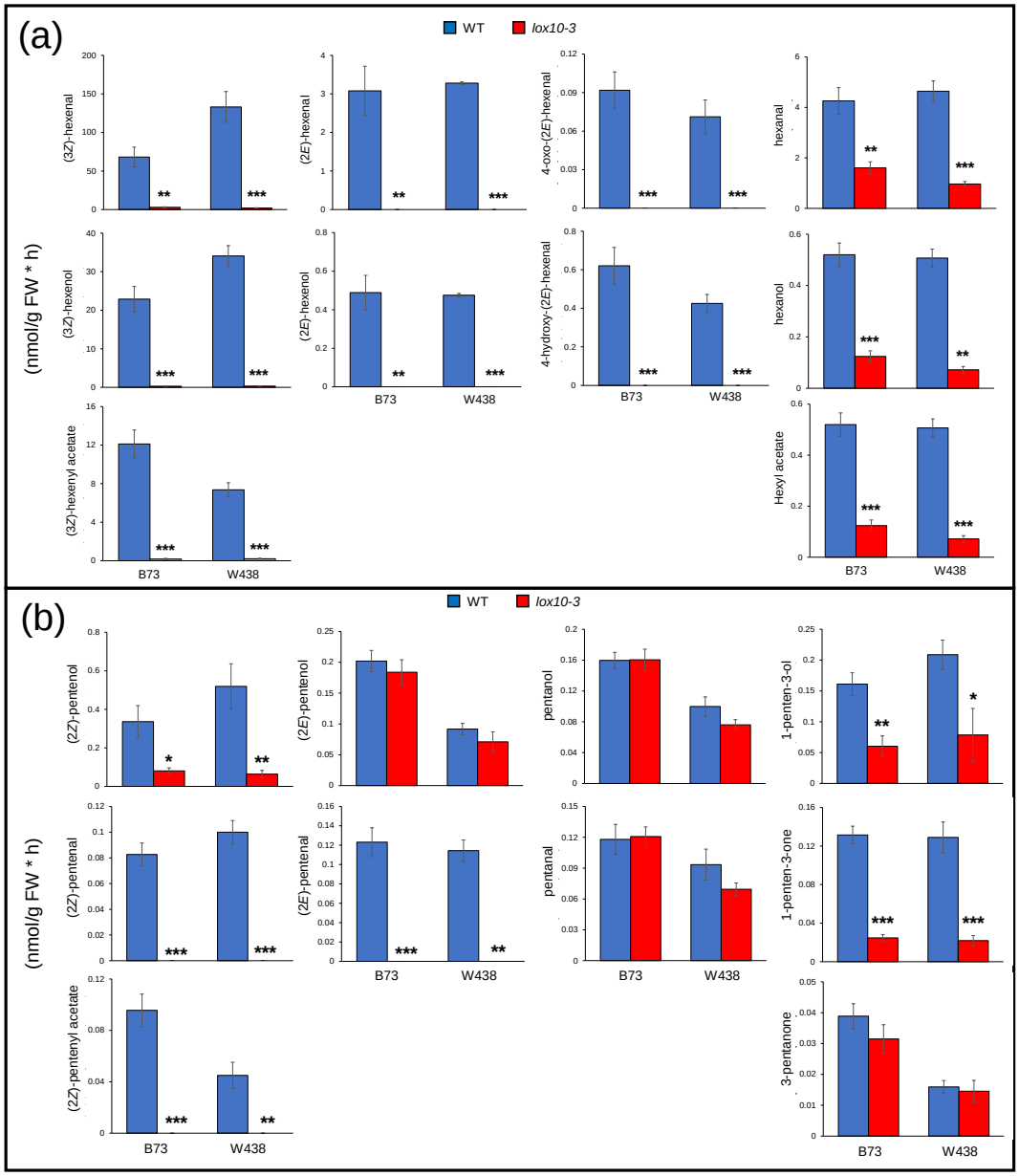

Figure 4 Wound-induced GLV and PLV emissions are greatly diminished in *lox10-3* mutants of maize. Volatiles were collected for 1 h after leaves of two WT inbred lines, B73 and W438 (blue), and *lox10-3* mutants (red) in each respective background, were cut into 1 cm pieces. (a) shows various GLVs and (b) shows various PLVs (mean ± SE, nmol per gram of fresh weight per hour). Student's T-test was performed to determine statistical difference between treatments for each individual inbred genetic background [p<.05 = (*), p<.005 = (**), p<.0005 = (***)] (n=4).

ZmLOX6 depends on substrate from a GLV-producing LOX for PLV synthesis

Both ZmLOX10 (this study) and ZmLOX6 (Gao et al., 2008; Tolley, 2020) have been established as important PLV-producing LOXs. As such, I next sought to clarify the potential interactions of ZmLOX6 and ZmLOX10 regarding their involvement in PLV synthesis. While it is possible that both LOX isoforms significantly contribute to PLV synthesis, their roles differ. As the major 13-LOX isoform in maize leaves, ZmLOX10 may provide much of the substrate for PLV synthesis (He et al., 2020), and may or may not also perform the cleavage reaction to synthesize PLVs. 13*S*-HPOT produced by the plastid-localized ZmLOX10 (Gorman et al., 2020) may also be utilized by the plastid-localized ZmLOX6 (Tolley et al., 2018), which cannot produce 13*S*-HPOT but can cleave it into PLVs and OTD (Gao et al., 2008). Unfortunately, exonic transposon-insertional ZmLOX6 mutants are not available in maize, therefore transgenic ZmLOX6-OE lines of *A. thaliana* in both WT Col-0 and *Atlox2-1* mutant Col-0 backgrounds (Tolley 2020) were utilized. AtLOX2 is the only GLV-producing LOX isoform in *A. thaliana* (Mochizuki et al., 2016) and is an ortholog of ZmLOX10 in maize (Borrego and Kolomiets, 2016).

In order to establish whether ZmLOX6 relies on the substrate from a GLV-producing LOX, I analyzed PLVs emitted by wounded leaves of WT Col-0, two ZmLOX6-OE lines, *Atlox2-1* mutants, and two lines in which *Atlox2-1* mutant overexpresses ZmLOX6-OE (*Atlox2-1* ZmLOX6-OE). As seen by Tolley (2020), both transgenic ZmLOX6-OE lines had significantly increased PLV emissions, except (2*Z*)-pentenyl acetate (Fig. 5). *Atlox2-1* mutants were lower than Col-0 for all PLVs,

reinforcing its status as the major PLV-producing LOX of *A. thaliana* (Mochizuki et al., 2016) (Fig. 5). However, the *Atlox2-1* ZmLOX6-OE lines displayed significantly lower levels of volatiles compared to sole transgenic ZmLOX6-OE lines, indicating that ZmLOX6-OE relies on AtLOX2 substrate for PLV synthesis (Fig. 5). Interestingly, PLVs were increased in the *Atlox2-1* ZmLOX6-OE lines relative to *Atlox2-1* mutants, suggesting that other 13-LOX isoforms may also provide a minor amount of substrate to ZmLOX6 (Fig. 5). Collectively, this indicates that while ZmLOX6 can use substrate from other LOXs, it is largely dependent on the substrate produced by a GLV-producing LOX isoform to synthesize PLVs. As such, it is likely that, in maize, ZmLOX6 depends on ZmLOX10 to produce PLVs, however, additional studies utilizing *lox6* and *lox6lox10* double mutants of maize are required to definitively resolve this hypothesis.

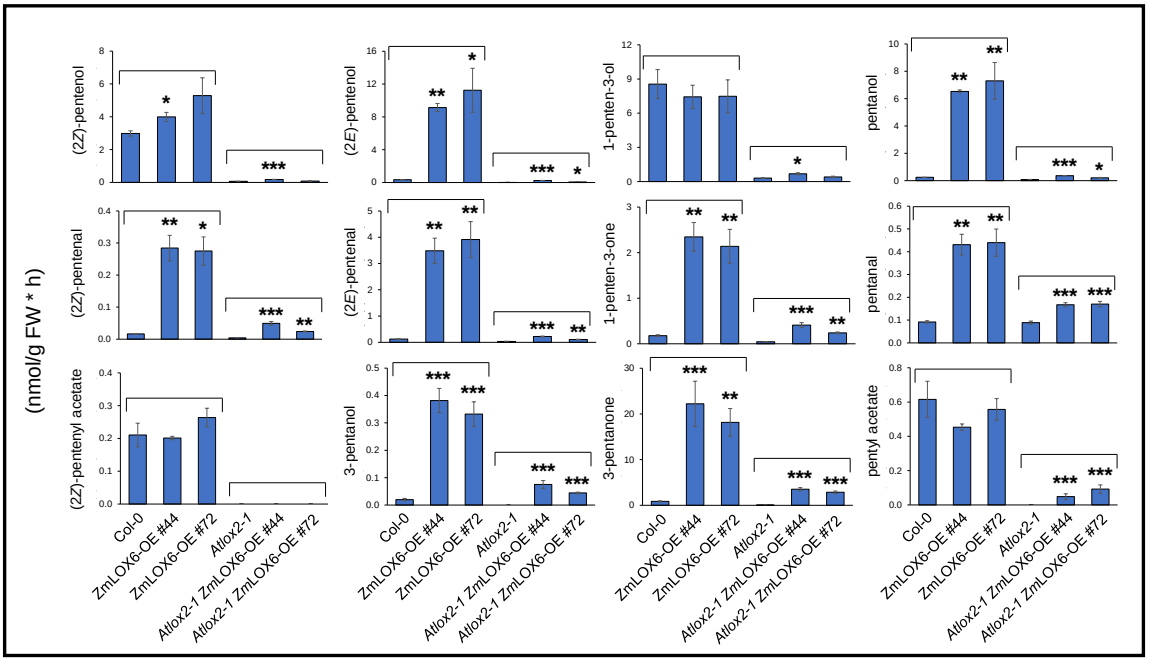

Figure 5 ZmLOX6 depends on AtLOX2, the GLV- and PLV-producing LOX, in transgenic ZmLOX6-OE lines of *A. thaliana*. Volatiles were collected for 1 h after leaves of two ZmLOX6-OE transgenic lines (line #44 and line #72), *Atlox2-1* mutants, and *Atlox2-1* ZmLOX6-OE mutant/transgenic lines (line #44 and line #72) in the Col-0 background were cut into 1 cm pieces. Shows various PLVs (mean ± SE, nmol per gram of fresh weight per hour). Dunnett's test was performed to determine statistical difference between Col-0 (control, left bracket) and ZmLOX6-OE transgenic lines treatments, and between *Atlox2-1* mutants (control, right bracket) and *Atlox2-1* ZmLOX6-OE mutant/transgenic lines [p<.05 = (*), p<.005 = (**), p<.0005 = (***)] (n=4).

The role of JA in PLV and GLV synthesis

GLVs and JA have a well-documented mutual synergism, with GLVs promoting synthesis of JA through induction of oxo-phytodienoate reductases (OPR) and JA promoting expression of LOX genes involved in GLV synthesis (Christensen et al., 2013). Given that JA promotes expression of LOXs, and LOXs are both the substrate provider and enzymatic catalysts for generation of PLVs, I measured PLVs and GLVs released by wounding the JA-deficient maize double mutant, *opr7-5opr8-2*. Wounded

opr7-5opr8-2 produced significantly less PLVs and GLVs than WT inbred B73, but were not as deficient as *lox10-3* mutants (Fig. 6). As reported previously (Christensen et al. 2013), *lox10-3* mutants were almost devoid of any GLVs, especially those derived from C18:3, and possessed greatly reduced PLV emissions compared to WT, except for pentanol, pentanal, and 3-pentanone (Fig. 6). Unlike the prior analysis of *lox10-3* mutants (Fig. 4b), (2*E*)-pentanol was significantly reduced in *lox10-3* mutants (Fig. 6). *opr7-5opr8-2* mutants displayed reductions in the emissions of GLVs, except for the acetate conjugates (3*Z*)-hexenyl acetate and hexyl acetate, which were almost as low as *lox10-3* mutants (Fig. 6). This suggests that JA signaling is critical for expression of CHATs. (2*Z*)-pentanol, (2*E*)-pentanol, (2*Z*)-pentenal, and (2*Z*)-pentenyl acetate emissions by *opr7-5opr8-2* mutants were statistically lower than WT, and many other PLVs displayed trends towards being lower but were not statistically significant (Fig. 6b). Collectively, these results suggest that JA is a positive regulator of PLV synthesis, and re-affirms that this is also the case for GLVs.

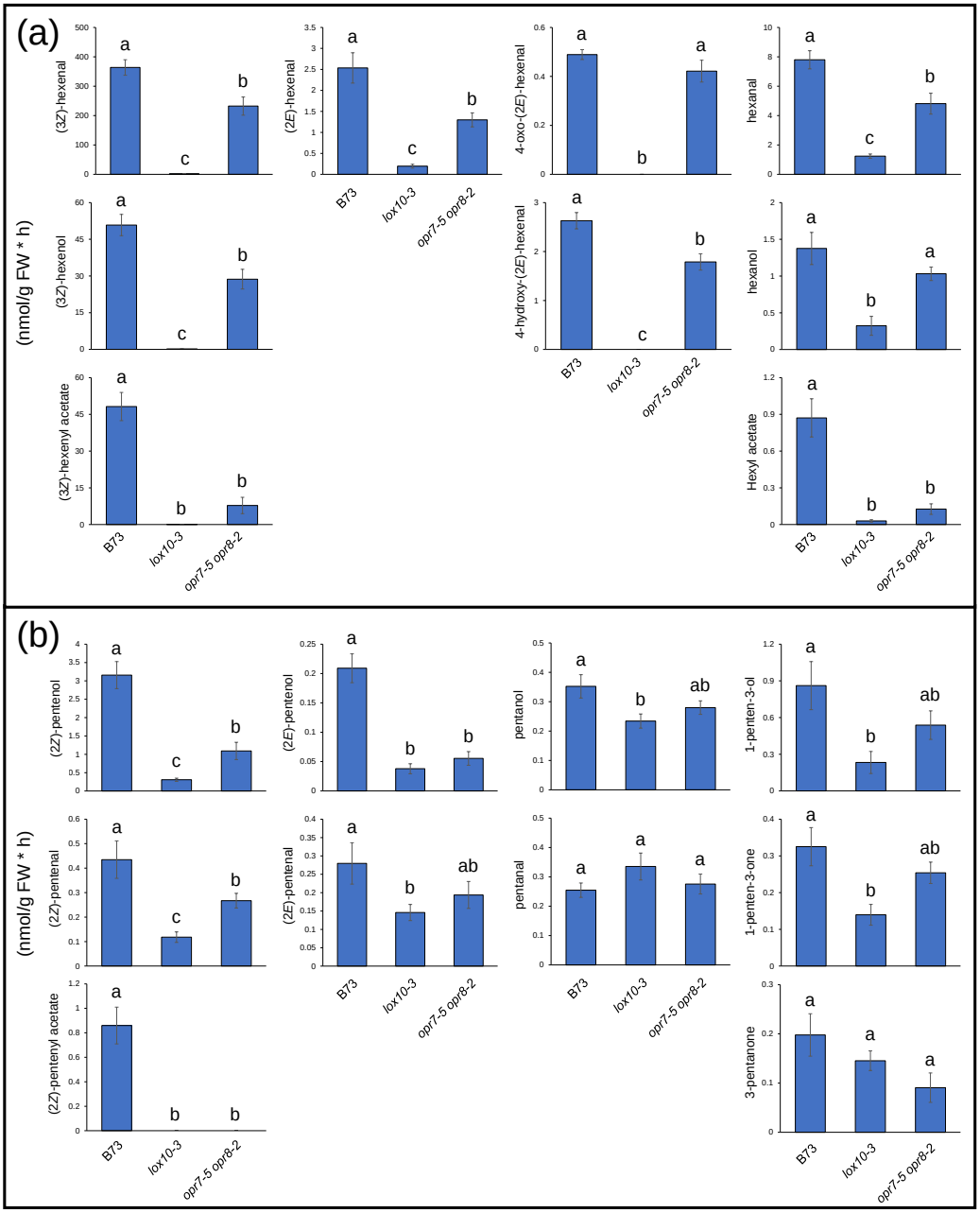

Figure 6 GLV and PLV emissions are diminished in *opr7-5opr8-2* and *lox10-3* mutants of maize. Volatiles were collected for 1 h after leaves of WT, *lox10-3*, and *opr7-5opr8-2* mutants in the B73 genetic background, were cut into 1 cm pieces. (a) shows various GLVs and (b) shows various PLVs (mean ± SE, nmol per gram of fresh weight per hour). Tukey's Test was performed to determine statistical difference between genotypes, where letters denote statistical significance (P<.05) (n=6).

Freeze-thaw treatment distorts the volatile profile of samples

One of the most popular methods used to analyze plant-derived volatiles requires flash-freezing plant tissue, and then allowing it to thaw (Shmelz et al., 2003; Chehab et al., 2006; Nyambura et al., 2011; Kihara et al., 2014; Savchenko et al., 2014; Mochizuki et al., 2016). Many times, this also includes grinding up the plant tissue prior to thawing. In order to understand if reported PLV emissions are accurate with this method, I analyzed freeze-thawed and manually wounded leaves of WT and *lox10-3* mutants in the B73 and W438 inbred genetic backgrounds and compared the two treatments. As with the previous experiment, wounding resulted in the emission of diverse PLVs and GLVs from both respective WTs, of which 18:3-derived volatiles were greatly diminished in *lox10-3* mutants (Fig. 7). Freeze-thawing of leaves resulted in significantly greater emissions of almost all PLVs in all genotypes, including many C18:2-derived PLVs (Fig. 7b). Interestingly, in the W438 background, *lox10-3* produced equivalent amounts of 1-penten-3-one, and even greater amounts of 3-pentanone (Fig. 7b). In the B73 background, *lox10-3* mutants produced more (2*E*)-pentenol upon freeze-thawing than WT (Fig. 7b). This suggests another LOX isoform may compensate for the absence of ZmLOX10 to produce these metabolites, perhaps ZmLOX6. (2*Z*)-pentenyl acetate was the sole PLV that experienced a sharp decrease in emission upon freeze-thawing (Fig. 7b). In fact, (2*Z*)-pentenyl acetate emission in all genotypes was either almost, or completely, abolished by freeze-thawing, suggesting this treatment results in the inactivation of the enzyme(s) responsible for its synthesis.

Freeze-thawing also increased the emission of many GLVs, and far more dramatically than the increase in PLVs (Fig. 7a). The most increased GLVs upon freeze thawing were those purported to be non-enzymatically generated, (2*E*)-hexenal, 4-hydroxy-(2*E*)-hexenal, 4-oxo-(2*E*)-hexenal, and the newly reported (2*Z*)-hexenal (Fig. 7a). Given its pattern of accumulation, it is likely produced non-enzymatically from (3*Z*)-hexenal, or possibly from (2*E*)-hexenal by an isomerase. As seen for acetate conjugates in the PLV pathway, all acetate conjugates in the GLV pathway were absent in freeze-thawed tissue.

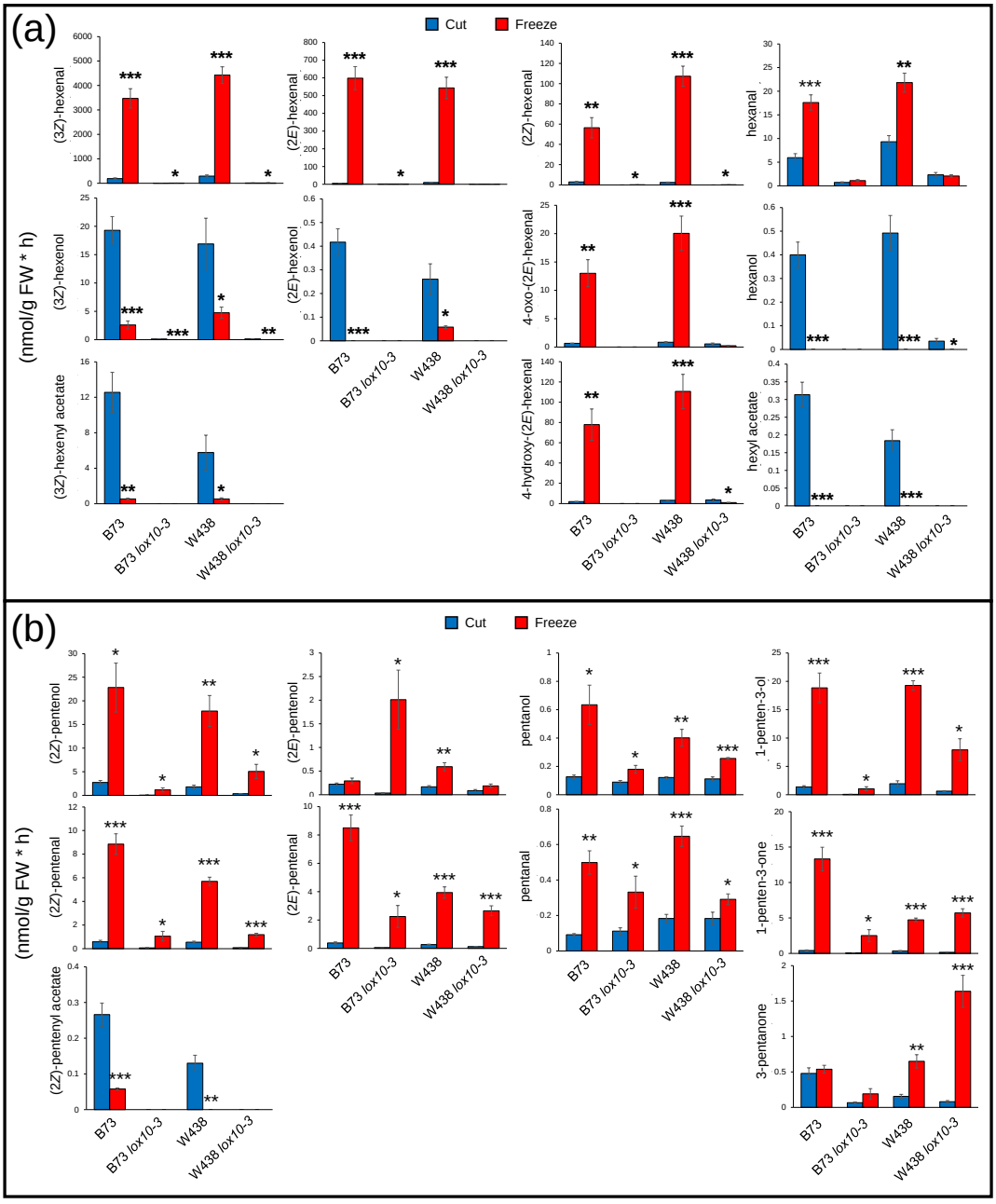

Figure 7 Freezing distorts the GLV and PLV profiles of maize. Volatiles were collected for 1 h after leaves of two inbred lines, B73 and W438, and *lox10-3* mutants in each respective background, were either cut into 1 cm pieces (blue) or briefly flash frozen in liquid nitrogen (red). (a) shows various GLVs and (b) shows various PLVs (mean ± SE, nmol per gram of fresh weight per hour). Student's T-test was performed to determine statistical difference between treatments for each individual genotype [p<.05 = (*), p<.005 = (**), p<.0005 = (***)] (n=4).

PLVs and GLVs emitted by Col-0 *A. thaliana* after freeze-thawing were also measured in order to determine if this effect was consistent throughout multiple species. As seen in maize, aldehyde GLVs were increased in *A. thaliana*, and GLV alcohols and acetates were diminished (Fig. 8a). Correspondingly, the (2*Z*)-pentenyl acetate was also decreased, while most other PLVs displayed increased emissions after freeze-thawing compared to normal wounding (Fig. 8b). Only pentanol, pentanal, (2*E*)-pentenol, and 1-penten-3-ol were not statistically increased by freeze-thawing, although the latter two displayed strong trends (Fig. 8b). Overall, freeze-thawing results for *A. thaliana* closely mirror those of maize, suggesting conservation of the relevant metabolic enzymes between different species.

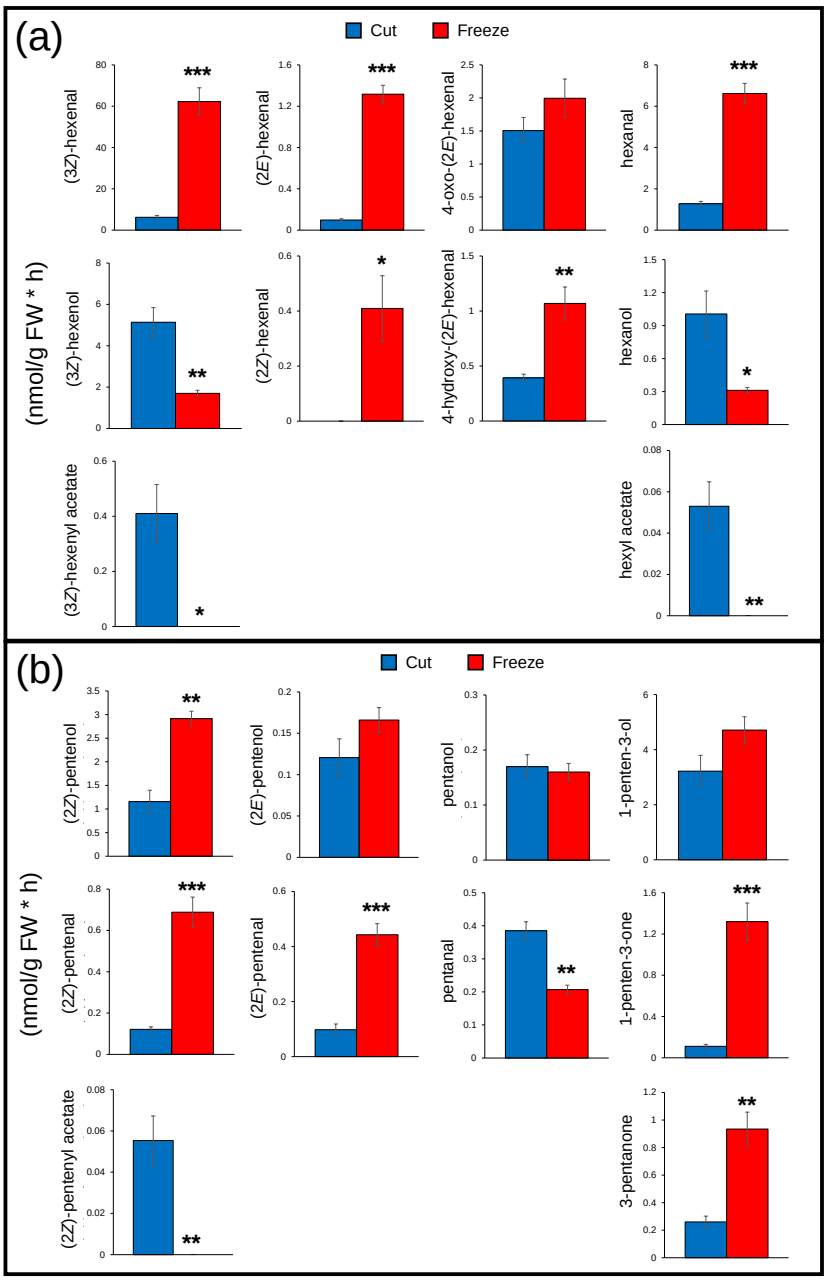

Figure 8 Freezing distorts the GLV and PLV profiles of *A. thaliana*. Volatiles were collected for 1 h after leaves of Col-0 were either cut into 1 cm pieces (blue) or briefly flash frozen in liquid nitrogen (red). (a) shows various GLVs and (b) shows various PLVs (mean ± SE, nmol per gram of fresh weight per hour). Student's T-test was performed to determine statistical difference between treatments for each individual genotype [p<.05 = (*), p<.005 = (**), p<.0005 = (***)] (n=4).

Collectively, these results suggest that the CHAT responsible for the conversion of GLV alcohols is irreversibly inactivated by freeze-thawing and that PLVs depend on a similar, if not the same, enzyme for generation of PLV acetate conjugates. Unlike PLVs however, freeze-thawing almost eliminated emissions of GLV alcohols in both species. This suggests that the enzymes performing conversion of GLV aldehydes to alcohols are also irreversibly inactivated by freezing. As GLV alcohols and PLV aldehydes are reportedly both synthesized by ADHs, albeit with opposite reactions, this suggests that different ADH isoforms may be responsible for PLV and GLV metabolism. Ultimately, this demonstrates that freeze-thawing distorts the profile of GLV and PLV emissions by interrupting metabolism of alcohols to acetate conjugates, and GLV aldehydes to alcohols. Given that ADH enzymes constitute a large family of enzymes that are also known to act on other volatiles (Spiers et al., 1998), this method should not be utilized to measure plant volatiles.

DISCUSSION

Though the order of PLV synthesis had been previously hypothesized (Salch et al., 1995), no experimental evidence had been reported to support it. In order to determine the order of synthesis in the PLV pathway, I exposed intact *A. thaliana* to individual pure, exogenous compounds and measured which volatiles were emitted as a result. Treatment with (2*Z*)-pentenol and 1-penten-3-ol produced nearly all other PLVs and no other exogenous treatment produced these volatiles (Fig. 3), validating their status as the primary PLVs synthesized from 13*S*-HPOT. This supports the hypothesis

that a C18:3 radical is produced, as is the case for other products of LOX-derived hydroperoxides (Mukhtarova et al., 2018), which undergoes a β-scission reaction that yields a pentadienyl radical that isomerizes into both (2*Z*)-pentenol and 1-penten-3-ol (Salch et al., 1995). Additionally, this suggests that PLVs do not result in the induction of PLV biosynthesis, indicating that PLVs emitted after PLV treatment are derivatized and re-emitted exogenous PLVs.

Oxidation of (2*Z*)-pentenol, pentanol, and 1-penten-3-ol into their corresponding aldehyde and ketones is also in alignment with previous hypotheses (Salch et al., 1995). Interestingly, while conversion of (2*E*)-pentenol to (2*E*)-pentenal occurred, the opposite reaction also occurred (Fig 3), suggesting that stoichiometry dictates the observed reaction. This was also true of pentanol and pentanal (Fig. 3). Given the strong correlation between emissions of (2*E*)-pentenal, (2*Z*)-pentenal, and (2*Z*)-pentenol, and the non-correlative emissions of (2*E*)-pentenol with these PLVs in maize (Fig. 4b & 7b) and non-transgenic *A. thaliana* (Fig. 5 & 8b), it is likely that (2*E*)-pentenol is derived from (2*E*)-pentenal that is isomerized from (2*Z*)-pentenal.

Unexpectedly, (2*Z*)-pentenol, (2*E*)-pentenol, 1-penten-3-ol, and 1-penten-3-one may also be respectively reduced to pentanol, 3-pentanol, and 3-pentanone (Fig. 3). This was unexpected, as reduction of carbon-carbon double bonds has not reported in the HPL pathway, indicating a PLV-specific reductase may facilitate this reaction. Additionally, though (2*Z*)-pentenol, (2*E*)-pentenol can be reduced to pentanol, pentanol may also be produced from 13*S*-HPOD substrate. The diminished impact of ZmLOX10 and AtLOX2 mutation, in maize and *A. thaliana* respectively, on PLV and GLV

synthesis from 13*S*-HPOD compared to that of 13*S*-HPOT (Fig. 4 & Fig. 5) supports this hypothesis. Similar to GLVs, (2*E*)-pentenol, (2*Z*)-pentenol, and pentanol appear to be acted on by a CHAT that produces the more chemically stable acetate conjugates, (2*E*)-pentenyl acetate, (2*Z*)-pentenyl acetate, and pentyl acetate, respectively (Fig. 3). Though pentanal and pentyl acetate can be formed from pentanol, this occurs at much lower rates than their alkene counterparts, indicating potential preference of alkenes over alkanes by the relevant ADH and CHAT enzymes. Interestingly, no acetate conjugate of 1-penten-3-ol was detected, indicating that the requisite CHAT(s) require a terminal hydroxyl group in the substrate they utilize.

Importantly, 1-penten-3-ol seems to be quickly oxidized to 1-penten-3-one, which is then readily reduced to 3-pentanone (Fig. 3). 3-pentanol also appears to be able to rapidly reduced to 3-pentanone, as well as converted into the previously undetected 3-methyl-2-pentanone. Similarly, pentanal was converted to pentanoic acid, which was not detected in volatile analysis of any plant tissues after wounding (Fig. 3). This suggests that 3-methyl-2-pentanone and pentanoic acid are either not normally synthesized or are normally synthesized in trace amounts.

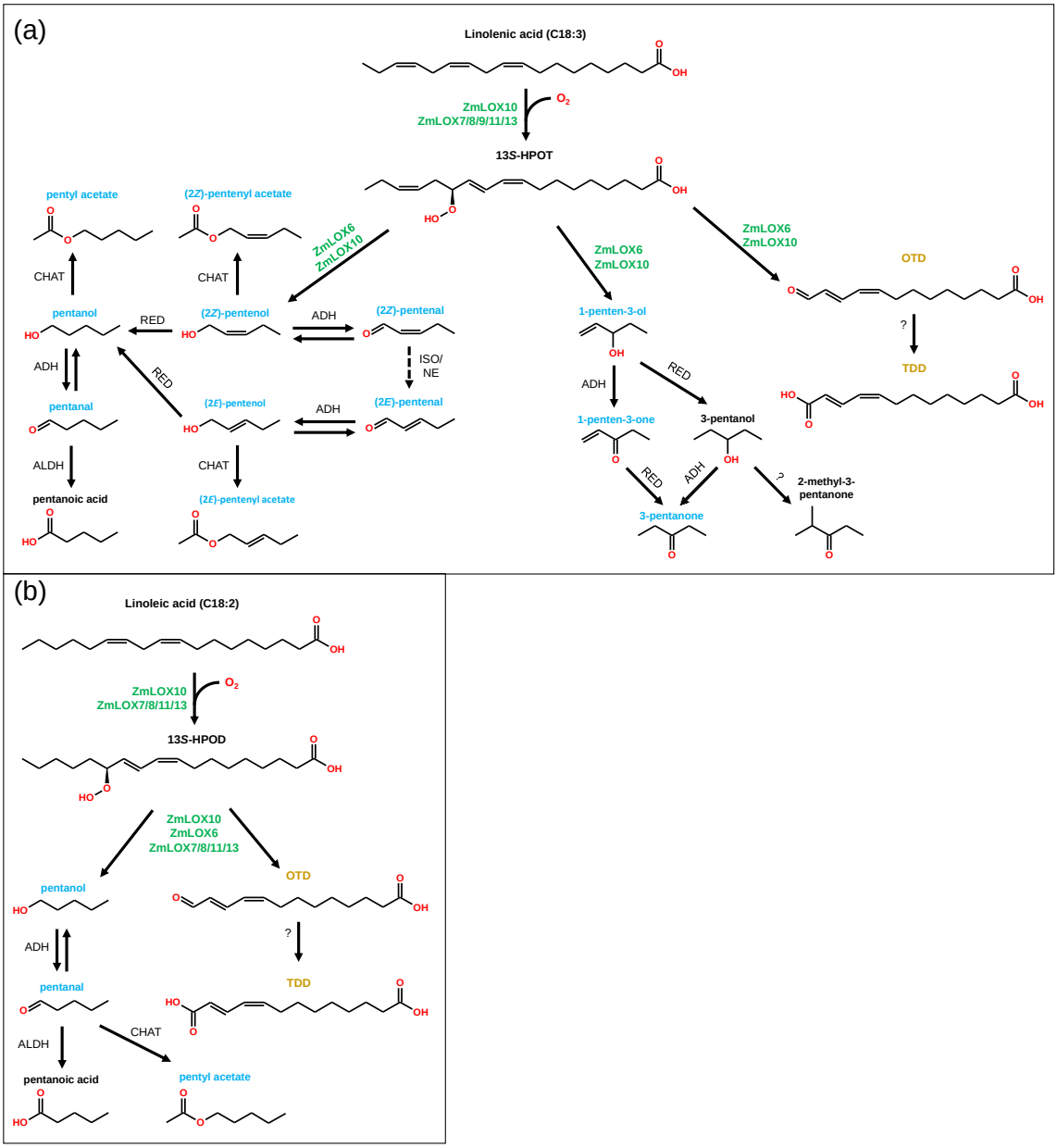

Figure 9 Working model of the PLV pathway in maize. (a) shows C18:3-derived and (b) C18:2-derived PLV pathways. Dashed arrows indicate possible reactions. Alcohol dehydrogenase (ADH), acetyl transferase (CHAT), reductase (RED), non-enzymatic (NE), isomerase (ISO). The names of PLVs are blue, the names of potential artificial or trace PLVs are black, and the names of 13-carbon compounds are orange. Adapted from Gardner et al. (1996).

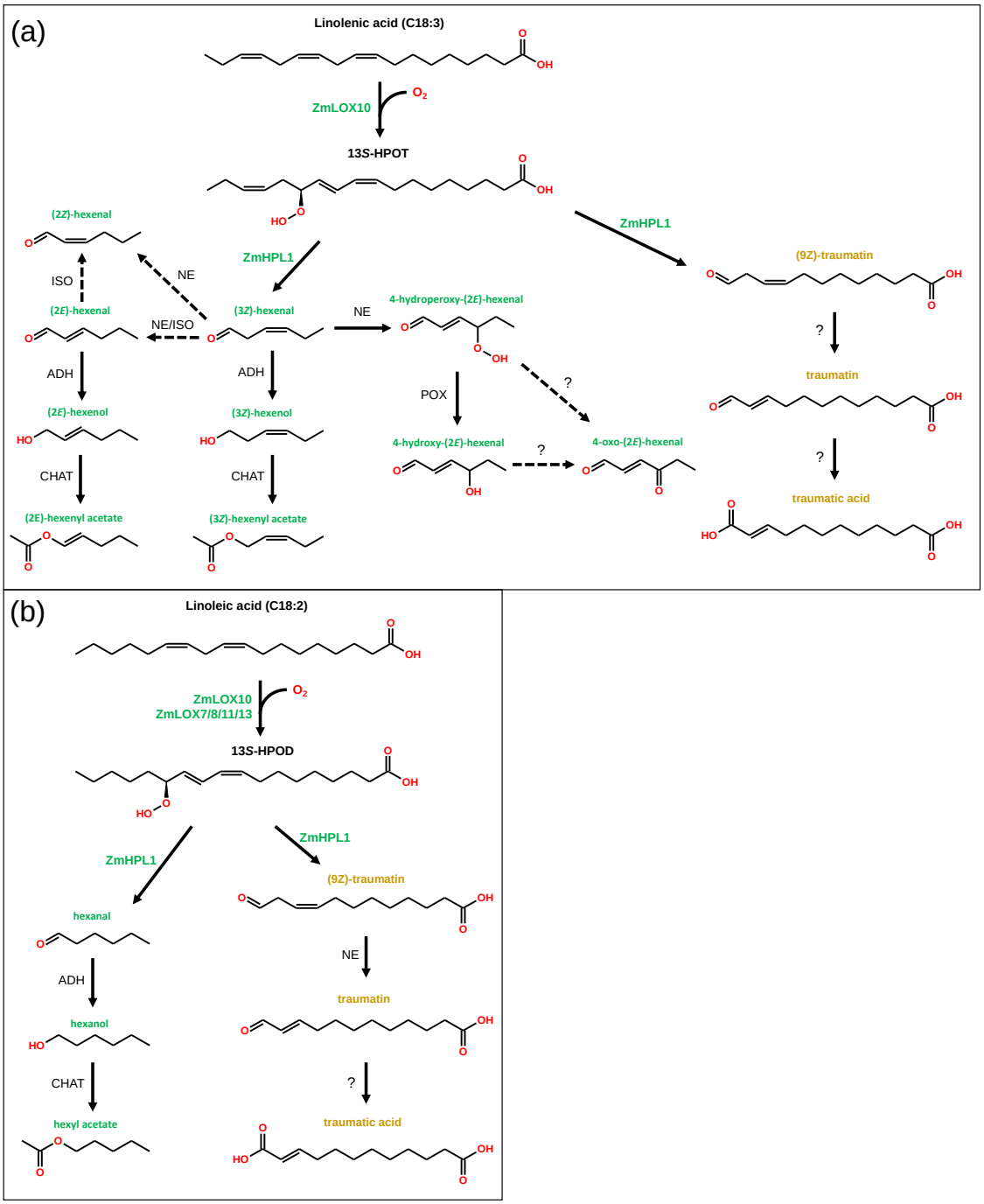

Figure 10 Working model of the HPL pathway in maize. (a) shows C18:3-derived and (b) C18:2-derived PLV pathways. Dashed arrows indicate possible reactions. Alcohol dehydrogenase (ADH), acetyl transferase (CHAT), peroxygenase (POX) non-enzymatic (NE), isomerase (ISO). The names of GLVs are green, the names of traumatins are orange. Adapted from Matsui et al. (2012).

Unlike GLV synthesis, there is scant information regarding PLV synthesis or function, despite the fact these volatiles are reported to be widely emitted in response to various stresses. I wanted to ascertain whether ZmLOX10, in addition to its role as the sole GLV-producing LOX isoform (Christensen et al., 2013), is also a major PLV-producing LOX isoform, as was reported in *A. thaliana* and tomato (Shen et al., 2014; Mochizuki et al., 2016). As these volatiles are reported to be produced in large quantities after wounding (Mochizuki et al., 2016), I wounded *lox10-3* mutants in two diverse genetic inbred backgrounds of maize, B73 and W438, and compared their GLV and PLV profiles. This analysis clearly revealed that ZmLOX10 is a major producer of most PLVs, with the notable exceptions of (2*E*)-pentenol, pentanol and pentanal. Importantly, pentanol and pentanal can also be derived from C18:2. ZmLOX10 also seemed to have only partially lower amounts of hexanal, hexanol, and hexyl acetate, indicating that it provides much less substrate to both the C18:2 GLV and PLV pathways compared to the C18:3 pathways.

As shown by Fischer et al. (2003), several soybean 13-LOXs showed PLV-synthesizing activity *in vitro*, although this activity was variable among different 13-LOXs. The maize LOX isoform, ZmLOX6, has already been noted to possess the ability to produce PLVs *in vitro* (Gao et al., 2008) and *in vivo* in transgenic ZmLOX6-OE lines of *A. thaliana* (Tolley, 2020). Furthermore, ZmLOX6 did not display the ability to oxygenate lipids *in vitro*, which suggests neo-functionalization of ZmLOX6 to specifically produce PLVs, highlighting their potential importance. As it is likely ZmLOX6 cannot produce its own substrate *in vivo*, it likely depends on 13*S*-HPOT

substrate produced by other LOX isoforms. As ZmLOX10 is the most highly expressed 13-LOX isoform, both ZmLOX6 and ZmLOX10 localize to chloroplasts (Tolley et al., 2018; Gorman et al., 2020), and both seem to play a role in PLV synthesis, it is possible they interact to produce PLVs. As a first step towards elucidating the interactions of these two LOX isoforms, I analyzed PLVs emitted in transgenic ZmLOX6-OE lines of *A. thaliana* that also possess a knockout mutation in AtLOX2. AtLOX2 is highly homologous to ZmLOX10 (Borrego and Kolomiets, 2016), and like ZmLOX10 in maize, is the major GLV- and PLV- producing LOX isoform in *A. thaliana* (Mochizuki et al., 2016). Compared to ZmLOX6-OE lines with a function AtLOX2, ZmLOX6-OE *Atlox2-1* transgenic/mutant lines displayed greatly impaired PLV emissions (Fig. 5). However, ZmLOX6-OE *Atlox2-1* transgenic/mutant lines displayed increased PLV emissions compared to *Atlox2-1* mutants, indicating that while ZmLOX6 is largely reliant on AtLOX2 for substrate, it may also utilize a small amount of substrate generated by other LOX isoforms (Fig. 5). Given the high homology and functionality between AtLOX2 and ZmLOX10, these results suggest that in maize, ZmLOX6 depends on ZmLOX10 to provide 13*S*-HPOT substrate, although it remains unclear as to whether ZmLOX10 may also directly cleave 13*S*-HPOT into PLVs.

Volatile analysis of maize (Fig. 4b) and *A. thaliana* (Fig. 5) resulted in the first reported detection of (2*Z*)-pentenyl acetate in plants. Given that PLVs emissions in *A. thaliana* had already been analyzed by Mochizuki et al. (2016), it was odd detection of this PLV was not reportedly detected. One of the major methods that Mochizuki et al. (2016) used to measure volatiles involved the flash freezing tissue and allowing it to

thaw while collecting volatiles. As suggested by Fall et al. (2001), flash-freezing may result in the impairment of ADH enzymes responsible for generation of GLV alcohols. Conversion of GLV aldehydes to alcohols is reportedly catalyzed by ADHs that are dependent on either NADPH (Tanaka et al., 2018) or NADH (Bate et al., 1998, Spiers et al., 1998). Conversely, NAD+ was reported to be necessary for two ADH isoforms of soybean that generate PLV aldehydes from alcohols (Gardner et al., 1996). Owing to the structural similarity of GLVs and PLVs, and the enzymes and co-factors that are responsible for their metabolism, it is likely GLV alcohols and PLV aldehydes are synthesized by the same or similar enzymes in a given species.

Comparisons of freeze-thawing and intact wounding volatile emissions confirmed that GLV alcohols and acetate conjugates were lowly emitted by maize and *A. thaliana* after freeze-thawing, but were highly emitted after wounding treatment (Fig 7a & 8a). This suggests that not just ADH, but also CHAT enzymes are significantly impaired by freeze-thawing. Oppositely, many putatively non-enzymatically generated GLVs such as (2*E*)-hexenal, (2*Z*)-hexenal, 4-hydroxy-(2*E*)-hexenal, and 4-oxo-(2*E*)-hexenal (Matsui et al., 2012) were heavily increased by freeze-thawing, as well as (3*Z*)-hexenal (Fig. 7a & 8a). These results were consistent in both maize genetic inbred backgrounds (Fig. 7a) as well as in Col-0 A. thaliana (Fig. 8a). Increased production of aldehydes derived from (3*Z*)-hexenal is likely the result of increased (3*Z*)-hexenal substrate availability for their synthesis, or because freeze-thawing simply causes more spontaneous reactions to occur. This however, does not explain the significantly elevated levels of (3*Z*)-hexenal. As GLVs are synthesized *de novo* after plants experience a stress

(Fall et al., 1999), these results suggest that plant LOXs and HPLs are still active when plant tissues thaw after freezing. Even though Col-0 is known to possess a mutation in its sole hydroperoxide lyase gene, HPL1 (Duan et al., 2005), it still produces small amounts of GLVs, indicating HPL1 retains some, albeit less, functionality. Similarly, (2*Z*)-pentenyl acetate emission was abolished by freeze-thawing in all genotypes of all species, indicating that a similar CHAT enzyme makes both GLV- and PLV-acetate conjugates (Fig. 7 & 8). While GLV alcohols were greatly diminished by freeze-thawing, PLV aldehydes were increased by freeze-thawing (Fig. 7 & 8). Given that both reactions are performed by ADHs, albeit opposite reactions, this was unexpected. This suggests that these reactions are performed by different ADH isoforms or that their co-factors or other requisite associated co-enzymes are differentially impacted by freezing. Given that ADHs regulate metabolism of many diverse metabolites and volatiles (Spiers et al., 1998), it's clear that freeze-thawing is an inherently flawed method of volatile analysis and that only intact tissue should be used for accurate volatile emission studies, especially those focusing on LOX-derived volatiles.

Though GLVs and PLVs are often co-emitted, they also share clear antagonism. This is evidenced by increases in PLV emission in *hpl* mutants (Vancanneyt et al., 2001; Salas et al., 2006; Shen et al., 2014). Since GLV and PLV synthesis requires substrate from the same LOXs, it is not surprising this is the case. However, as GLVs are known as prominent inducers of JA (Engelberth et al., 2004) and JA is a prominent inducer of LOXs (Melan et al., 1993; Yan et al., 2012). To unravel the relationship between JA and PLVs, I wounded the JA-deficient double mutant, *opr7-5op8-2* and observed GLV and

PLV emissions relative to WT and *lox10-3* mutants. It was clear that *opr7-5op8-2* mutants were significantly hindered in their ability to synthesize PLVs and GLVs, although this difference was not quite as drastic as in *lox10-3* mutants (Fig. 6). This is likely a result of decreased LOX expression, revealing that both GLV and PLV syntheses are partially dependent on JA signaling in maize. These results are also in agreement with analysis of the respective GLV, traumatin and traumatic acid, and PLV, OTD, non-volatile counterparts of wounded *opr7-5op8-2* mutant leaves (He et al., 2020). Furthermore, all GLV and PLV acetate conjugates were relatively more diminished in *opr7-5op8-2* mutants than other types of GLVs or PLVs (Fig. 6). This indicates that CHAT enzymes are a part of the HPL and LOX branches that are especially dependent on JA signaling.

Collectively, these results make it clear that there are differences in PLV synthesis and emission among different plant species, and even genetic inbred backgrounds of maize. It is equally clear that ZmLOX10 is responsible for the synthesis of a significant portion of PLVs in maize, in addition to being the sole-GLV producing LOX (Christensen et al., 2013). This is especially true of PLVs and GLVs that are derived from C18:3, with ZmLOX10 generating relatively little PLVs and GLVs derived from C18:2. However, ZmLOX6-OE lines of *A. thaliana* emit an abundance of PLVs, suggesting ZmLOX6 may also play an important role in maize PLV synthesis (Tolley, 2020) (Fig. 5). Given the dual role of LOXs in the synthesis of PLVs, synthesis of both the hydroperoxide substrate and β-scission cleavage reaction, it is difficult to ascertain whether ZmLOX10 simply provides substrate to other LOXs such as ZmLOX6, or

whether ZmLOX10 may also perform the β-scission cleavage reaction. Given its high homology to AtLOX2, the only LOX isoform involved in PLV synthesis in *A. thaliana*, it is likely that it serves both roles. However, the specific roles of ZmLOX10 and ZmLOX6 regarding PLV synthesis can only be answered by performing protein interaction assays between ZmLOX6 and ZmLOX10, as well as volatile analysis of *lox6* single and *lox6lox10* double mutants of maize. These questions should be addressed in future works looking into maize volatile oxylipin synthesis.

CHAPTER IV

GREEN LEAF VOLATILES AND JASMONIC ACID ENHANCE SUSCEPTIBILITY TO ANTHRACNOSE DISEASES CAUSED BY COLLETOTRICHUM GRAMINICOLA IN MAIZE[*]

INTRODUCTION

Colletotrichum graminicola

Colletotrichum is one of the most widespread and prolific genera of plant pathogenic fungi in the world (Dean et al., 2010). *Colletotrichum graminicola* is an economically relevant representative of this genus that is capable of causing annual billion-dollar losses of yield in the United States alone (Oestreich, 2005). Though *C. graminicola* infects several tissues of maize, its most devastating forms of disease arise from infection of stalks and leaves, which result in anthracnose stalk rot (ASR) and anthracnose leaf blight (ALB). Infection begins with germination of conidia 12 h after contact with the plant surface and is followed by formation of melanized appressoria within 24 h (Vargas et al., 2012). A penetration peg is then formed after 24-36 h, which leads to a phase of biotrophic colonization by primary hyphae (Mims & Vaillancourt, 2002; Vargas et al., 2012). After approximately 48-72 hours the fungus switches to a phase of necrotrophic growth. This is characterized by the formation of thinner

[*] Re-printed with permission from "Green leaf volatiles and jasmonic acid enhance susceptibility to anthracnose diseases caused by Colletotrichum graminicola in maize" by Gorman, Z., Christensen, S.A., Yan, Y., He, Y., Borrego, E. and Kolomiets, M.V., 2020. *Molecular Plant Pathology, 21* (5), pp.702-715, Copyright by John Wiley and Sons.

secondary hyphae that kill cells prior to infection, which results in the formation of necrotic lesions on infected tissues (Bergstrom & Nicholson, 1999; Mims & Vaillancourt, 2002; O'Connell et al., 1985; Vargas et al., 2012; Wharton et al., 2001). Though disease progression of *C. graminicola* is well documented, less is known regarding defenses employed by maize against it. Existing literature implicates salicylic acid (SA), jasmonic acid (JA), and other various metabolites as potential regulators of defense against *C. graminicola*; however, genetic evidence has not yet been provided to validate these hypotheses (Balmer et al., 2013; Miranda et al., 2017; Vargas et al., 2012).

Jasmonic acid

JA and GLVs are well known oxylipins produced in the lipoxygenase (LOX) pathway (Andreou & Fuessner, 2009; Borrego & Kolomiets, 2016; Feussner & Wasternack, 2002). JA biosynthesis in the AOS pathway begins in the chloroplast with the oxygenation of C18:3 by a 13-LOX to form 13*S*-hydroperoxy octadecatrienoic acid (13*S*-HPOT) (Blée, 2002; Howe & Shilmiller, 2002). 13*S*-HPOT is subsequently acted upon by a 13-AOS and then an allene oxide cyclase (AOC) to form (+)-*cis*-12-oxo-phytodienoic acid (12-OPDA), which possesses signaling activity distinct from JA (Dave et al., 2011; Dave & Graham, 2012; Kramell et al., 2000; Ribot et al., 2008; Stintzi et al., 2001; Taki et al., 2005; Vick & Zimmerman, 1983). 12-OPDA is then transported to the peroxisome where it is reduced to OPC-8:0 (8-[3-oxo-2-cis-[(*Z*)-2-pentenylcyclopentyl]octanoic acid) by an oxo-phytodienoate reductase (OPR). Maize possesses two functionally redundant JA-producing OPRs, ZmOPR7 and ZmOPR8 (Yan et al., 2012). OPC-8:0 undergoes three rounds of β-oxidation to form (+)-7-*iso*-JA,

which itself is biologically inactive (Staswick & Tiryaki, 2004). Once synthesized, JA may be converted into a variety of derivatives, including methyl jasmonate (MeJA) and the main biologically active conjugate, (+)-7-*iso*-jasmonyl-isoluecine (JA-Ile) (Caarls et al., 2017; Fonseca et al., 2009; Staswick & Tiryaki, 2004; Vick & Zimmerman, 1983; Wasternack & Strnad, 2018; Yan et al., 2016). JA signaling regulates many diverse physiological processes and is a key regulator of defense response to wounding, herbivory, and pathogen infection via induction of defensive metabolites and proteolytic enzymes (Farmer & Ryan, 1990; Howe & Jander, 2008; Rodriguez-Saona et al., 2001) or emission of volatile organic compounds (VOCs), such as GLVs (Kessler et al., 2001), which recruit insect parasitoids (Allman & Baldwin, 2010; Turlings et al., 1995).

Green leaf volatiles

GLVs are an important class of VOC and are produced in the HPL pathway, functioning in inter- and intra-plant signaling, plant-insect communication, and defense against a litany of environmental stresses. GLVs include C_6 aldehydes, alcohols, and their corresponding esters, and are almost ubiquitously emitted in response to abiotic and biotic stresses. As with JA, GLV biosynthesis begins in chloroplasts with oxygenation of C18:3 by a 13-LOX to produce 13*S*-HPOT (Blée, 2002; Borrego & Kolomiets, 2016; Howe & Schilmiller, 2002). Maize possesses a single LOX isoform, ZmLOX10, that supplies substrate to the HPL pathway for GLV biosynthesis (Christensen et al., 2013). A 13-HPL acts upon ZmLOX10-derived 13*S*-HPOT to form a short-lived hemi-acetal, which quickly breaks into C_6 GLVs and traumatin, a C_{12} compound (Mukhtarova et al., 2018). Exposure to GLVs induces broad spectrum defense to various stresses through

upregulation of a variety of defense-related genes, including genes involved in the biosynthesis and signaling of JA (Bate & Rothstein, 1998; Christensen et al., 2013; Engelberth et al., 2004; Engelberth et al., 2007; Engelberth et al., 2013; Farag et al., 2005; Frost et al., 2008; Hirao et al., 2012; Yamauchi et al., 2015). In addition to altering plant responses, GLVs can also directly inhibit growth of fungal and bacterial pathogens (Hamilton-Kemp et al., 1992; Kishimoto et al., 2006; Major et al., 1960; Nakamura & Hatanaka, 2002; Prost et al., 2005; Shiojiri et al., 2006; Zeringue & McCormick, 1989).

Thus far, the effects of GLVs on plant-pathogen interactions have almost exclusively been studied in the *Arabidopsis-Botrytis cinerea* pathosystem, where GLVs induce resistance (Archbold et al., 1997, Kishimoto et al., 2006; Kishimoto et al., 2008; Shijori et al., 2006). In this pathosystem, defense conferred by GLVs is likely mediated through increased JA-dependent signaling, which typically induces resistance to necrotrophic pathogens (Thomma et al., 1998). JA shares strong antagonism with another important defense phytohormone, salicylic acid (SA), which typically induces resistance to (hemi)-biotrophic pathogens (Glazebrook, 2005). Utilizing the maize GLV-deficient mutant, *lox10*, and the JA-deficient double mutant, *opr7 opr8*, I show that GLVs facilitate susceptibility to *C. graminicola* through JA-dependent suppression of SA shortly after inoculation.

RESULTS

GLV- and JA-deficiency results in increased resistance to ASR

To investigate the roles of GLVs and JA in ASR, I inoculated stalks of *lox10* mutants in two different genetic backgrounds, W438 and B73, with *C. graminicola*. Mutants displayed significantly smaller lesions relative to their respective near-isogenic line (NIL)-wild-types (WT), indicating increased resistance to ASR (Fig. 11a-c). Furthermore, mutants in both genetic backgrounds were equally resistant, indicating ZmLOX10 function in mediating susceptibility is well-conserved across diverse genetic backgrounds (Fig. 11a-c). Since GLVs are one of the major LOX10-derived products and are well-known inducers of JA synthesis (Engelberth et al., 2004), I hypothesized that the increased resistance in *lox10* mutants is due to reduced JA. To test whether JA is a susceptibility factor for ASR, I inoculated stalks of single *opr7-5* and *opr8-2* mutants, *opr7-5 opr8-2* double mutants, and their respective NIL-WTs. Of these genotypes, only the *opr7-5 opr8-2* double mutant is devoid of JA, while *opr7-5* and *opr8-2* single mutants maintain WT levels of JA due to functional redundancy of the ZmOPR7 and ZmOPR8 genes (Yan et al., 2012). Accordingly, only *opr7-5 opr8-2* double mutants displayed increased resistance against ASR, whereas *opr7-5* and *opr8-2* single mutants and their respective NIL-WTs all exhibited equally large lesions (Fig. 11d). Taken together, these results imply that *lox10* and *opr7-5 opr8-2* mutant resistance is due to reduced GLV and JA biosynthesis.

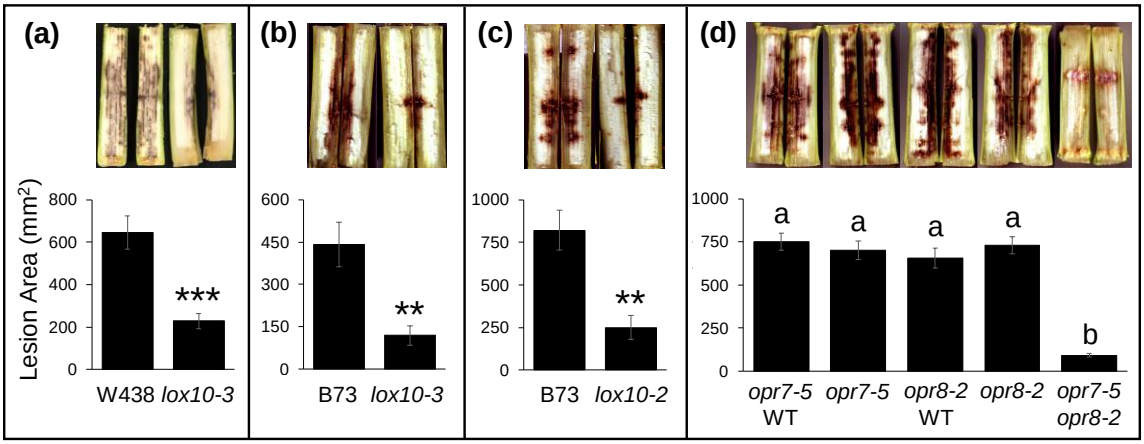

Figure 11 *lox10* and *opr7-5 opr8-2* mutant stalks are more resistant to *C. gramnicola*. (a) shows representative stalks of WT and *lox10-3* mutants in the W438 genetic background 11 dpi. (b) shows *lox10-2* and (c) shows *lox10-3* mutants and their near-isogenic WTs in the B73 genetic background 10 dpi. (d) shows stalks of *opr7-5*, *opr8-2*, and *opr7-5 opr8-2* mutants and their respective WTs in the B73 background 10 dpi. Stalks were split and imaged and lesions were quantified from the digital images. [Mean ± SE, (mm^2)]. For (a,b,c) Student's T-test was used to determine statistical significance [p<.005 = (**), p<.0005 = (***)]. Tukey's HSD test was used to determine statistical significance for (d) where different letters denote statistical difference (p<.05) (n=10).

Increased resistance to ASR correlates with reduced JA and increased SA

To investigate the biochemical mechanisms behind increased resistance of both GLV- and JA-deficient mutants, I used liquid chromatography tandem mass spectrometry (LC-MS/MS) to quantify accumulation of diverse hormones and metabolites, including SA, and the jasmonates, 12-OPDA, JA, and JA-Ile, during ASR progression in *lox10-3* and *opr7-5 opr8-2* mutant stalks. *lox10-3* mutants were significantly impaired in their ability to accumulate 12-OPDA throughout the course of infection, as well as in uninoculated controls (Fig. 12a). Similarly, *opr7-5 opr8-2* mutants accumulated low levels of 12-OPDA at 1 day post inoculation (dpi) (Fig. 12e). Unlike in *lox10-3* mutants however, levels of 12-OPDA in *opr7-5 opr8-2* mutants

recovered to WT levels after 3 dpi, presumably due to increased synthesis of 12-OPDA by ZmLOX10. This suggests that ZmLOX10 is a major producer of 12-OPDA in stalks.

JA and JA-Ile accumulation was also impaired in *lox10-3* mutants, but as in WT stalks, steadily increased throughout the duration of the experiment (Fig. 12b,c). As expected, *opr7-5 opr8-2* mutants are largely devoid of JA and JA-Ile, with the notable exception of 5 dpi, where JA, but not JA-Ile, exceeded levels seen in WT stalks (Fig. 12f,g). This induction of JA was unexpected, as *opr7-5 opr8-2* mutants were thought to be JA-deficient (Yan et al., 2012). However, many fungi are able to directly synthesize JA themselves (Oliw et al., 2019; Tsukada et al., 2010), so I hypothesized that JA detected in *opr7-5 opr8-2* mutants was synthesized and secreted by *C. graminicola* in order to reduce host defenses. To test this hypothesis, I measured jasmonates in *C. graminicola* mycelial mass filtered from liquid culture, as well as the liquid media itself. Much to our surprise, no jasmonates of any kind were detected in either *C. graminicola* biomass or the liquid media in which it was grown (data not shown).

Metabolite analysis revealed that SA is elevated in *lox10-3* and *opr7-5 opr8-2* mutant stalks relative to their respective WTs (Fig. 12d,h). Both mutants display elevated levels of SA at 1 dpi relative to their respective WTs. *opr7-5 opr8-2* mutants were particularly high, which is likely a result of them possessing higher basal SA, a result not observed in *lox10-3* mutants (Fig. 12d,h & Fig. 13). Importantly, the most significant differences of jasmonates and SA between both mutants and their respective WTs occur at the earliest timepoints of infection, which coincide with a phase of biotrophic growth by *C. graminicola* (Fig. 12). Overall, *lox10-3* and *opr7-5 opr8-2*

mutant resistance seems to correlate with increased SA and decreased JA in stalks at early stages of infection.

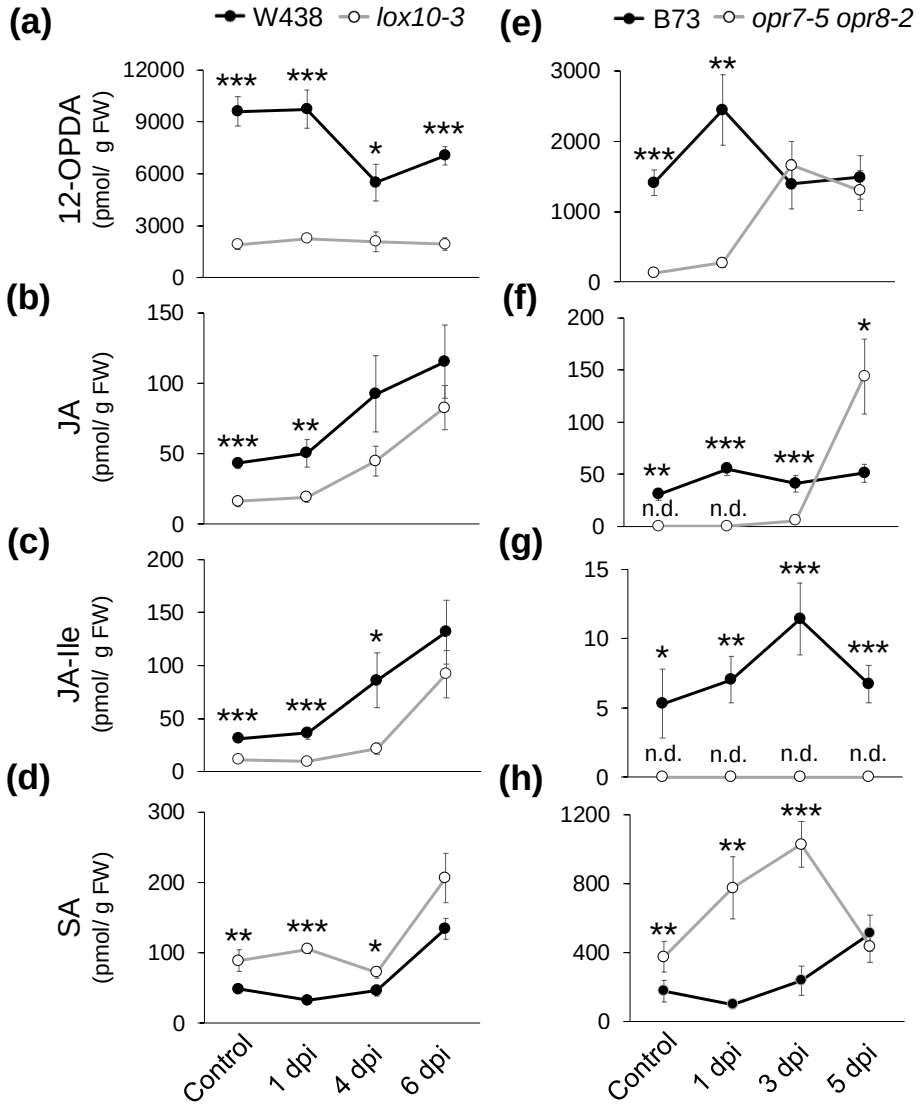

Figure 12 Hormone analysis shows jasmonates are low or absent, and SA is high, in *lox10-3* and *opr7-5 opr8-2* mutant stalks after inoculation. The left column shows 12-OPDA (a), JA (b), JA-Ile (c), and SA (d) levels in WT and *lox10-3* mutant stalks in the W438 background 1, 4, and 6 dpi. The right column shows 12-OPDA (e), JA (f), JA-Ile (g), and SA (h) levels in WT and *opr7-5 opr8-2* mutants stalks in the B73 after infection. (n.d. = not detected). Control = mock-treated 1 dpi. (Mean ± SE, pmol per gram of fresh weight). Student's T-test was used to determine statistical difference between genotypes of each timepoint/treatment [p<.05 = (*), p<.005 = (**), p<.0005 = (***)] (n=5).

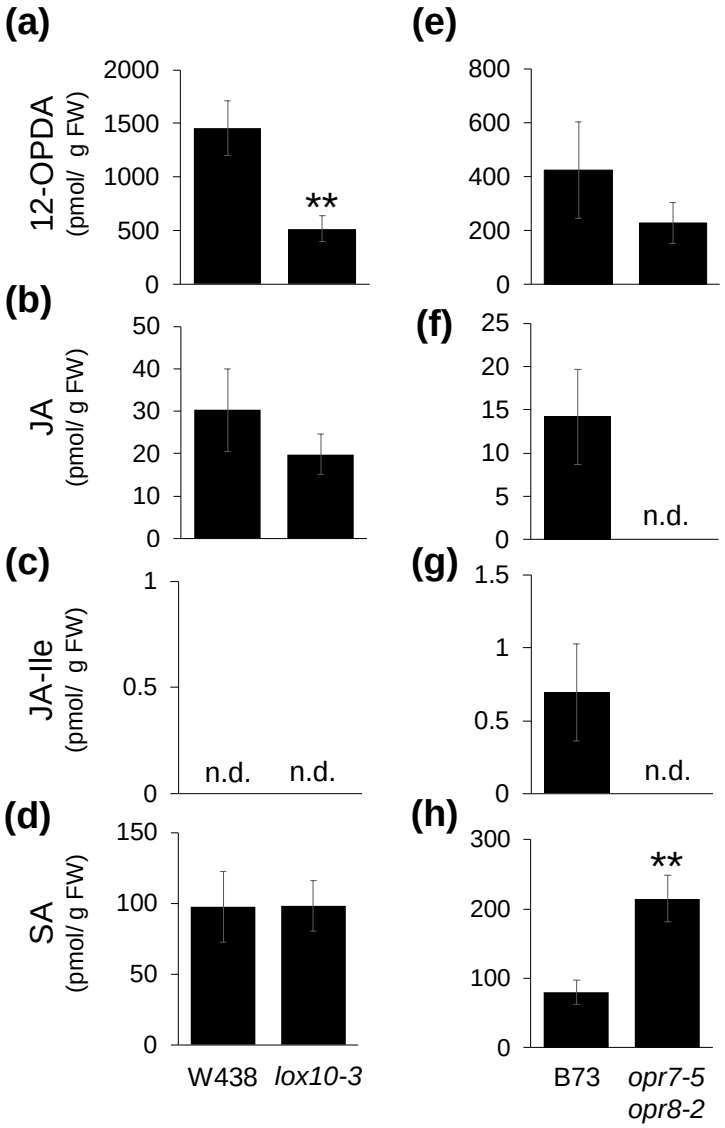

Figure 13 Basal hormone analysis of *lox10-3* and *opr7-5 opr8-2* mutant stalks shows that 12-OPDA is low in *lox10-3* mutants and SA is high in *opr7-5 opr8-2* mutants. The left column of the figure show amounts of 12-OPDA (a), JA (b), JA-Ile (c), and SA (d) levels in untreated WT and *lox10-3* mutant stalks in the W438 background. The right column of the figure shows 12-OPDA (e), JA (f), JA-Ile (g), and SA (h) levels in untreated WT and *opr7-5 opr8-2* mutant stalks in the B73 background. (Mean ± SE, pmol per gram of fresh weight) (n.d. = no detection). Student's T-test was used to determine statistical difference between genotypes [p<.005 = (**)] (n=5).

GLV- and JA-deficiency results in increased resistance to ALB

To test whether GLVs and JA mediate susceptibility to *C. graminicola* in leaves, I drop-inoculated *C. graminicola* spore suspension onto leaves of *lox10-2* and *lox10-3* mutants in the W438 and B73 backgrounds, as well as *opr7-5 opr8-2* mutants in the B73 background. Similar to ASR, ALB assays consistently showed that both *lox10-2* and *lox10-3* mutant leaves in both genetic backgrounds displayed significantly smaller lesions compared with their WT counterparts (Fig. 14). Additionally, *opr7-5 opr8-2* mutant leaves also had significantly smaller lesions compared with WT (Fig. 14c), and in direct side-by-side comparisons were similar to lesions on *lox10-3* mutant leaves. Overall, this confirms that, as with ASR, GLVs and/or other ZmLOX10-derived products and JA promote virulence of *C. graminicola*.

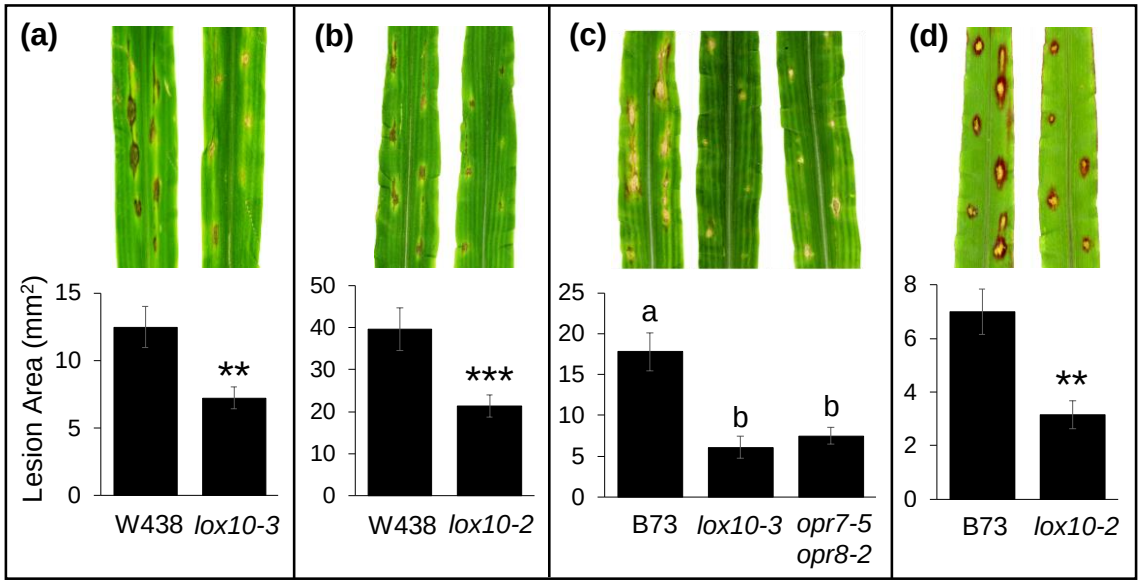

Figure 14 *lox10* and *opr7-5 opr8-2* mutant leaves are resistant to *C. graminicola.* Shows the mean areas of lesion after inoculation of *lox10-2* (b) & (d), *lox10-3* (a) & (b), and *opr7-5 opr8-2* (b) mutants. (a) & (b) show *lox10-2* and *lox10-3* mutants in the W438 background. (c) & (d) shows *lox10-2*, *lox10-3*, and *opr7-5 opr8-2* mutants in the B73 background. Leaves were harvested 5 (a) & (c) or 6 (b) & (d) dpi and scanned to produce digital images from which lesion areas were measured. [Mean ± SE, lesion area (mm^2)]. For (a,b,d), Student's T-test was performed to determine statistical significance of lesion areas [$p<.005$ = (**), $p<.0001$ = (***)]. Tukey's HSD test was performed for (c), where different letters denote statistical significance ($p<.05$) (n=5).

Increased resistance to ALB correlates with reduced JA and increased SA

To determine if the same mechanisms behind ASR resistance of *lox10-3* and *opr7-5 opr8-2* mutant stalks also underlie ALB resistance in leaves, I quantified 12-OPDA, JA, JA-Ile, and SA throughout progression of ALB in leaves of *lox10-3* and *opr7-5 opr8-2* mutants. As in stalks, 12-OPDA and JA levels are low in *lox10-3* mutants throughout the duration of disease progression (Fig. 15a). JA-Ile largely mimicked this same pattern, but after 5 dpi, *lox10-3* mutants accumulated more JA-Ile than WT (Fig. 15c). *opr7-5 opr8-2* mutant leaves, with the exception of 1 dpi, displayed lower amounts of 12-OPDA compared with WT, similar to results obtained for stalks (Fig. 15e). Unsurprisingly, *opr7-5 opr8-2* mutant leaves were devoid of JA or JA-Ile throughout 3 dpi (Fig. 15f,g), but at 5 dpi, both accumulated to levels greater than seen in WT (Fig. 15f,g). This late and robust accumulation of JA in *opr7-5 opr8-2* mutant leaves at 5 dpi mirrors results in stalks, but unlike in stalks of *opr7-5 opr8-2* mutants, also includes a proportionate increase of JA-Ile. Interestingly, this late increase in JA and/or JA-Ile is seen in leaves of both *lox10-3* and *opr7-5 opr8-2* mutants, which characteristically produce low amounts of JA. These results again suggest potential differing roles of JA during biotrophic and necrotrophic phases of growth.

As in stalks, SA is elevated in *lox10-3* mutant leaves throughout the course of infection (Fig. 15d). In *opr7-5 opr8-2* mutant leaves, SA levels were equal to WT throughout infection (Fig. 15h). This was surprising given the high amounts of SA seen in *opr7-5 opr8-2* mutant stalk tissues. However, it is important to note that the levels of SA prior to infection (0 dpi), were strikingly higher relative to WT. Furthermore, the

levels of SA in leaves of *opr7-5 opr8-2* mutant were much higher compared to the amounts detected in their stalks. This suggests that high basal amounts of SA present in *opr7-5 opr8-2* mutant leaves may prevent initial colonization by *C. graminicola*, resulting in limited infection and thus limited defense induction. Conversely, *lox10-3* mutants possess high amounts of SA after infection, but as in stalks, have normal basal levels of SA. This suggests that although the mechanisms behind SA-related defense in *lox10-3* and *opr7-5 opr8-2* mutant leaves and stalks are different, both mutants are resistant due to enhanced amounts of SA. Taken in concert with the relatively low amount of jasmonates present in both mutants, especially at earliest points of infection, this suggests that early ZmLOX10-, ZmOPR7-, and ZmOPR8-dependent accumulation of JA suppresses SA-mediated defense against *C. graminicola*. However, in addition to producing potent JA-inducing GLVs, ZmLOX10 may also provide substrate for synthesis of a variety of other metabolites, including JA (Borrego & Kolomiets, 2016). As such, it was unclear whether ZmLOX10 increases JA through GLV-dependent induction, direct synthesis of JA, both, or other ZmLOX10-derived metabolites.

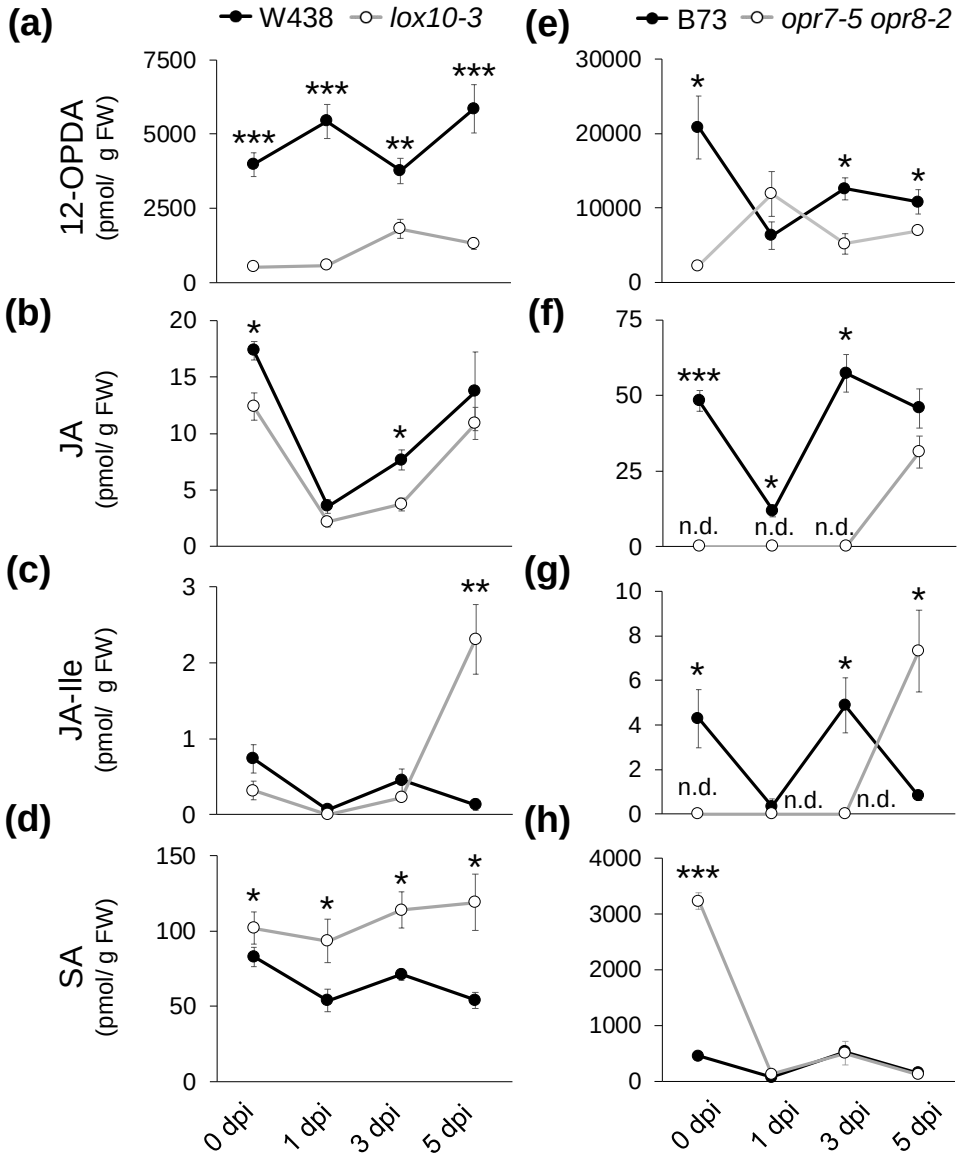

Figure 15 Hormone analysis shows jasmonates are low or absent, and that SA is high, in *lox10-3* and *opr7-5 opr8-2* mutant leaves before or throughout infection. The left column shows 12-OPDA (a), JA (b), JA-Ile (c), and SA (d) levels in WT and *lox10-3* mutants leaves in the W438 background 0, 1, 3, and 5 dpi. The right column shows 12-OPDA (e), JA (f), JA-Ile (g), and SA (h) levels in WT and *opr7-5 opr8-2* mutant leaves in the B73 background 0, 1, 3, and 5 dpi. 0 dpi plants were untreated. (Mean ± SE, pmol per gram of fresh weight). (n.d. = not detected). Student's t-test was used to determine statistical difference between genotypes of each timepoint/treatment [p<.05 = (*), p<.005 = (**), p<.0005 = (***)] (n=6).

LOX10 localizes to chloroplasts, the site of JA and GLV biosynthesis

I first sought to establish whether ZmLOX10 localizes to chloroplasts, the known site of both GLV and JA biosynthesis, as with other GLV-producing LOXs (Bell et al., 1995; Chehab et al., 2006; Mochizuki et al., 2016; Shen et al., 2014). Using maize containing YFP-tagged ZmLOX10 (LOX10-YFP), Christensen et al. (2013) previously reported that ZmLOX10 localized to unknown microbodies but its localization to plastids was uncertain. To further understand ZmLOX10 localization, I performed additional confocal microscopy on LOX10-YFP lines and found ZmLOX10 also localizes to chloroplasts (Fig. 16). ZmLOX10 seems to most prominently accumulate in chloroplasts of bundle sheath cells and guard cells, as well as in chloroplasts of mesophyll cells, albeit to a lesser degree. These results suggest that 13*S*-HPOT produced by ZmLOX10 may potentially feed into the AOS pathway for JA synthesis as well as into the HPL pathway for GLV synthesis.

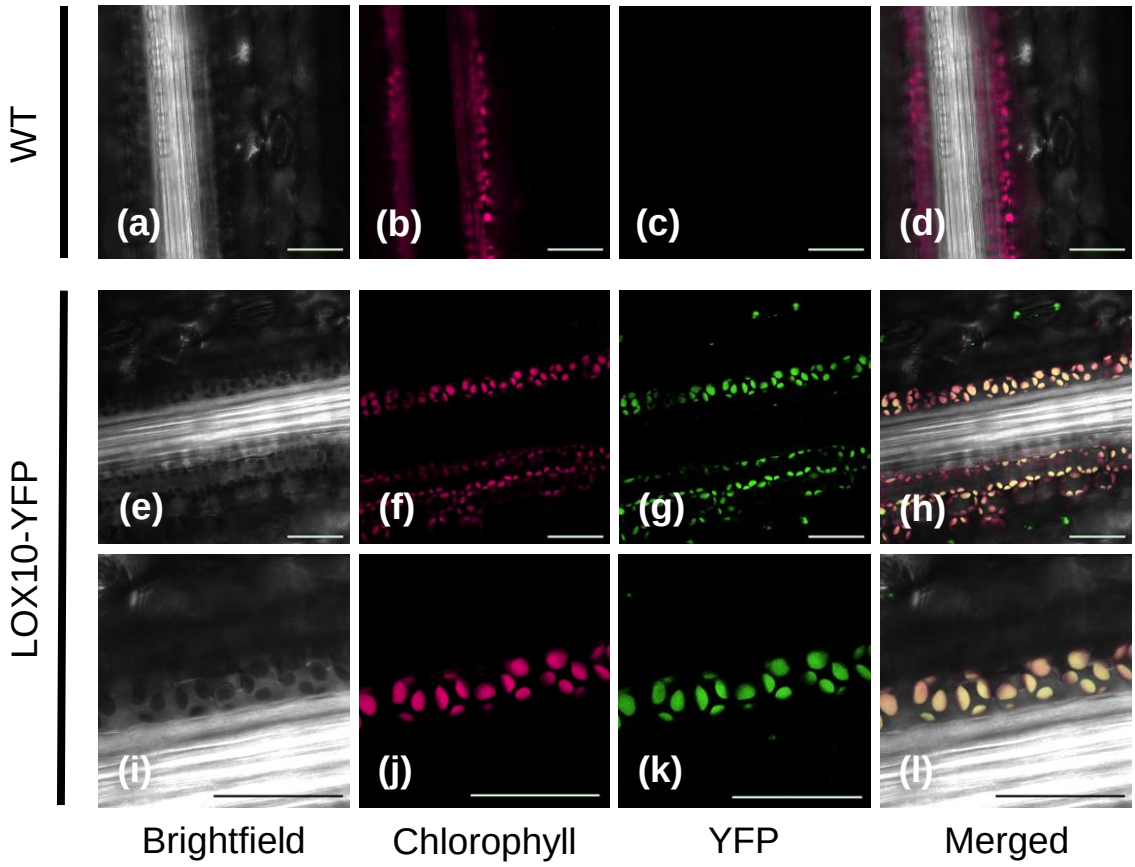

Figure 16 LOX10-YFP tagged maize lines reveal that ZmLOX10 localizes to chloroplasts of bundle sheath cells. (a-d) show images of untransformed leaves of B73 inbred line and (e-l) show images of transgenic lines in the B73 background expressing YFP-tagged LOX10 (LOX10-YFP) under its native promoter, where (e-h) show images comparable to (a-d) and (i-l) show zoomed-in views of (e-h) detailing LOX10 localization to bundle sheath chloroplast (i-l). Columns in order of left to right show brightfield views, chlorophyll autofluorescence, YFP fluorescence, and a merged view. (Scale bars = 50 μm).

GLVs mediate susceptibility to *C. graminicola* through induction of JA

To uncover the mechanism behind LOX10-mediated JA induction, I exposed *lox10-3* and *opr7-5 opr8-2* mutants to exogenous GLV treatment for 1 h prior to inoculation of their leaves. Treatment consisted of a mixture containing 10 nmol of each major GLV molecular species emitted by maize, (*Z*)-3-hexenal, (*Z*)-3-hexenol, and (*Z*)-3-hexenyl acetate. Exposure of *lox10-3* mutants to GLVs resulted in lesion sizes equal to those observed on WT controls, and were significantly larger than those on *lox10-3* mutant controls (Fig. 17a). In contrast, *opr7-5 opr8-2* mutants exposed to GLVs did not display increased susceptibility compared to *opr7-5 opr8-2* mutant controls (Fig. 17b). These results show that small amounts of GLVs can rescue *lox10-3* mutant resistance, but are unable to rescue JA-deficient *opr7-5 opr8-2* mutants (Fig. 17a,b). This supports the hypothesis that GLVs induce JA synthesis in a non-ZmLOX10 dependent manner, which ultimately suppresses SA and leads to susceptibility.

To confirm that rescue of *lox10-3* mutants by GLV exposure is mediated by increased JA, I exposed *lox10-3* mutants to GLVs and quantified 12-OPDA, JA, and JA-Ile. Accumulation of these jasmonates was significantly diminished in *lox10-3* mutant controls compared to WT controls, however, JA and JA-Ile levels in *lox10-3* mutants were restored after GLV exposure (Fig. 17c,d,e). Interestingly, 12-OPDA was not increased by GLV exposure (Fig. 17c). This could be due to GLV induction of genes in the AOS pathway downstream of 12-OPDA synthesis, such as ZmOPR7 and ZmOPR8 (Christensen et al., 2013), and/or ZmLOX10 is the major producer of 12-OPDA. These

results suggest that among many potential ZmLOX10-derived metabolites, GLVs specifically induce susceptibility to *C. graminicola* through induction of JA.

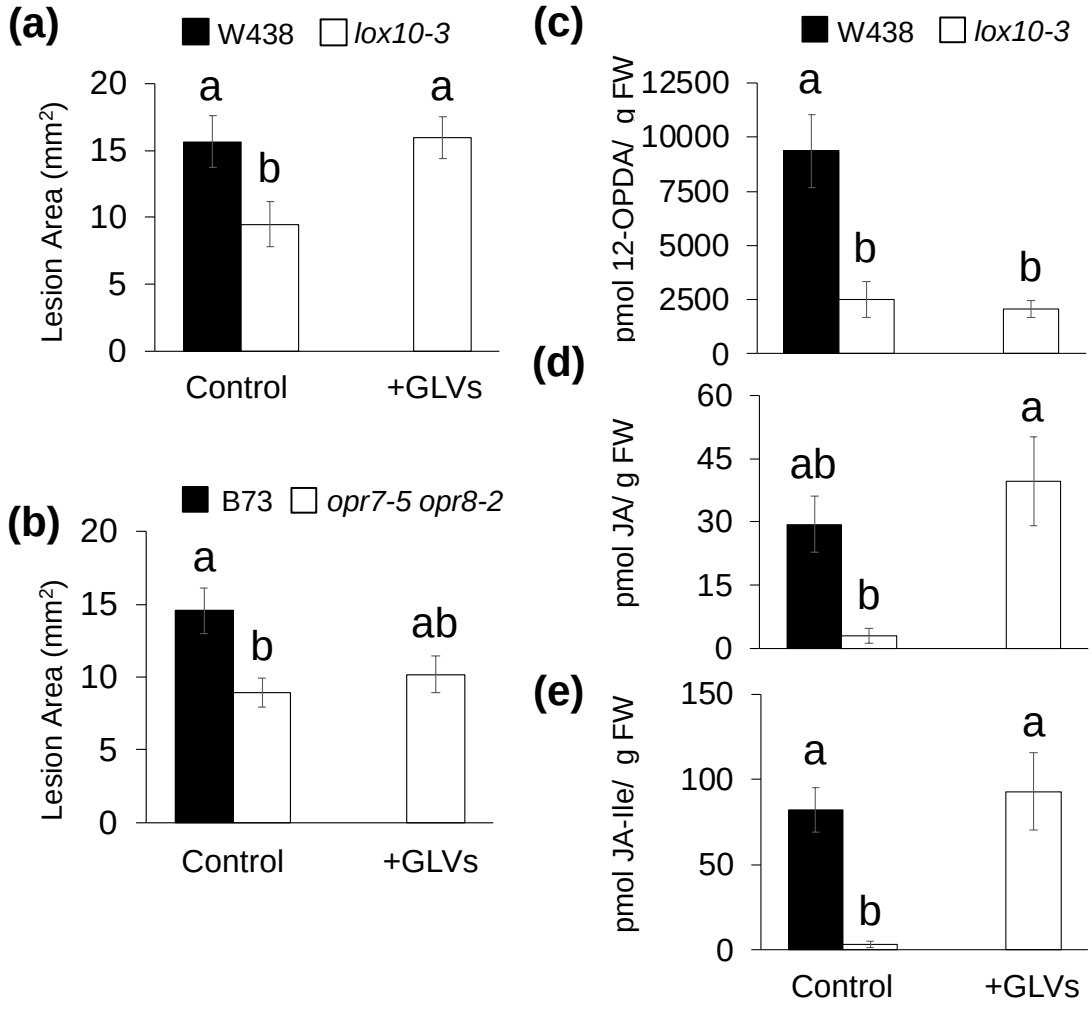

Figure 17 GLV exposure rescues *lox10-3* mutant, but not *opr7-5 opr8-2* mutant, susceptibility by increasing JA and JA-Ile. *lox10-3* and *opr7-5 opr8-2* mutants in the W438 (a) or B73 (b) backgrounds were exposed to either an exogenous GLV mixture or triacetin (control) for 1 h, followed by inoculation with *C. graminicola*. Infected leaves were harvested and scanned 4 dpi to produce digital images from which lesions were measured [Mean ± SE, (mm^2)]. 12-OPDA (c), JA (d), and JA-Ile (e) were measured in *lox10-3* mutants after GLV exposure (Mean ± SE, pmol per gram of fresh weight). Tukey's HSD test was used to determine statistical significance in, where different letters denote statistical significance ($p<.05$) (n=6).

SA induces defense and JA promotes susceptibility to *C. graminicola*

SA is commonly required for resistance to biotrophs or hemi-biotrophs and is implicated in systemic acquired resistance (SAR) to *C. graminicola* in maize (Balmer et al., 2013), but the roles of JA and SA in local infections remain untested. To confirm these respective roles, I exposed WT, *lox10-3*, and *opr7-5 opr8-2* mutants to methyl salicylate (MeSA) or methyl jasmonate (MeJA) prior to infecting their leaves with *C. graminicola*. WT plants in both the W438 and B73 backgrounds exposed to MeSA exhibit significantly smaller lesions compared with their respective controls, and were comparable to *lox10-3* and *opr7-5 opr8-2* mutant controls (Fig. 18a,b). Oppositely, WT plants in the W438 background exposed to MeJA exhibited larger lesions than WT controls (Fig. 18c). This increased susceptibility due to exogenous MeJA was not seen in the B73 background (Fig. 18d). MeSA was unable to further decrease lesion sizes in *lox10-3* or *opr7-5 opr8-2* mutants compared to their respective controls, presumably due to their innate saturation of SA-dependent defenses (Fig. 18a,b). Conversely, exposure to MeJA rescued susceptibility of both *lox10-3* and *opr7-5 opr8-2* mutants. These results conclusively showed that SA induces resistance and JA promotes susceptibility to *C. graminicola*, and confirmed that high SA and low JA early in the infection process are responsible for *lox10-3* and *opr7-5 opr8-2* mutant resistance.

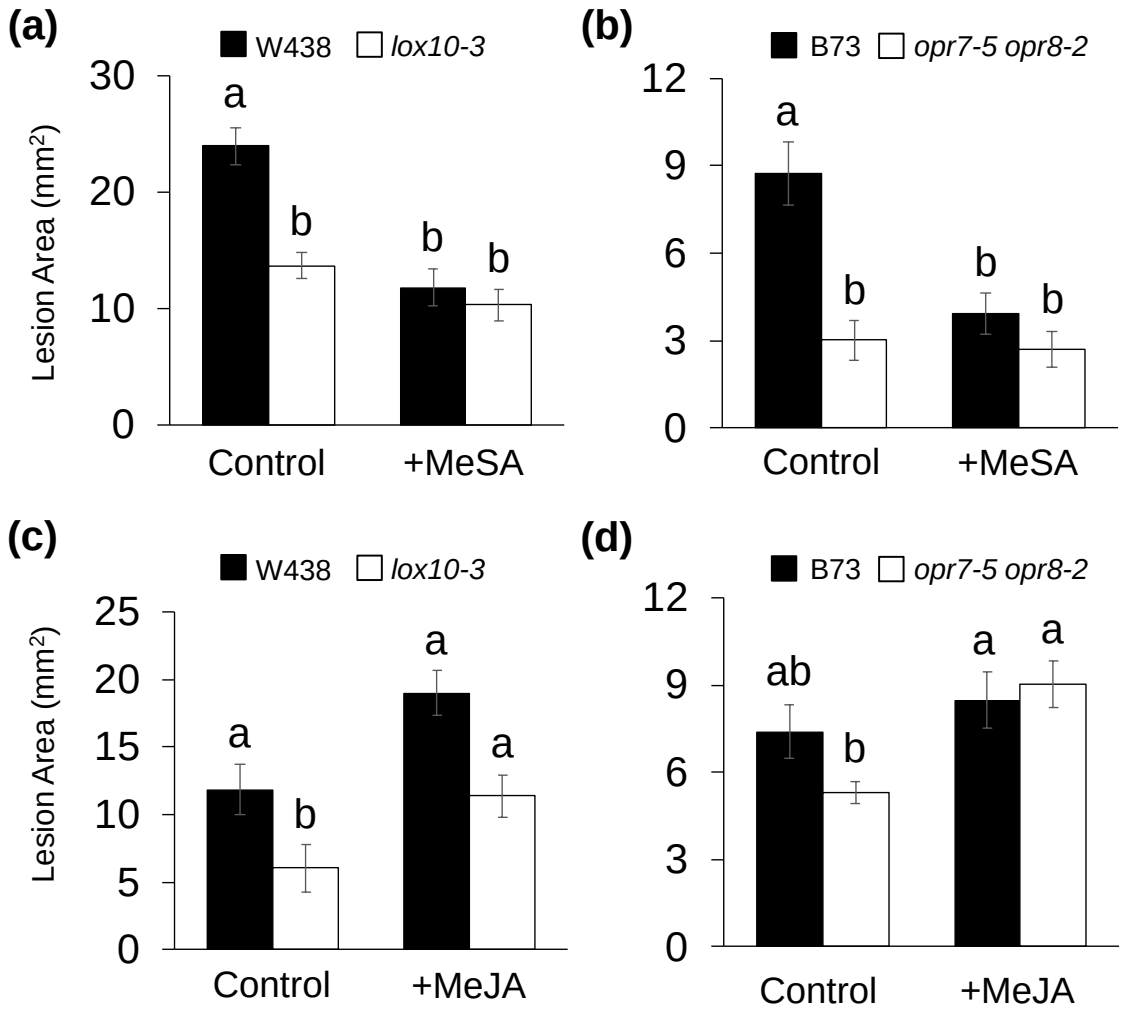

Figure 18 Treatment with MeJA rescues susceptibility in *lox10-3* and *opr7-5 opr8-2* mutants while treatment with MeSA increases resistance in WT. WT and *lox10-3* mutant in the W438 genetic background (a) & (b) and WT and *opr7-5 opr8-2* mutants in the B73 genetic background were exposed to either MeSA (a) & (b), MeJA (c) & (d), or ethanol (control) before inoculation with *C. graminicola*. Treatments consisted of exposing plants to 10 µmol MeSA or MeJA dissolved in ethanol, or ethanol (control) for 2 (a,b) or 6 (c,d) h. Leaves were harvested and scanned 4 dpi to produce digital images from which lesions were measured [Mean ± SE, (mm^2)]. Tukey's HSD test was used to determine statistical significance, where different letters denote statistical significance ($p<.05$) (n=5).

GLVs, but not JA, induce susceptibility after the switch to necrotrophy by *C. graminicola*

As GLVs and JA are known to aid in defense against necrotrophic pathogens, I sought to better clarify the roles of these metabolites after the switch to necrotrophy. To determine this, leaves of both *lox10-3* and *opr7-5 opr8-2* mutants were inoculated and infection was allowed to proceed for 3 days. After 3 dpi and the formation of visible lesions, I exposed the infected plants to either GLVs or MeJA and leaves were harvested after 6 dpi. As with the treatment before inoculation, GLV treatment during necrotrophy was able to rescue WT-levels of susceptibility in *lox10-3* mutants (Fig. 19a). However, MeJA treatment only slightly, but not significantly, enhanced susceptibility of *lox10-3* and *opr7-5 opr8-2* mutants (Fig. 19b,c). This indicates that JA only significantly contributes to disease progression during the earliest points of infection, when *C. graminicola* grows biotrophically, but not during the necrotrophic phase of growth. Furthermore, this indicates that while GLVs rely on JA induction for susceptibility during biotrophic growth, these molecules contribute to susceptibility through unknown, JA-independent mechanisms during necrotrophic growth.

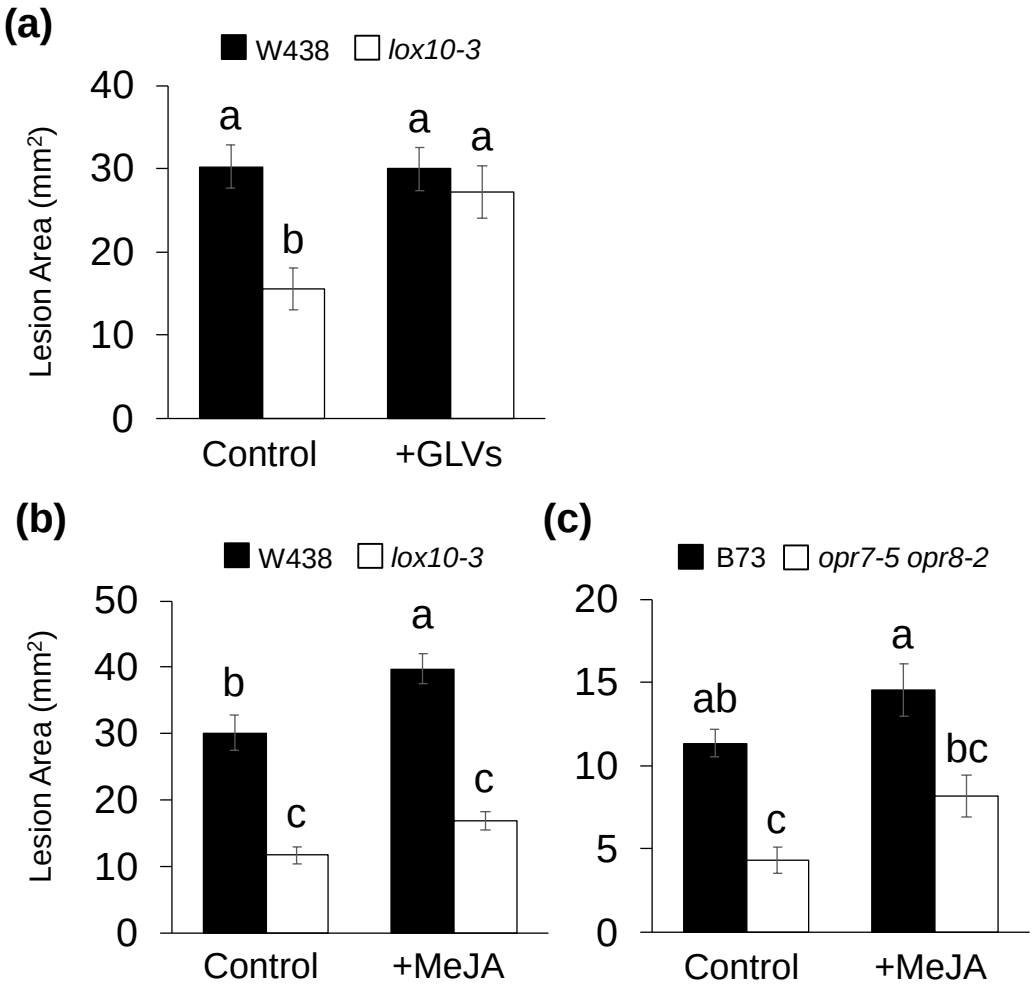

Figure 19 GLV treatment during necrotrophy rescues susceptibility in *lox10-3* mutants, but MeJA treatment does not. *lox10-3* and *opr7-5 opr8-2* mutants were inoculated with *C. graminicola* and infection was left to proceed for 3 days before they were exposed to GLVs (a), MeJA (b,c), and their respective control treatments (triacetin and ethanol, respectively). Leaves were harvested and scanned 6 dpi to produce digital images from which lesions were measured [Mean ± SE, (mm^2)]. Tukey's HSD test was used to determine statistical significance, where different letters denote statistical significance.

DISCUSSION

Inoculation of stalks and leaves of GLV-deficient *lox10* mutants and JA-deficient *opr7-5 opr8-2* mutants clearly revealed that ZmLOX10 and JA are susceptibility factors

during *C. graminicola* infection (Fig. 11 & Fig. 14). Importantly, resistance was observed in *lox10-2* and *lox10-3* mutants in both the B73 and W438 genetic backgrounds, indicating ZmLOX10-mediated susceptibility is conserved across diverse genetic backgrounds in leaves and stalks. As ZmLOX10, ZmOPR7, and ZmOPR8 are involved in the synthesis and/or induction of JA, it was not surprising that *lox10-3* and *opr7-5 opr8-2* mutant stalks and leaves displayed impaired accumulation of several jasmonates during the early stages of infection. However, I was surprised to find that *lox10-3* mutant leaves and *opr7-5 opr8-2* mutant leaves and stalks experienced increased amounts of JA at later stages of infection, 5-6 dpi, after the switch to necrotrophy (Fig. 13 & Fig. 16). Interestingly, *opr7-5 opr8-2* mutant leaves, but not stalks, also accumulated JA-Ile at this time, which could be due to differences in JAR expression between the two tissue types. I hypothesized this JA was directly synthesized and secreted by *C. graminicola*, but no jasmonates of any kind were detected in analysis of either *C. graminicola* or its growth media (data not shown). Despite this result, I cannot rule out that *C. graminicola* is directly producing this JA, as it may require physical or chemical cues and/or access to plant substrate from the plant surface to initiate JA biosynthesis. Alternatively, it is possible this JA was synthesized by the plant through a non-ZmOPR7/OPR8 dependent pathway, as has been reported for *opr3* mutants in *Arabidopsis* (Chini et al., 2018). Despite its unknown origins, this late JA increase reveals a possible shift in the role of JA upon the switch from biotrophy to necrotrophy. Ultimately however, *lox10-3* and *opr7-5 opr8-2* mutant leaves and stalks possess low

amounts of jasmonates during the early stages of infection, which are likely the most critical for establishing effective SA-mediated defense.

In contrast to JA, *lox10-3* and *opr7-5 opr8-2* mutants had higher amounts of SA in both stalks (Fig. 13d,h) and leaves (Fig. 13d,h). *lox10-3* mutant stalks and leaves had similar levels of SA compared with WT prior to infection (Fig. 13d, Fig. 15d), but had significantly higher amounts as soon as 1 dpi (Fig. 12d, Fig. 15d). Unlike *lox10-3* mutants, stalks and leaves of *opr7-5 opr8-2* mutants have high basal amounts of SA compared to WT (Fig. 13h). As early as 1 dpi, stalks of *opr7-5 opr8-2* experience even greater accumulation of SA relative to WT (Fig. 12h), however the amount of SA in leaves of *opr7-5 opr8-2* mutants returns to WT levels after 1 dpi (Fig. 15h). This is likely because of the incredibly high amounts of SA present in *opr7-5 opr8-2* mutant leaves, which are significantly higher than in stalks. This high basal amount may effectively prevent infection, thus resulting in diminished defense hormone induction. It should be noted that all leaves, but not stalks, of all genotypes experience a decrease in most metabolites and hormones 1 dpi. This is attributed to the inoculation method for leaves, which involved a 24 h incubation in a humidity chamber with comparatively limited air flow and available light for photosynthesis. The relatively high amounts of SA present in both *lox10-3* and *opr7-5 opr8-2* mutants before or soon after infection (1 dpi) directly coincide with appressoria formation and initiation of biotrophic growth by *C. graminicola* (Vargas et al., 2012). Reactive oxygen species (ROS) are rapidly produced by plants upon infection via SA signaling and are involved in fungal defense and growth inhibition, including *C. graminicola* (Albarouki & Deising, 2013; Apostol et

al., 1987; Mellersh et al., 2002). It is possible that the quick induction of SA-related defenses inhibits catalase-mediated degradation of H_2O_2, allowing buildup of H_2O_2 around points of appressorial penetration, which stops penetration and/or growth of *C. graminicola*.

The mechanism behind low concentrations of JA was clear in *opr7-5 opr8-2* mutants, but less so in *lox10-3* mutants as GLV-producing LOXs are also usually the major JA-producing LOXs. In maize, there are several LOXs that may directly contribute to JA synthesis, such as ZmLOX8, a known producer of JA in response to wounding (Acosta et al., 2009; Christensen et al., 2013). As such, there was uncertainty as to whether ZmLOX10 increases JA upon inoculation through direct synthesis, through GLV-mediated signaling, both, or perhaps through other ZmLOX10-derived metabolites. Previous microscopy of LOX10-YFP in maize did not show ZmLOX10 localization to plastids, despite it containing a predicted plastid localization signal and LOX10 protein being previously isolated from chloroplasts (Christensen, et al., 2013; Majeran et al., 2005). As such, I first wanted to confirm if ZmLOX10 localizes to chloroplasts, the initial site of both GLV and JA synthesis. These new results clearly detail ZmLOX10 localization to chloroplasts of bundle sheath, mesophyll, and guard cells, indicating potential for JA biosynthesis (Fig. 16). These findings agree with analysis of ZmLOX10 by ChloroP software, which predicts the presence of a 58 amino acid chloroplast transit peptide (Nemchenko et al., 2006), and with prior proteome analysis revealing LOX10 is abundant in both mesophyll and bundle sheath plastids (Majeran et al., 2005).

To uncover the mechanism behind ZmLOX10-mediated increase of JA upon infection, I exposed *lox10-3* and *opr7-5 opr8-2* mutants to GLVs prior to infection. The GLV mixture contained (3*Z*)-hexenal, (3*Z*)-hexenol, and (3*Z*)-hexenyl acetate because these GLVs were specifically emitted by maize in response to *C. graminicola* infection (Constantino, 2017). GLV exposure of *lox10-3* and *opr7-5 opr8-2* mutants resulted in a full rescue of susceptibility in *lox10-3* mutants, but not *opr7-5 opr8-2* mutants (Fig. 17a,b). Furthermore, GLV exposure restored JA and JA-Ile in *lox10-3* mutants (Fig. 17c). This result agreed with previous analysis of JA in *lox10-2* mutants after GLV exposure (Christensen et al., 2013). This demonstrated that GLVs alone can induce susceptibility to *C. graminicola* and that GLV-mediated susceptibility, at least during biotrophy, requires intact JA signaling. Furthermore, this showed that biologically relevant amounts of GLVs increase JA and susceptibility independent of direct LOX10 JA synthesis. Remarkably, 12-OPDA levels were not rescued in *lox10-3* mutants exposed to GLVs, suggesting that LOX10 is the major producer of 12-OPDA. This also indicates that GLV-mediated JA induction is achieved by activation of steps in the AOS pathway following AOC-mediated synthesis of 12-OPDA, implicating ZmOPR7 and ZmOPR8 as potential specific targets of GLVs for JA induction (Christensen et al., 2013).

Exposure of *lox10-3* and *opr7-5 opr8-2* mutants to MeJA restored WT levels of susceptibility in both mutants (Fig. 18c,d), agreeing with the low levels of jasmonates detected in both mutants at early stages of infection. Conversely, MeSA exposure was unable to induce further resistance in either mutant, which is likely due to their already

saturated SA-dependent defense signaling before or upon infection. Furthermore, MeSA was also able to induce resistance in WT on par with either mutant and MeJA was able to induce further susceptibility of WT only in the W438 background, which could be due to underlying differences in the two backgrounds (Fig. 18). These data provide strong genetic and chemical evidence that JA is a susceptibility factor, and that SA provides resistance, to *C. graminicola*.

However, as both *lox10-3* and *opr7-5 opr8-2* mutant leaves displayed low initial amounts of JA, followed by high amounts after 5 dpi, I sought to determine if the role of JA and GLVs changed after the shift from biotrophic growth to necrotrophic growth of *C. graminicola*. Exposure of *lox10-3* and *opr7-5 opr8-2* mutants to MeJA after 3 days of infection, after the switch to necrotrophy, was not able to rescue susceptibility as with the treatment before inoculation (Fig. 19b,c). This indicates that while JA initially acts as a susceptibility factor, its contribution to susceptibility becomes negligible after the fungus switches to a necrotrophic phase of growth. In contrast to JA, GLVs were still able to restore susceptibility in *lox10-3* mutants after the switch to necrotrophy (Fig. 19a). This shows that during necrotrophy, GLVs rely on other mechanisms than JA after the switch to necrotrophy. These mechanisms remain unknown and should be the subject of future studies. Furthermore, this shows that GLVs contribute to susceptibility in both phases of growth. This result contrasts with the previous study by Ameye et al. (2015), in which GLV treatment after the switch to necrotrophy by another hemi-biotroph, *Fusarium graminearum*, in wheat induced resistance. The role GLVs play in plant-pathogen interactions may largely depend on the lifestyle of the pathogen, however I do

not discount the possibility that the effect of GLVs on plant-pathogen defense is pathosystem-specific.

Little is known regarding maize defense mechanisms against *C. graminicola*. JA, SA, and other metabolites were suggested to be important for defense, but these hypotheses were not investigated with the use of knockout mutants or exogenous chemical treatment. Using JA- and GLV-deficient mutants, I have definitively shown that JA, and GLVs by virtue of JA induction, cause maize susceptibility to *C. graminicola* in the biotrophic phase of growth. Much of this susceptibility can be attributed to JA-mediated antagonism of SA-related defenses at this time, although there could be additional SA-independent effects of JA or GLVs responsible as well. This is particularly true of GLV-mediated susceptibility during necrotrophy. This suggests that ZmLOX10, ZmOPR7, ZmOPR8, and other genes involved in synthesis or induction of GLVs and JA, are potential targets for induction by *C. graminicola* shortly after colonization. It is important to note that herbivory and mechanical damage are strong inducers of GLVs and JA in maize (Christensen et al., 2013) and that ASR frequency in field settings show a direct correlation with herbivory by European corn borer (ECB) (*Ostrinia nubilalis*) (Bergstrom and Nicholson, 1999; Keller et al., 1986; Venard and Vaillancourt, 2007). This is in part because ECB can vector *C. graminicola* and allow it to bypass the tough rind of the stalk. However, this work reveals a critical biochemical mechanism behind this correlation may also be the suppression of SA-mediated defenses by GLV and JA induction upon herbivory (Bergstrom and Nicholson, 1999; Venard and Vaillancourt, 2007). This study also expands upon the known functions of GLVs in

plant-pathogen interactions, adding to a small number of publications that show GLVs can induce susceptibility to (hemi)-biotrophs (Ameye et al., 2015; Scala et al., 2013; Tong et al., 2012).

CHAPTER V

DARK-INDUCED GLV EMISSIONS TRIGGER JASMONIC ACID BIOSYNTHESIS AND ESTABLISH PRIMING AGAINST FALL ARMYWORM, AND FACILITATE STOMATE CLOSURE

INTRODUCTION

Plants are complex organisms that are required to withstand numerous biotic and abiotic stresses. Oxylipins have recently emerged as a group of structurally and functionally diverse signals that regulate responses to many of these stresses, as well as a variety of developmental processes. Lipoxygenases (LOXs) are the best-known group of enzymes that produce these oxylipins. LOXs are largely divided into two classes depending on the respective carbon position they dioxygenate, 9-LOX or 13-LOX, producing 9- or 13-hydroperoxides, respectively, primarily utilizing linoleic (C18:2) and linolenic acid (C18:3) as substrates. These hydroperoxides serve as substrates for seven different branches of the LOX pathway including the hydroperoxide lyase (HPL) and allene oxide synthase (AOS) branches (Feussner & Wasternack, 2002). Collectively, these branches produce a vast array of diverse oxylipins (He et al., 2020).

Though most LOX branches are largely understudied, the HPL and AOS branches have been well-characterized. The HPL branch produces C_6 green leaf volatiles (GLV) and the C_{12} oxo-acids, traumatins. In maize, ZmLOX10 is the only LOX isoform known to provide substrate to ZmHPL1 for GLV synthesis (Christensen et al., 2013). GLVs are an important class of volatile organic compounds (VOCs) that are emitted in

response to various stresses, including mechanical damage (Fall, 1999; Arimura, 2000, 2005; Halitschke, 2004), herbivory (Turlings et al., 1995; Farag & Pare, 2002; Allman & Baldwin, 2010), pathogen infection (Croft et al., 1993; Shiojiri et al., 2006; Frost et al., 2008; Piesik et al., 2011; Ponzio et al., 2013), drought (Wenda-Piesik et al., 2011; Savchenko et al., 2014), photosynthesis (Savchenko et al., 2017), and heat and cold stress (Copolovici et al., 2012).

Though not an obvious stress, GLVs are also emitted in large amounts after light-to-dark transitions by diverse plant species (Brilli et al., 2011; Jardine et al., 2012) including sorghum and maize (Chamberlain et al., 2006). Furthermore, dark-induced GLV emissions were found to occur in plants grown in conditions that include sharp (Fall et al., 1999; Graus et al., 2004; Brilli et al., 2011; Jardine et al., 2012) and somewhat more gradual light-to-dark transitions (Chamberlain et al., 2006). After wounding or transition from light-to-dark, GLVs are rapidly emitted, about 30 seconds to 15 minutes after light-to-dark transitions, though the composition of the volatile blend experiences temporal shifts throughout this time (Fall et al., 1999; Graus et al., 2004; Brilli et al., 2011; Jardine et al., 2012). Importantly, dark-induced GLV emission depends on the *de novo* synthesis of GLVs by LOXs and HPLs (Fall et al., 1999). Though the emission of GLVs upon light-to-dark transitions is well-documented, the mechanisms and implications of this phenomenon have yet to be investigated.

GLVs likely evolved as systemic volatile plant signals, however other plants have evolved to “eavesdrop” on these signals in order to establish defensive priming in anticipation of external stressors (Engelberth et al., 2004; Baldwin et al., 2006; Turlings

and Erb, 2018). Insects have also evolved the ability to perceive and interpret plant volatile cues, and use this information to locate host plants, evaluate their health status, and to find prey (Kessler and Baldwin, 2001; Allman and Baldwin, 2010; Franco et al., 2017; Turlings and Erb, 2018; Rojas et al., 2018; Grunseich et al., 2020). Though insects are adept at perceiving GLVs and locating host plants (Gouinguené et al., 2005), GLVs also prime plant defenses against a variety of stresses, including insect herbivory (Baldwin et al., 2006; Engelberth et al., 2007; Ton et al., 2007; Timilsena et al., 2019). One of the best-known mechanisms of GLV-induced priming is the induction of jasmonic acid (JA) biosynthesis (Engelberth et al., 2004; Engelberth et al., 2007; Christensen et al., 2013; Gorman et al., 2020).

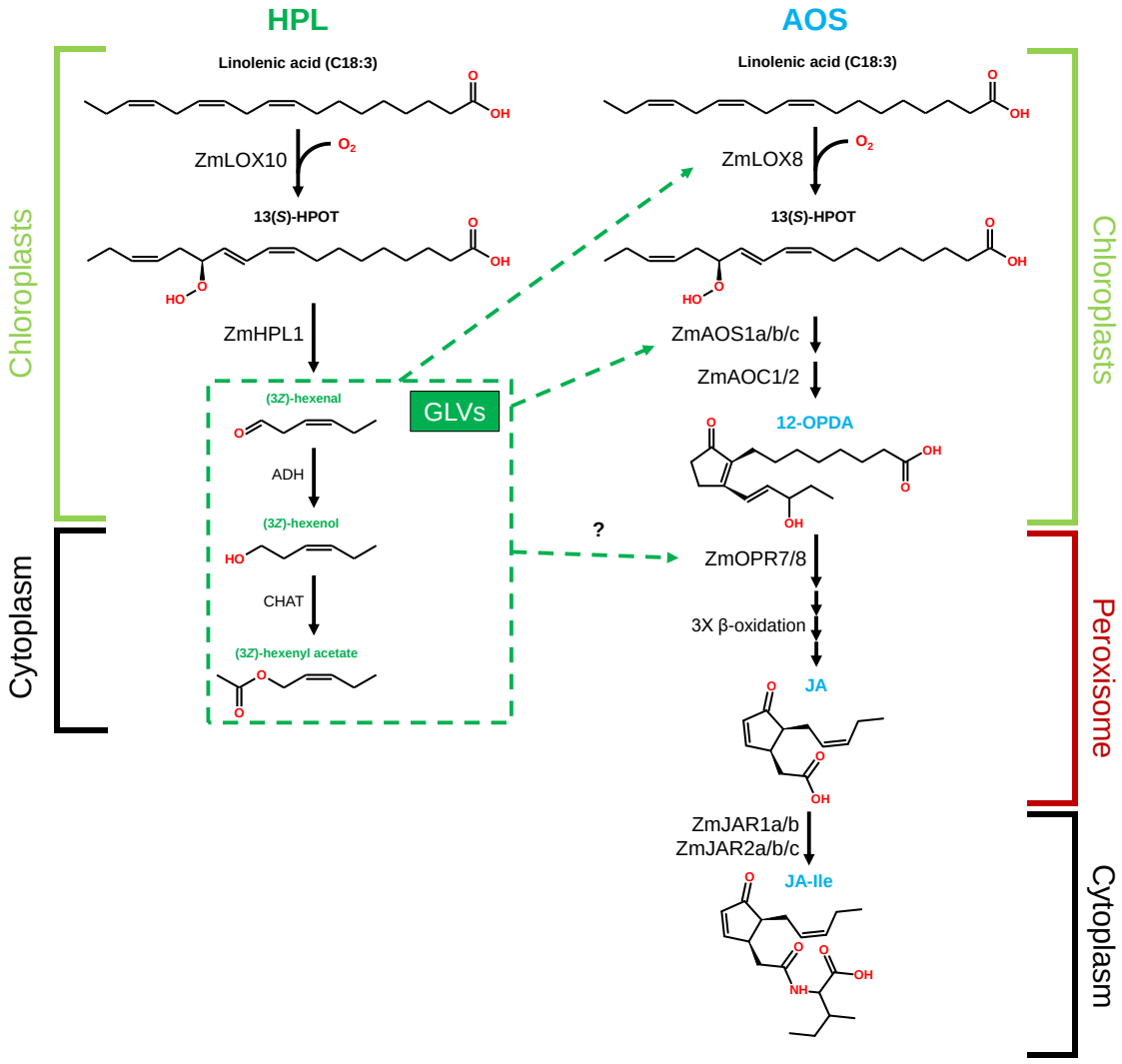

Figure 20 Working model of GLV and JA interactions in maize. Dashed arrows indicate signaling. Hydroperoxide lyase (HPL); allene oxide synthase (AOS); green leaf volatiles (GLVs); 12-oxo-phydienoic acid (12-OPDA); jasmonic acid (JA); jasmonic acid isoleucine (JA-Ile); alcohol dehydrogenase (ADH); cis-3-hexenol acetyl transferase (CHAT). Green names denote HPL-derived metabolites, blue names denote AOS-derived metabolites. Adapted from Acosta et al. (2009), Matsui et al. (2012), Borrego & Kolomiets (2016).

While JA and its downstream biologically active derivative, jasmonyl-isoleucine (JA-Ile), are increased by GLV exposure, its precursor, 12-oxo-phytodienoic acid (12-OPDA), is not (Engelberth et al., 2004; Engelberth et al., 2007; Gorman et al., 2020). 12-

OPDA displays signaling activity that is partly independent of JA signaling, and represents a separate and distinct signaling molecule (Dave and Graham, 2012; Maynard et al., 2018; Wang et al., 2020a; Wang et al., 2020b; Gorman et al., 2020). JA regulates many plant physiological processes, including defense against insect herbivory. JA governs insect defense by regulating trichome development (Li et al., 2004), priming synthesis of GLVs and other VOCs that participate in direct and indirect insect defenses (Rodriguez-Saona et al., 2001; He et al., 2020), induce proteinase inhibitor synthesis (Felton et al., 1994; Chen et al., 2007), and induce expression of many other defense-related genes (Howe & Jander, 2008). Collectively, JA is a critical hormone for defense against insect herbivory.

Spodoptera frugiperda, commonly known as fall armyworm (FAW), is a major pest in the Americas, Africa and Eastern Asia (Huang et al., 2014; Day et al., 2017). FAWs cause significant damage throughout their larval stages by defoliating of plant tissue, and damaging stalks and ears of maize, which leads significant yield and economic loss in countries around the world (Sparks, 1979, Sena et al., 2003; Day et al., 2017). Lines of maize that possess higher levels of JA display increased resistance compared to lines possessing lower levels of JA (Analka et al., 2009; Shivaji et al., 2010). GLV-deficient *lox10* mutants of maize are also deficient in OPDA and JA upon wounding (He et al., 2020), and display increased susceptibility to both *Spodoptera exigua* (Christensen et al., 2013) and FAW (Rojas et al., 2018), implicating GLVs as critical components of plant defense against insects. Given the prominent role of GLVs

in maize defense against insect herbivores, this study investigates the impact of light-to-dark released GLVs on maize defense against FAW.

Synthesis of GLVs (Joo et al., 2018), JA (Goodspeed et al., 2012; Shin et al., 2012), and many other phytohormones are known to be controlled by the circadian clock (Jouve et al., 1999; Blázquez et al., 2002; Bancos et al., 2006; Thain et al., 2004). The circadian clock is comprised of a series of inter-connected feedback loops that are maintained by circadian clock oscillators. The circadian clock regulates circadian rhythm, which increases organisms' fitness by helping them anticipate and prepare for cyclical events, such as the onset of darkness. In addition to be partially controlled by the circadian clock, JA can conversely partially regulate the clock by inducing expression of *AtMYC2* in *Arabidopsis*, a prominent JA-induced transcription factor (Kazan, 2013) which directly binds to the promoter of AtSPA1, a far-red phytochrome suppressor (Gangappa and Chattopadhyay, 2010; Gangappa et al., 2013). Because of the synergistic relationship between GLVs and JA and the cyclical nature of dark-emitted GLVs, I also investigated the role of ZmLOX10 in the regulation of circadian clock oscillators.

Photosynthesis requires gas exchange between plants and the surrounding environment, and this process is mediated by the closing and opening of stomata. In addition to their role in JA induction, GLVs are known to induce closing of stomata in tomato and *Arabidopsis* (Savchenko et al., 2014; López-Gresa et al., 2018). Rapid stomatal closure after the photoperiod has ended is important for conservation of water and drought resistance. As such, this study investigated the role of GLVs in the regulation of stomata in maize. Collectively, this study seeks to elucidate the biological

implications of light-to-dark GLV emissions both in terms of regulating stomata closure and priming against insect herbivory.

RESULTS

ZmLOX10-derived GLVs are emitted in response to light-to-dark transitions

Release of GLVs by maize hybrid lines after light-to-dark transitions was previously reported by Chamberlain et al. (2006). I first wanted to establish if GLVs are also synthesized by the maize inbred line, W438, and if GLV synthesis at this transition time is dependent on ZmLOX10. To do this, I collected and analyzed volatiles from W438 inbred wild-type (WT) and near-isogenic *lox10-3* mutants in the W438 background using gas chromatography mass spectrometry (GC-MS). Volatiles were collected for 1 h before and after an entrained light-to-dark switch (end of the normal photophase, beginning of normal scotophase). GLV emissions were greatly increased upon darkness in WT, and were absent in *lox10-3* mutants, indicating that light-to-dark GLV emissions occur in the W438 background, and are ZmLOX10-dependent (Fig. 21a). GLVs were lowly emitted during the photophase, consistent with their role as stress-response metabolites. (3*Z*)-hexenal was the most highly emitted GLV, both before and after the light-to-dark transition, followed by (3*Z*)-hexenyl acetate and (3*Z*)-hexenol. Though (2*E*)-hexenal was previously reported to be emitted after light-to-dark transitions (Chamberlain et al., 2006), it was not detected in this study.

To determine if GLV emission specifically occur as a result of light-to-dark transitions, and not according as a result of circadian rhythm, I analyzed volatiles

collected 1 h before and 1 h after entrained and non-entrained light-to-dark switches (middle of the normal photophase). Non-entrained light-to-dark transitions elicited large GLV emissions, resulting in even greater amounts than after diurnal light-to-dark transitions (Fig. 21b). Though the overall amount of GLVs released by non-entrained transitions was greater, the proportion of different GLVs relative to one another remained consistent between the two types of transition. Once again (2*E*)-hexenal was not detected. These results suggest that GLVs are emitted in response to changes in light regimes, rather than circadian rhythm. Though pentyl leaf volatiles (PLVs) emissions after light-to-dark transitions have been reported (Brilli et al., 2011), no PLVs were detected in these experiments. Since GLVs are known to induce JA in maize (Engelberth et al., 2004; Christensen et al., 2013; Gorman et al., 2020), I next sought to determine whether these dark-induced GLV emissions trigger increases in JA biosynthesis.

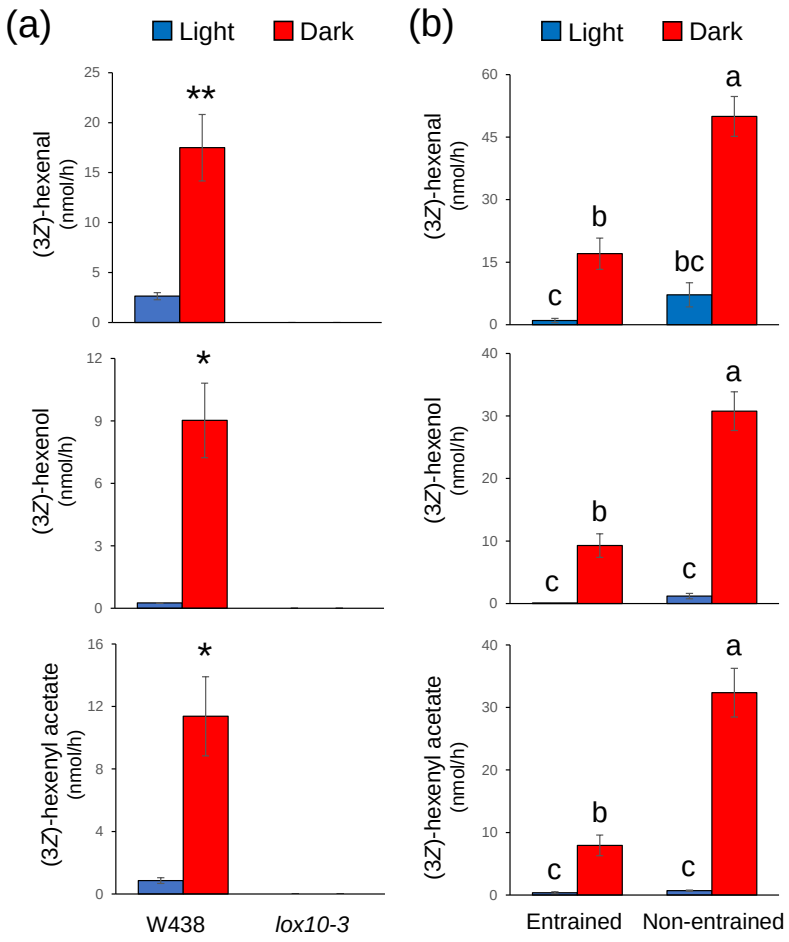

Figure 21 GLVs produced by ZmLOX10 are emitted after the onset of dark. Figure shows the mean amount of the GLVs, (3*Z*)-hexenal, (3*Z*)-hexenol, and (3*Z*)-hexenyl acetate emitted 1 h before (blue) or after (red) the onset of darkness. (a) shows the amounts of GLVs emitted after transition after a diurnal transition to dark in WT and *lox10-3* mutants in the W438 background. (b) shows the amount of GLVs released after both diurnal (end of the photophase) and non-diurnal (middle of the photophase) transitions to dark. Analytes are reported in (nmol/h). (a) Student's T-test was used to determine statistical significance between light and dark emissions [$p<.05$ = (*), $p<.005$ = (**)] (n=4). (b) Tukey's Test was used to determine statistical significance of (b), where letters denote statistical significance ($p=.05$) (n=4).

Jasmonates accumulates in response to light-to-dark transitions

In order to determine if GLVs elicit the synthesis of JA after light-to-dark transitions, we profiled a variety of phytohormones and oxylipins in the leaves and roots

of WT and *lox10-3* mutants in the W438 background using liquid chromatography tandem mass spectrometry (LC-MS/MS). Both JA and JA-Ile were increased in WT as early as 30 min after the onset of darkness (Fig. 22b,c). Levels of JA largely receded to pre-dark levels after 1 h, but JA-Ile levels continued to climb, reaching their peak 1 h after darkness and fading to near pre-dark levels at 3 h after the onset of darkness. *lox10-3* mutants exhibited no change in JA or JA-Ile throughout the time course, despite possessing similar pre-dark levels of jasmonates compared to WT. Though JA and JA-Ile were increased in response to darkness, their precursor, 12-OPDA, remained unchanged (Fig. 22a). This indicates that dark-induced regulation of JA-synthesis likely occurs at a step in the AOS pathway after 12-OPDA formation, as is known to be the case with GLV-mediated induction of JA (Engelberth et al., 2007; Gorman et al., 2020). Traumatin (TAN) and its derivative, traumatic acid (TA), were also transiently increased 30 min after the onset of darkness (Fig. 22d,e). These quick transient spikes of these HPL-derived metabolites correlate well with the rapid emission of GLVs after light-to-dark transitions. The LOX-branch product, 13-oxo-9(*Z*)-11(*E*)-tridecedienoic acid (OTD), was not induced by the onset of darkness and experienced a slight decrease in accumulation 1 h after dark (Fig. 22e). As PLVs and OTD are simultaneously synthesized, these results suggest that they are not synthesized in response to darkness in maize.

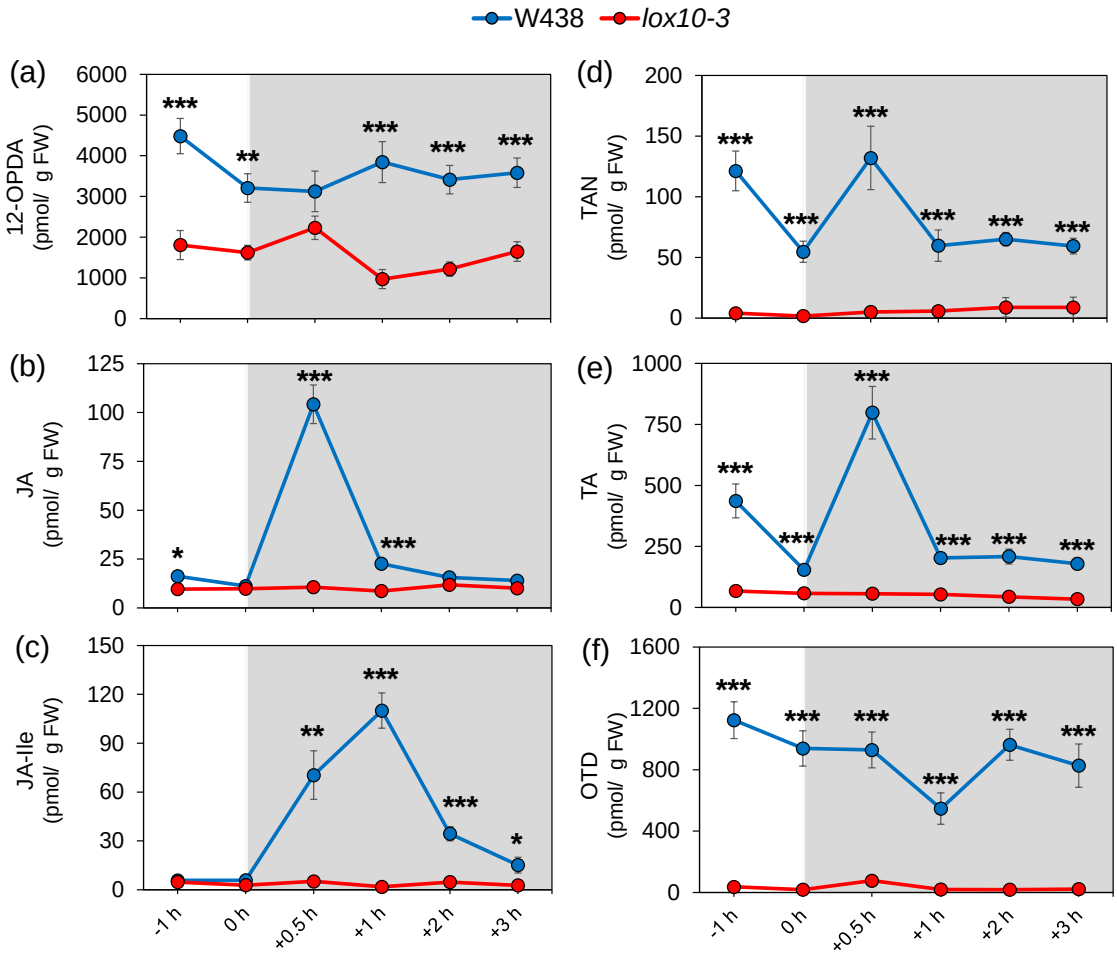

Figure 22 ZmLOX10 is required for induction of jasmonates and traumatins after the onset of darkness. Figure shows the amount of (a) 12-OPDA, (b) JA, (c) JA-Ile, (d) TAN, (e) TA and (f) OTD in W438 inbred (blue) or *lox10-3* mutants (red) at various timepoints just before and throughout the night (nmol/g FW). Bars indicate standard error (n=8). White background indicates timepoints during the photophase whereas grey background indicates timepoints during the scotophase. Student's T-test was used to determine statistical difference between the genotypes at every timepoint (* = p<.05), (** = p<.005), (*** = p<.0005).

LC-MS/MS analysis of maize roots revealed that JA and JA-Ile slightly increase in WT in response to darkness (Fig. 23b,c). This occurred much more gradually and significantly less than in maize leaves (Fig. 23b,c). Both jasmonates exhibited increasing trends 30 min and continued until at least 3 h after darkness. Unlike leaves, *lox10-3*

mutant roots exhibited accumulation patterns similar to WT, though overall amounts were still lower in *lox10-3* mutants compared to WT (Fig. 23). As in leaves, 12-OPDA does not appear to increase in roots of either WT or *lox10-3* mutants in response to dark (Fig. 23a). TAN was not detected in roots, likely because HPL1 is lowly expressed in maize roots (Hoopes et al., 2019). Although TA was detected, it was likely non-enzymatically generated by spontaneous interactions of esterified hydroperoxyl fatty acids (Zoeller et al., 2012). Accordingly, there few differences between amounts of TA between WT and *lox10-3* mutants (Fig. 23d). Collectively, these results reveal that only maize leaves sharply respond to light-to-dark transitions by increasing synthesis of jasmonates and that ZmLOX10 is critical in this process. It is still unclear as to whether ZmLOX10 leads to increases in JA biosynthesis through GLV-mediated signaling or whether ZmLOX10 directly provides substrate to the AOS pathway.

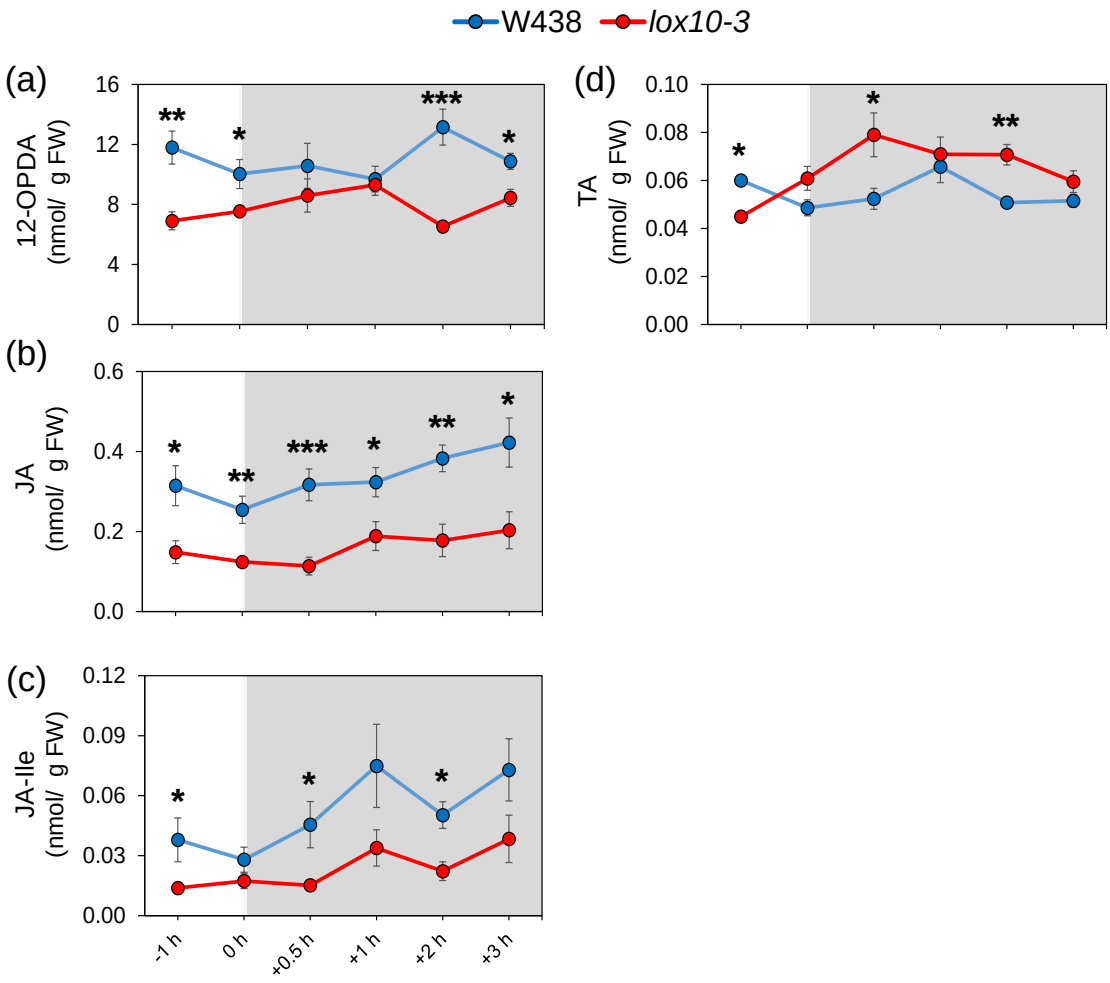

Figure 23 Roots do not experience a sharp increase of jasmonates upon the onset of dark. Figure shows the amount of (a) 12-OPDA, (b) JA, (c) JA-Ile, and (d) TA in W438 inbred (blue) or *lox10-3* mutants (red) at various timepoints just before darkness and throughout the night (nmol/g FW). Bars indicate standard error (n=8). White background indicates timepoints during the photophase whereas grey background indicates timepoints during the scotophase. Student's t-test was used to determine statistical difference between treatments at timepoint [p<.05 = (*), p<.005 = (**), p<.0005 = (***)] (n=6).

GLVs released after light-to-dark transitions increase jasmonates in leaves

In order to determine whether dark-induced JA synthesis is dependent on GLV or JA produced directly by ZmLOX10, I exposed *lox10-3* mutants to either triacetin or a

GLV mixture containing (3*Z*)-hexenal, (3*Z*)-hexenol, and (3*Z*)-hexenyl acetate dissolved in triacetin, for 30 min beginning at the light-to-dark transition. This mixture mimicked the GLVs that were highly emitted after light-to-dark transitions (Fig. 21). GLV-exposed *lox10-3* mutants exhibited a large, sharp, transient increases of JA and JA-Ile 30 min after the onset of darkness, which eventually receded back to control levels after 2 h (Fig. 24b,c). While JA and JA-Ile were increased by GLV treatment, 12-OPDA was not induced (Fig. 24a). In summary, GLV treatment resulted in *lox10-3* mutants exhibiting the same dark-induced responses of 12-OPDA, JA, and JA-Ile as WT plants, indicating that GLVs emitted in response to the onset of dark are responsible for increases in jasmonates at this time. These results clearly indicate that ZmLOX10-derived GLVs emitted after the onset of darkness result in the strong and transient accumulation of jasmonates and *lox10-3* mutants are capable of producing JA, presumably by other functional 13-LOX isoforms, when complemented with exogenous GLVs.

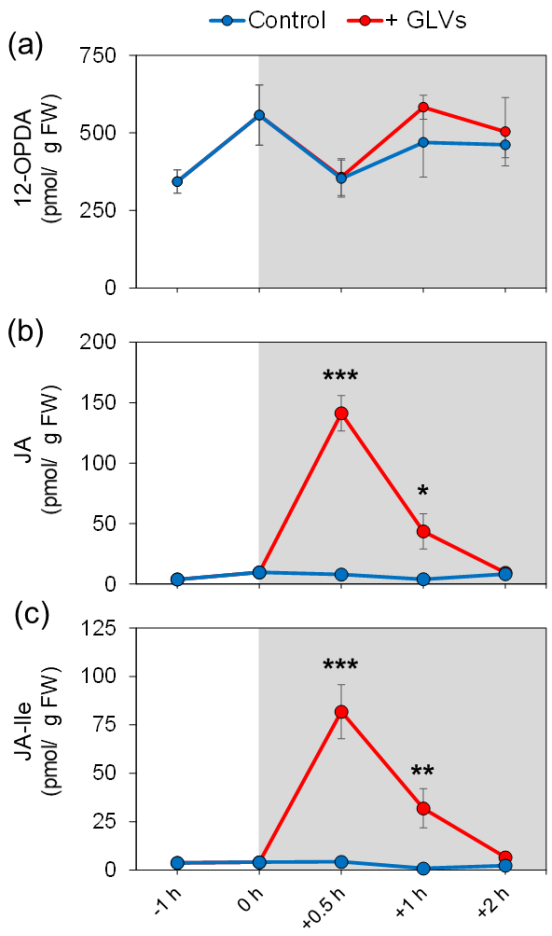

Figure 24 Exogenous GLV treatment rescues dark-induced JA accumulation in *lox10-3* mutants. The graphs show the amount of (a) 12-OPDA, (b) JA, (c) JA-Ile in *lox10-3* mutants exposed to either control treatment (ethanol, blue) or a GLV mixture (red) after the onset of darkness. Plants were exposed for 30 min starting at the onset of darkness (0 h) Jasmonates were measured at various timepoints just before and after dark treatment (pmol/g FW). White background indicates timepoints during the photophase whereas grey background indicates timepoints during the scotophase. Student's t-test was used to determine statistical difference between treatments at timepoint [$p<.05$ = (*), $p<.005$ = (**), $p<.0005$ = (***)] (n=6).

ZmLOX10 induce JA signaling through ZmLOX8 after light-to-dark transitions

In order to ascertain the various processes that may be impacted by sudden increases of GLVs and jasmonates in leaves in response to darkness, I carried out

RNAseq-based global transcriptome analysis of leaves of WT W438 inbred and *lox10-3* mutants. From this analysis, I generated a heatmap displaying the relative amounts of transcripts of each gene across each genotype and timepoint. All genes were divided into six major clusters based on the relative similarity of their expression across the different genotypes/timepoints. Clusters IV and V exhibit differences in gene expression between WT and *lox10-3* mutants before dark, with Cluster V containing genes that are more highly expressed in WT and Cluster IV consisting of genes that are more highly expressed in *lox10-3* mutants (Fig. 25). Cluster VI shows genes that are not differentially regulated between the two genotypes during the day, but are suppressed in *lox10-3* mutants after dark. Cluster I genes largely exhibit patterns opposite to those in Cluster VI. The largest and most pertinent clusters, Cluster II and Cluster III, are comprised of genes that are differentially regulated in WT and *lox10-3* mutants after darkness, with Cluster II genes displaying strong induction in *lox10-3* mutants and Cluster III genes exhibiting substantial increases in WT (Fig. 25). These two clusters contain the genes that exhibit the greatest contrast in the expression levels between *lox10-3* mutant and WT response to darkness and highlight the important role that ZmLOX10 plays in maize transcriptional responses to darkness. These results suggest that GLVs induce Cluster III genes and suppresses Cluster II genes. Collectively, this analysis revealed moderate differences in gene expression between WT and *lox10-3* mutants before light-to-dark transitions, but extensive transcriptional differences 1 h afterwards.

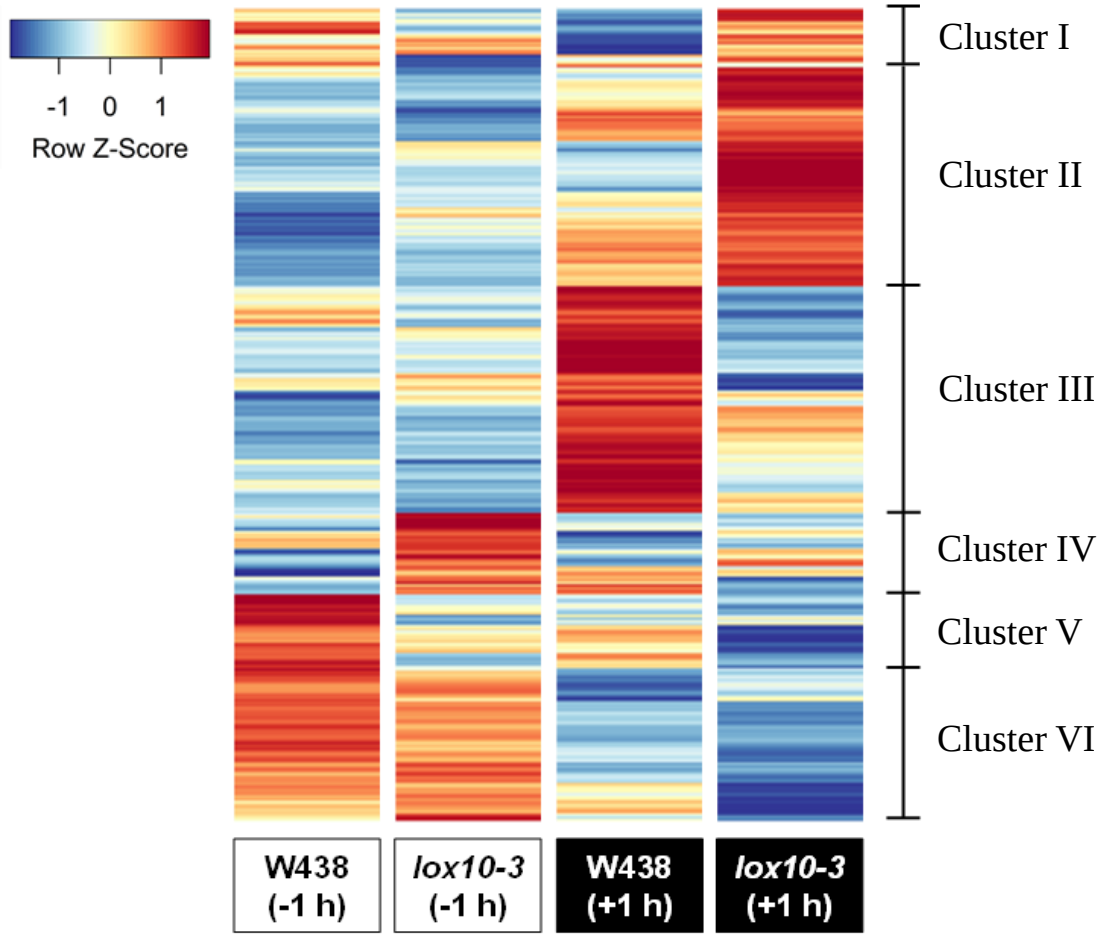

Figure 25 ZmLOX10-mediated signaling controls expression of multiple genes differentially regulated during light-to-dark transitions. Figure shows heatmap of transcripts levels of WT and *lox10-3* mutant leaves in the W438 background 1 hour before (-1 h) or 1 hour after (+1 h) dark. Heatmap shows differences in gene expression among different genotypes/timepoints using Z-score (blue=low, red=high) of fragments per kilobase million (FPKM). Genes were placed in 6 different groups based on similarity of expression pattern across all timepoints/genotypes. Each genotype/timepoint represents a sample consisting of 4 plants.

Unsurprisingly, many of the genes identified in Cluster III were related to JA signaling (Fig. 25). In order to further ascertain the expression of these genes over a more extended timecourse, I further analyzed the expression of key JA-related genes with qPCR. Using the ΔΔCT method, expression of these select genes at timepoints

during the scotophase was compared to the -1 h timepoint, the sole timepoint during the photophase, within each individual genotype (Livak and Schmittgen, 2001). In WT, both *ZmLOX8* and *ZmLOX10* are increased in response to darkness, although their respective patterns of induction differ (Fig. 26a,b). In WT, *ZmLOX10* exhibited a gradual increase in expression, steadily rising throughout the timecourse (Fig. 26a), whereas *ZmLOX8* sharply rose in WT at +1 h before steadily decreasing back to pre-dark levels (Fig. 26b). *ZmAOS1c*, an AOS isoform thought to be involved in the synthesis of 12-OPDA and JA in maize (Borrego and Kolomiets, 2016), exhibited a similar pattern to *ZmLOX8* (Fig. 26c). Contrary to WT, *lox10-3* mutants did not experience induction of either *ZmLOX8* and *ZmAOS1c* after the light-to-dark transition (Fig. 26b,c). Interestingly, *ZmOPR7* and *ZmOPR8* did not increase in either genotype in response to the onset of dark, with expression of both decreasing after dark (Fig. 26d,e).

I also tested the expression of the JA-responsive transcription factors, Zmbhlh91 and *ZmMYC7*. This revealed that 1 h after darkness, *ZmMYC7* transiently increased in WT, but not in *lox10-3* mutants (Fig. 26e). Zmbhlh91 also appeared to follow this same trend, but was far less inducible (Fig. 26f). Finally, the JA signaling repressors, *ZmJAZ2* and *ZmJAZ3*, also exhibited large transient spikes in WT, but not in *lox10-3* mutants (Fig. 26h,i). These results indicate that GLV-mediated increases in JA biosynthesis may be due to the transient transcriptional induction of *ZmLOX8* and *ZmAOS1c*, agreeing with previous results showing that ZmLOX8 provides the substrate for the synthesis of a large portion of JA in maize (Christensen et al., 2013). Oppositely, transcript accumulation of *ZmOPR7* and *ZmOPR8* is not induced upon darkness, suggesting that

transcription of these genes is not a mechanism by which GLVs induce JA biosynthesis after light-to-dark transitions. Together with the metabolite data, the exact mechanisms behind GLV-mediated JA induction after light-to-dark transitions are currently unclear. However, these results showed that JA-signaling directly coincided with JA-Ile biosynthesis (Fig. 22c).

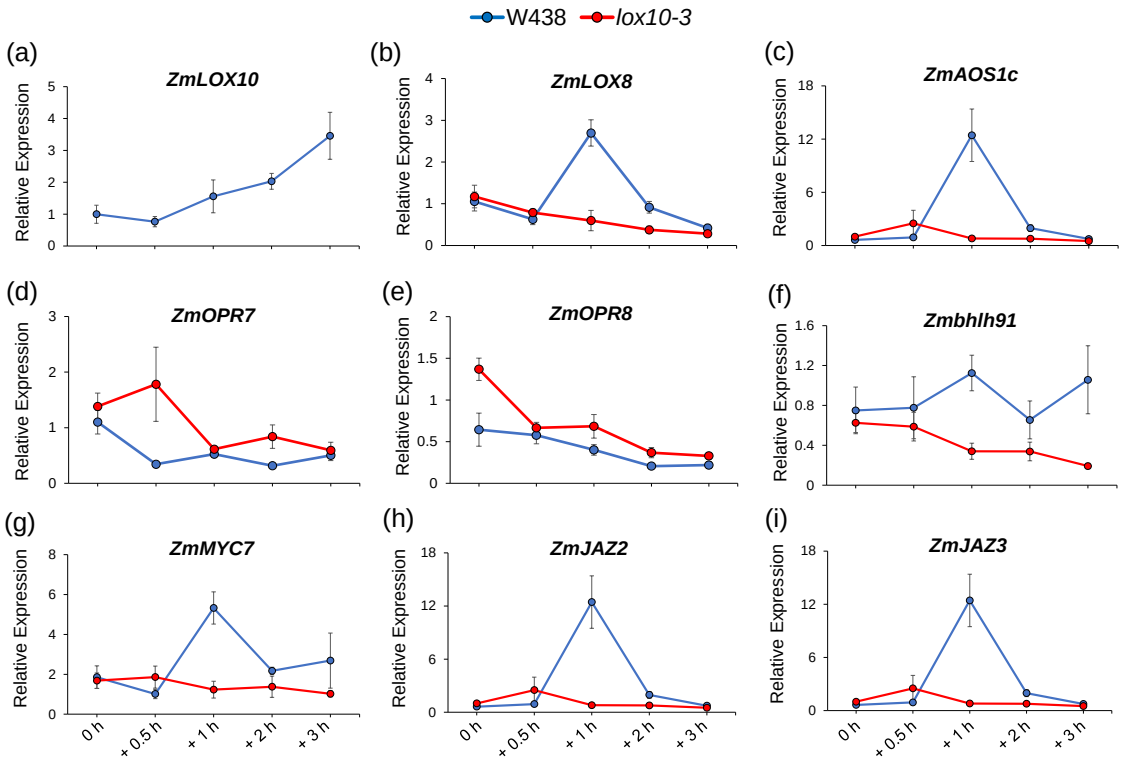

Figure 26 Transcript accumulation of JA biosynthesis and signaling genes is increased after darkness in a ZmLOX10-dependent manner. Figure shows the relative expression of (a) *ZmLOX10*, (b) *ZmLOX8*, (c) *ZmAOS1c*, (d) *ZmOPR7*, (e) *ZmOPR8*, (f) *Zmbhlh91*, (g) *ZmMYC7*, (h) *ZmJAZ2*, and (i) *ZmJAZ3* after darkness in leaves of WT W438 inbred (blue) and *lox10-3* mutants (red) in the W438 background. Relative expression was calculated by the ΔΔCT method (Livak and Schmittgen, 2001), where all timepoints are compared to the (-1 h) timepoint (the timepoint before the onset of dark). Expression greater than 1 indicates higher expression than at (-1 h), and lower than 1 indicates lesser expression than at (-1 h). All bars represent standard error (n=4).

Dark-induced GLV emissions result in long-term, cyclic priming to FAW

GLVs released upon darkness induce synthesis of JA and result in widespread gene induction, however the physiological implications of this phenomenon remain unknown. As ZmLOX10 and JA are known to be involved in defense against insect herbivores (Christensen et al., 2013; Rojas et al., 2018), I first sought to determine if GLVs released after light-to-dark transitions increase resistance to herbivory by FAW. To test this hypothesis, I exposed WT and *lox10-3* mutants to either triacetin (control), or an exogenous mixture of GLVs containing (3*Z*)-hexenal, (3*Z*)-hexenol, and (3*Z*)-hexenyl acetate dissolved in triacetin, for 30 min starting at the light-to-dark transition. Afterwards, GLVs were allowed to diffuse from the chambers in order to prevent any direct effects of GLVs on FAW. A single FAW, 4th instar, was placed on the 3rd leaf of each plant in a clip cage. The FAWs were left in the clip cages to feed for approximately 16 h, but did not begin feeding until the early hours of the photophase, approximately 8 h after being placed on the leaves. *lox10-3* mutants exposed to control treatment had far more leaf area consumed than WT, showing *lox10-3* mutants are more susceptible to herbivory by FAW than WT (Fig. 27a). This is in agreement with previous analysis of *lox10* mutant susceptibility to FAW (Rojas et al., 2018). GLV treatment resulted in greatly reduced amounts of damage in *lox10-3* mutants, which was equivalent to WT. This indicates that GLV exposure at the time of light-to-dark transition is able to rescue *lox10-3* mutant to WT levels of resistance for at least 16 h post exposure. This suggests that GLV emissions upon light-to-dark results in long-term defense priming.

To ascertain how long this priming may last, I reared neonate FAWs on WT and *lox10-3* mutants that were exposed, daily, to either GLVs or control treatment at the onset of diurnal dark period (Fig. 27b). The neonates were allowed to move and feed freely on the plants continuously for 7 days of the duration of the experiment. After 7 days of feeding, the average weight of the FAWs reared on each genotype/treatment was recorded. FAWs that were reared on control *lox10-3* mutants were significantly heavier than those of WT plants exposed to control treatment (Fig. 27b). GLV exposure resulted in significantly reduced weights of FAWs reared on *lox10-3* mutants, which were equal to those reared on WT (Fig. 27b). Since FAWs were allowed to freely feed on the plants for 7 days and the treatments only occurred once a day at the start of the scotophase, these results suggest that dark-induced GLV emissions result in priming of maize defenses against FAW for approximately 24 h.

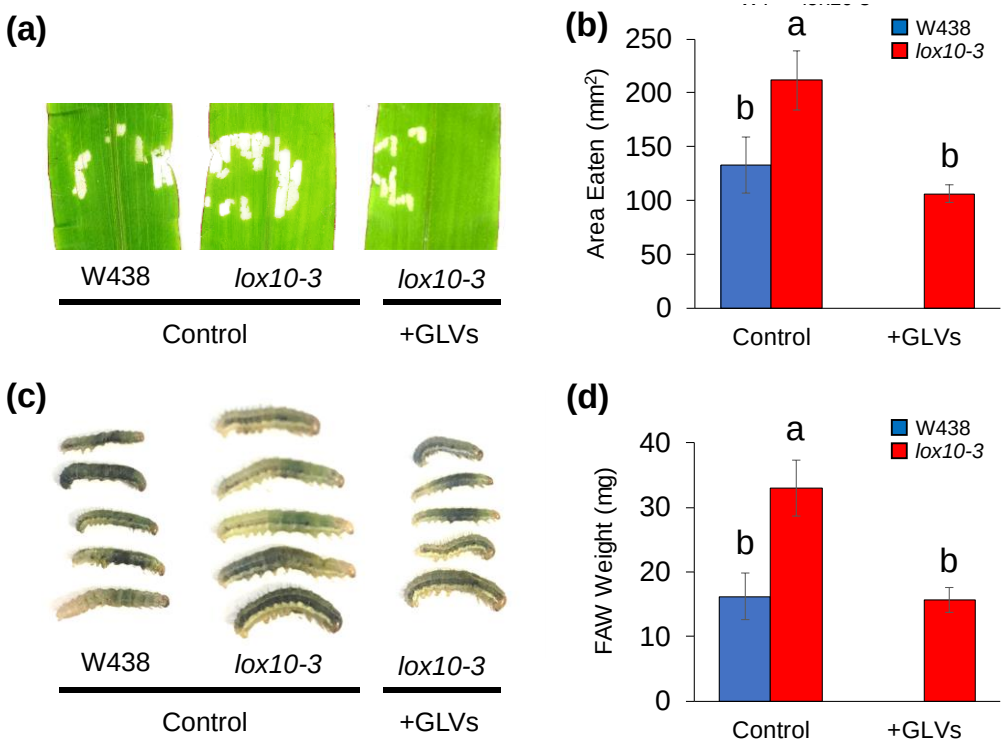

Figure 27 GLV exposure at the onset of dark rescues *lox10-3* susceptibility to FAW and inhibits FAW weight gain. (a) and (b) show the result of a FAW feeding assay, in which WT and *lox10-3* mutants were exposed to GLVs or triacetin (control) for 30 min after dark, and then a 4th instar FAW was placed on a leaf in a clip cage and allowed to feed for 16 h. Leaves were scanned afterwards and analyzed with ImageJ software to determine the area of leaf eaten. (a) shows representative images of leaves after feeding. (b) shows the mean of area (mm^2) eaten in W438 (blue) and *lox10-3* mutants (red). (c) and (d) shows weights of neonate FAW after feeding for 7 days on WT and *lox10-3* mutants that were exposed to GLVs or triacetin (control) for 30 min every day at the onset of dark. (c) shows representative FAW after 7 days of feeding. (d) shows mean weight of FAW after 7 days of feeding on W438 (blue) or *lox10-3* mutants (blue). Different letters denote statistical significance (Tukey's HSD).

Dark-induced GLV emissions do not regulate circadian rhythm

Dark-induced GLV emissions represent a rhythmic event, prompting the hypothesis that it may contribute to the regulation of the circadian clock. To test this hypothesis, I profiled gene expression of two morning element oscillators, ZmCCA1 and

ZmLHY1, and two evening element oscillators, ZmTOC1 and ZmTOC2, in both WT and *lox10-3* mutants over the course of 24 h. Using the ΔΔCT method, I compared the expression of these genes in *lox10-3* mutants to WT at each individual timepoint (Fig. 28a-d). This showed that all four genes were downregulated at the ZT14 timepoint, just 2 h before the onset of darkness. Though this timepoint represents the greatest differences between WT and *lox10-3* mutants, it also occurs at the timepoint furthest away from the light-to-dark transition, making it unlikely that these differences arise from GLVs emitted at this time. At the ZT20 timepoint, the middle of the scotophase, *ZmTOC1* and *ZmLHY1* were upregulated in *lox10-3* mutants.

I next wanted to determine if these differences between WT and *lox10-3* mutants occur at times when these genes are normally highly expressed. Using the ΔΔCT method, I compared the expression of all timepoints of *ZmCCA1* and *ZmLHY1* to the ZT12 timepoint, and all timepoints of *ZmTOC1* and *ZmTOC2* to the ZT 4 timepoint, within each individual genotype (Fig. 28e-h). There were modest differences in the expression patterns of these genes between WT and *lox10-3* mutants, with *ZmLHY1* expression at ZT14 and ZT20 exhibiting slight alterations in *lox10-3* mutants, although these differences seemed to be relegated to individual timepoints, rather than part of a larger pattern (Fig. 28f). Furthermore, both of these timepoints occur at times of low *ZmLHY1* expression. Both *ZmTOC1* and *ZmTOC2* exhibited a slight decrease at ZT14 that was not present in WT (Fig. 28g,h). Though this timepoint coincides with their respective peak expressions, this difference is once again only present at this one timepoint, with the nearest timepoints appearing to maintain patterns consistent with

WT. Ultimately, there were few differences in expression or the expression patterns of these circadian clock oscillators between WT and *lox10-3* mutants. The timepoints containing these differences were isolated, with adjacent timepoints exhibiting no alterations in *lox10-3* mutants. Because these circadian clock oscillators are critical components of the circadian clock, these results suggest that dark-induced GLV emissions do not contribute to the regulation of circadian rhythm.

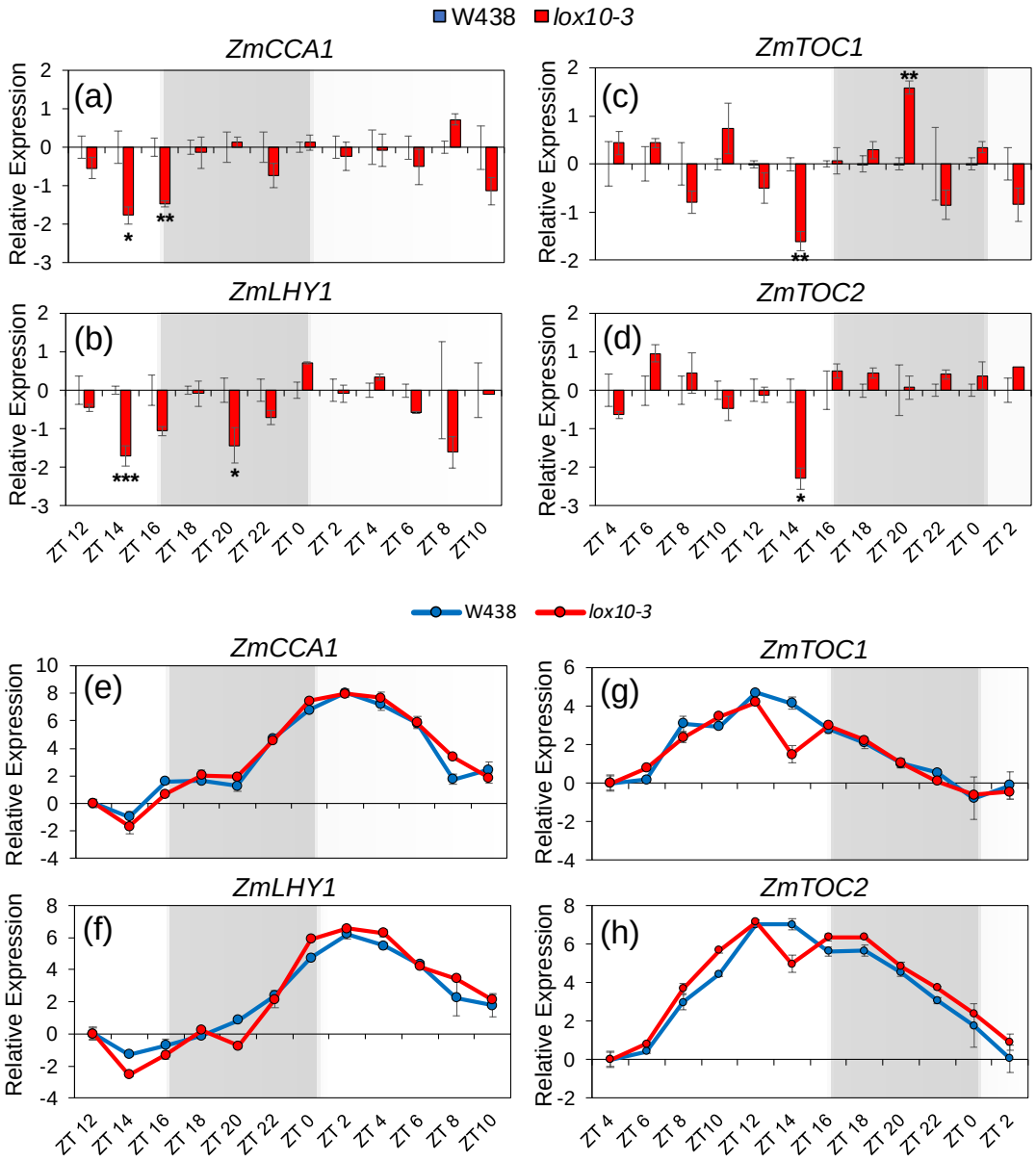

Figure 28 Expression of circadian clock oscillators are largely unaffected by ZmLOX10. (a-d) shows the expression of *ZmCCA1* (a), *ZmLHY1* (b), *ZmTOC1* (c), and *ZmTOC2* (d) in *lox10-3* mutants (red) relative to WT (blue) at each timepoint. (e-h) shows the expression of the morning loop oscillators, *ZmCCA1* (e) and *ZmLHY1* (f), and the evening loop oscillators, *ZmTOC1* (g) and *ZmTOC2* (h), at every timepoint in WT and *lox10-3* mutants relative to the ZT 12 (a & b) or ZT 4 (c & d) timepoints. Background color indicates light/dark. Data shown is the mean of the log of ΔΔCT. All bars represent standard error. Student's T-test was used to determine statistical difference between genotypes at every timepoint (* = p<.05), (** = p<.005), (*** = p<.0005).

GLVs facilitate closure of stomata

Light-to-dark transitions represent a switch from photosynthetic to non-photosynthetic conditions, after which plants are known to close their stomata in order to prevent water loss (Costa et al., 2007). GLVs have previously been shown to induce closure of stomata in *Arabidopsis*, and aid in drought tolerance (Savchenko et al., 2014). To determine if this was also the case in maize, I first wanted to determine if ZmLOX10 protein is localized to guard cells, the cells that modulate aperture of stomata. To do this, I looked at the stomata of transgenic lines of maize containing YFP-tagged ZmLOX10 (LOX10-YFP), expression of which is driven by the LOX10 native promoter (Mohanty et al., 2009). LOX10-YFP was clearly localized to the chloroplasts of guard cells, confirming that ZmLOX10 protein is indeed guard cell-localized (Fig. 29g,h). Taken together with prior ZmLOX10 localization to chloroplasts of mesophyll and bundle sheath cells (Gorman et al., 2020), this shows that ZmLOX10 localizes to plastids in an array of different cell types.

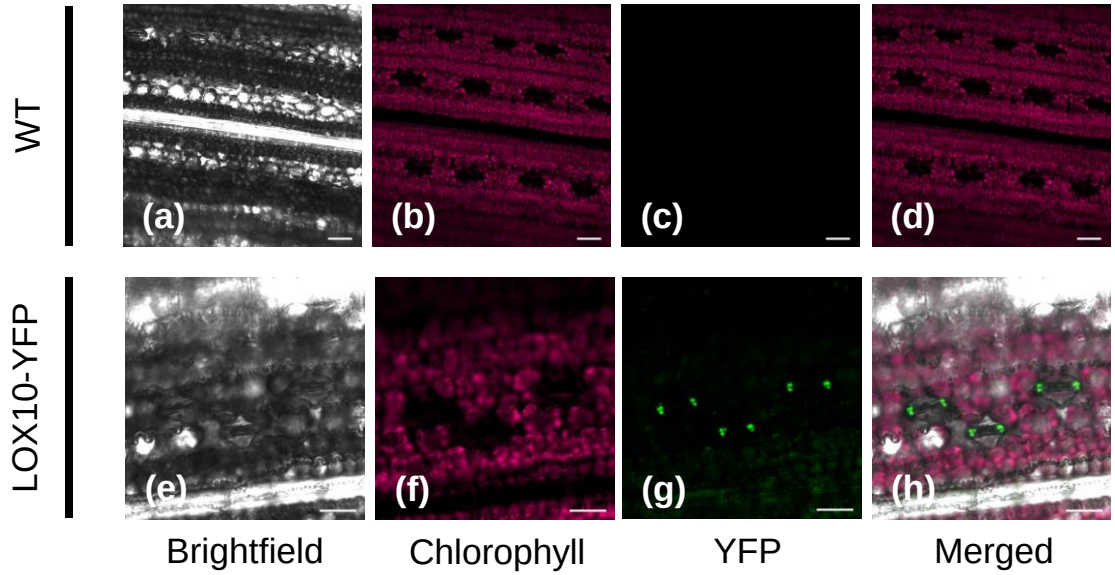

Figure 29 LOX10-YFP tagged maize lines show that LOX10 localizes to chloroplasts of guard cells. (a-d) show images of untransformed leaves of B73 inbred line and (e-l) show images of transgenic lines in the B73 background expressing YFP-tagged LOX10 (LOX10-YFP) under its native promoter. (a-d) shows LOX10-YFP is not present in WT leaves, including in guard cells. (e-h) details localization of LOX10-YFP to chloroplasts of guard cells. Columns in order of left to right show brightfield views, chlorophyll autofluorescence, YFP fluorescence, and a merged view. YFP signal is absent in untransformed lines (c), but abundant in LOX10-YFP lines (g) where it overlaps with chlorophyll autofluorescence (h). Scale bars represent 50 µm.

Next, I measured the aperture of stomata on epidermal peels of WT and *lox10-3* mutants. This revealed that *lox10-3* mutant stomatal apertures were almost twice as wide as those of WT (Fig. 30a-c). To determine if GLV-deficiency was the reason for wider stomatal apertures in *lox10-3* mutants, I treated epidermal peels of WT and *lox10-3* mutants with various GLVs and measured their resulting apertures. I also treated them with abscisic acid (ABA), a known inducer of stomata closure, as a control. Treatment with all GLVs significantly decreased stomatal aperture in *lox10-3* mutants, but only (3*Z*)-hexenal and (2*E*)-hexenal closed stomata in WT plants (Fig. 30c). Importantly,

individual GLV treatments of *lox10-3* mutants resulted in equivalent, or even lesser, stomatal apertures than WT controls, indicating that GLVs were able to rescue stomatal closure in *lox10-3* mutants. (3*Z*)-hexenal and (2*E*)-hexenal were the most effective GLVs, resulting in the equal or lesser stomatal apertures compared to ABA treatment (Fig. 30c). (2*E*)-hexenal was particularly noteworthy as it displayed the most potent activity compared to other GLV molecular species. As such, I established a dose-dependent effect of (2*E*)-hexenal on stomatal aperture. As little as 10 µM of (2*E*)-hexenal was able to establish significant stomatal closure in both WT and *lox10-3* mutants (Fig. 30d). There were no significant differences found between concentrations of 10-50 µM in either genotype, however 100 µM resulted in even stronger closure in WT (Fig. 30d). These results show that GLVs are potent signals for closure of stomata and may aid in nightly stomatal closure.

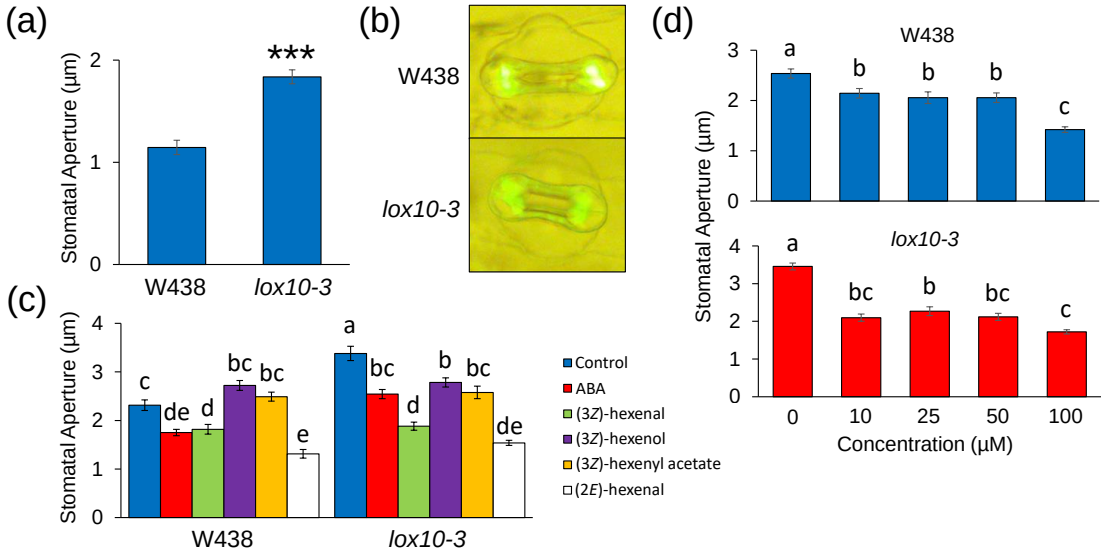

Figure 30 GLVs aid in stomatal closure. Figure shows the difference in stomatal aperture between W438 inbred line and *lox10-3* mutant epidermal peels with no treatment (a) and (b), in response to various GLV treatments 100 µM (c), and in response to dose-dependent treatment with (2*E*)-hexenal (d). Students T-test was used to determine statistical significance for (a) (*** = p<.0001) (n>100). Tukey's test was used for (c) and (d) (p<.05) (n>100), where different letters denote statistical significance.

DISCUSSION

GLVs are emitted in response to various biotic and abiotic stresses, including after light-to-dark transitions. This phenomenon has been documented to occur in many diverse species, including maize (Fall et al., 1999; Graus et al., 2004; Brilli et al., 2011; Jardine et al., 2012), but its physiological significance remains unknown. Using WT and *lox10-3* mutants in the W438 genetic inbred background, I have shown that GLVs emitted upon diurnal light-to-dark transitions are ZmLOX10-dependent, as are all other documented instances of GLV emissions in maize (Fig. 1) (Christensen et al., 2013). The most prominently emitted GLVs were (3*Z*)-hexenal, (3*Z*)-hexenol, and (3*Z*)-hexenyl

acetate. These volatiles were emitted in the same relative proportions, but to overall greater amounts, after non-diurnal light-to-dark transitions (Fig. 1b). This could be because *ZmLOX10* and *ZmHPL1* are both at their respective maximal levels of expression in the middle of the photoperiod (Nemchenko et al., 2006), the time at which the non-entrained light-to-dark switch was implemented. Another reason could be the increased availability of substrate for synthesis of GLVs, as the amount of GLVs synthesized in response to stress is directly correlated to the amount of photosynthetically assimilated carbon (Loreto et al., 2006; Brilli et al., 2011).

Though (2*E*)-hexenal was previously reported to be the most prominently emitted GLV in maize after light-to-dark transitions (Chamberlain et al., 2006), it was not detected in our analysis. This could be due to differences between the maize hybrids that were used by Chamberlain et al. (2006) and the inbred line used in this study. It is also possible that this aldehyde was previously misidentified. PLVs had also previously been reported to be emitted in response to light-to-dark transitions by several tree species (Brilli et al., 2011; Jardine et al., 2012), however they were not detected in this study either. This is likely due to the differences in the methods used in those studies, which employed the use of proton-transfer reaction mass spectrometry of headspace air, and this study, which performed GC-MS analysis of volatiles dynamically collected onto volatile traps. It is also possible this could be due to innate differences between the LOX and HPL pathways of maize and the other plant species used in those studies.

I chose to collect volatiles for 1 h after light-to-dark transitions in order to ensure that all volatiles that were emitted in response to dark were collected, but GLVs were

likely emitted much more quickly, within seconds of dark until about 20 min afterwards (Fall et al., 1999; Graus et al., 2004; Brilli et al., 2011; Jardine et al., 2012). Following the emission of (3*Z*)-hexenal, (3*Z*)-hexenol, and (3*Z*)-hexenyl acetate, WT plants experienced an increase of several non-volatile oxylipins, all of which were dependent on ZmLOX10 (Fig. 22). This included the C_{12} compounds, TAN and TA, which are derivatives of (9*Z*)-traumatin, an oxylipin synthesized alongside GLVs during ZmHPL1-mediated cleavage of lipid hydroperoxides (Matsui, 2006). (9*Z*)-traumatin is quickly and spontaneously converted to TAN, which is then further metabolized into TA (Kallenbach et al., 2011). Both TAN and TA showed sharp transient spikes in accumulation 30 min after light-to-dark transition (Fig. 22d,e). Given the rapid nature of GLV synthesis, it is likely the true peaks of these metabolites were at earlier timepoints closer to the light-to-dark transition. Oppositely, OTD, the C_{13} counterpart to PLVs, was not increased in response to light-to-dark transition (Fig. 22e). This suggest that GLVs and traumatins are specifically synthesized in response to light-to-dark transitions.

Synthesis of jasmonates was induced as early as 30 min after dark in WT, with JA peaking at this time and JA-Ile peaking 1 h after the light-to-dark transition (Fig. 22b,c). Both jasmonates began to quickly recede towards pre-dark levels after their respective peaks, displaying the stepwise conversion of JA into JA-Ile, the main biologically active jasmonate. 12-OPDA did not exhibit any changes throughout the timecourse in either genotype, which led me to hypothesize that induction of jasmonate synthesis occured downstream of 12-OPDA synthesis (Fig. 22a). This pattern of jasmonate, but not 12-OPDA, induction in response GLV exposure has been previously

reported (Engelberth et al., 2007; Gorman et al., 2020), making GLV the most likely signals driving JA synthesis downstream of 12-OPDA synthesis. Importantly, the amount of 12-OPDA present in maize tissues if far greater than JA, suggesting only a small fraction of 12-OPDA gets converted to JA (Fig. 22a-c and Fig. 23a-c). Interestingly, gene expression analysis indicated that expression of *ZmLOX8* and *ZmAOS1c*, but not *ZmOPR7* and *ZmOPR8*, was increased in a ZmLOX10-dependent manner after the onset of dark (Fig. 26b-e). Furthermore, the induction of these genes directly correlated to induction of JA-Ile. These results indicate that equivalent amounts of 12-OPDA and jasmonates may be synthesized after light-to-dark transitions, or that GLV regulation of the AOS pathway at steps past the formation of 12-OPDA occurs at the translational or post-translational level.

Though ZmLOX10 has little impact on basal levels of jasmonates before the light-to-dark switch, it was critical for transient induction of jasmonates in leaves after light-to-dark transitions. As previously shown, *lox10-3* mutants were largely deficient in 12-OPDA at all timepoints (Christensen et al., 2013; Gorman et al., 2020; He et al., 2020), again implicating ZmLOX10 as the major 12-OPDA producing LOX isoform of maize (Fig. 22a and Fig. 23b). *lox10-3* mutants were also almost devoid of TAN and TA, much like GLVs. OTD levels were also extremely low in *lox10-3* mutants, as noted by He et al. (2020), confirming that ZmLOX10 is both the major GLV and PLV producing LOX isoform (Fig. 22d-f). Treatment of *lox10-3* mutants with GLVs was able to induce a transient spike in JA and JA-Ile, but not 12-OPDA, exhibiting the same pattern seen in WT, and confirming that jasmonate induction in leaves after dark is due to GLVs

emission after light-to-dark transitions. The transient induction of JA-Ile mirrored that of JA in *lox10-3* mutants, rather than exhibiting a slightly more drawn pattern of induction, as was seen in WT plants (Fig. 22b,c and Fig. 24b,c). This could be because ZmLOX10 represses JAR enzymes, which facilitate conversion of JA to JA-Ile.

RNAseq analysis of the maize leaf transcriptome during light-to-dark transition revealed that many genes are misregulated at the transcriptional level in *lox10-3* mutant leaves compared to WT (Fig. 25). While there was some differential regulation 1 h before dark, Clusters IV and V, there were significantly more genes misregulated 1 h after darkness found in Clusters II and III. ZmLOX10 was responsible for induction of of multiple genes after darkness, represented by Cluster III, and also suppression of many others, Cluster II. Many of the most differentially regulated genes found in Cluster III were related to JA biosynthesis and signaling, which led me to perform additional gene expression analysis of these genes, via qPCR, at several different timepoints around the light-to-dark transition. As mentioned above, the JA-biosynthesis genes, *ZmLOX8*, *ZmLOX10*, and *ZmAOS1c*, were upregulated after dark in a ZmLOX10-dependent manner (Fig. 26a-c), however *ZmOPR7* and *ZmOPR8* were not. Several markers of JA signaling, *ZmMYC7*, *ZmJAZ2*, and *ZmJAZ3*, exhibited strong induction in WT in response to the onset of dark, with *Zmbhlh91* exhibiting a less robust response (Fig. 26f-i). Furthermore, these JA-response genes and the JA-biosynthetic genes, *ZmLOX8* and *ZmAOS1c*, experienced sharp and transient transcript accumulation 1 h after dark that mirrored the accumulation of JA-Ile (Fig. 22c). Interestingly, *ZmLOX10* transcripts accumulated in a gradual manner after the onset of dark, slowly increasing throughout

the duration of the experiment (Fig. 26a). This pattern was in stark contrast to other dark-inducible genes analyzed, as well as the accumulation patterns of JA-Ile. This data suggests that if JA is synthesized by induction of a LOX isoform after light-to-dark transitions, it is likely that ZmLOX8 is responsible for dark-induced JA biosynthesis. Given the stark transcriptional differences between WT and *lox10-3* mutants during light-to-dark transitions, it appears that dark-synthesized GLVs, and consequently jasmonates, play a profound role in gene regulation in maize after light-to-dark transitions.

While maize leaves experienced large, sharp increases of JA and JA-related signaling after light-to-dark transitions, this was not the case for either WT or *lox10-3* mutant roots (Fig. 23). Rather, JA and JA-Ile were gradually increased after the onset of darkness in a non-ZmLOX10-dependent manner, although *lox10-3* mutants still possessed overall lower levels of jasmonates compared to WT (Fig. 23b,c). As in leaves, roots did not experience altered levels of 12-OPDA in response to darkness, and ZmLOX10 was once again shown to be a major producer of 12-OPDA (Fig. 23a). TAN was not detected in roots of both genotypes, indicating that ZmHPL1 is not active in roots, matching its low expression in root tissue (Hoopes et al., 2019). Only trace amounts of TA were detected in roots, with a slight trend of higher levels in *lox10-3* mutants compared to WT (Fig. 23d). Since the enzymatically driven precursor of TA, TAN, was not detected, it is likely TA in roots was generated non-enzymatically through interactions of hydroperoxide groups of esterified 13*S*-hydroperoxy-octadecatrienoic acid and 13*S*-hydroperoxy-octadecadienoic acid in lipid membranes, as is reported for its

9-LOX counterpart, azaleic acid (Zoeller et al., 2012). Since GLVs produced upon darkness are only produced in leaves, roots may not be adequately exposed to the volatiles or may not be capable of responding to GLVs (Doan et al., 2020).

Assays utilizing FAW demonstrated that dark-induced GLV emissions resulted in significant defense against FAW. Damage assays showed that untreated *lox10-3* mutants were much more susceptible to FAW compared to WT, with approximately twice as much leaf area consumed (Fig. 27a). This correlated well with previous analysis of *lox10-3* mutant susceptibility to FAW (Rojas et al., 2018). Exposing *lox10-3* mutants to GLVs restored their resistance to FAW (Fig. 27a). Unexpectedly, FAW in this experiment did not begin feeding until the early hours of the morning, approximately 8 h after the onset of darkness and GLV treatment, suggesting that dark-induced GLVs provide long-lasting priming against insect herbivory. This notion was confirmed by an additional feeding assay that observed the weight gain of FAW on WT and *lox10-3* mutants that were exposed to GLVs on a daily basis. Though GLV exposure occurred daily at the time of diurnal light-to-dark transition, FAW were allowed to freely move and feed on the plants for 7 days. These results mirrored the damage assay, with FAW neonates reared on *lox10-3* mutants exhibiting almost double the weight of those reared on WT and daily GLV exposure resulted in equal FAW weights between WT and *lox10-3* mutants (Fig. 27b). Because GLV treatment was limited from the time of the light-to-dark transition to 30 min afterwards and FAW were allowed to feed freely throughout the duration of the experiment, these results indicate that dark-induced GLV and JA

synthesis in maize leaves results in significant priming against insect feeding that lasts for up to 24 h.

Since GLVs and JA are rapidly synthesized at the onset of darkness in a cyclic, diurnal manner and JA is known to influence genes that regulate circadian rhythm (Gangappa and Chattopadhyay, 2010; Gangappa et al., 2013), I hypothesized that they might exert some influence over the circadian clock at this time. However, analysis of WT and *lox10-3* mutants revealed that the circadian clock is largely unaltered in *lox10-3* mutants. Only minor, sporadic differences in expression of *ZmCCA1* and *ZmLHY1*, two morning loop oscillators, and *ZmTOC1* and *ZmTOC2*, two evening loop regulators, were detected in *lox10-3* mutants compared to WT (Fig. 28). Furthermore, these differences were greatest before the light-to-dark switch took place, when *ZmCCA1* and *ZmLHY1* are expressed at the lowest levels. While ZmLOX10 might regulate expression of these genes at this time, it is likely not through dark-induced GLV and JA synthesis. Most importantly, these slight differences did not result in any substantial sustained differences in rhythmic expression of these genes, only causing a disturbance in *ZmTOC1* and *ZmTOC2* two hours before the light-to-dark transition (Fig. 28c,d). Collectively, these results indicate that the circadian clock remains well entrained in *lox10-3* mutants despite the absence of dark-emitted GLVs.

While GLVs do not appear to play a role in maintaining circadian rhythm, they do appear to play a role in stomatal closure. LOX10-YFP lines clearly display localization of ZmLOX10 to chloroplast of guard cells, indicating that it may play a role in the regulation of stomata function. (Fig. 29) Correspondingly, *lox10-3* mutants have

much wider stomatal apertures compared to WT, and GLV treatment rescues this phenotype by closing stomata (Fig. 30). All tested GLVs were able to induce stomatal closure and restore WT-like apertures in *lox10-3* mutants, however (3*Z*)-hexenol and (3*Z*)-hexenyl acetate did not result in enhanced stomatal closure in WT (Fig. 30c). Similarly, Savchenko et al. (2014) observed that (3*Z*)-hexenal, but not (3*Z*)-hexenol resulted in stomatal closure of WT *Arabidopsis*. In tomato, several (3*Z*)-hexenol derivatives exerted strong closure of stomata (López-Gresa et al., 2018); however, these GLVs were not detected of maize and thus were not tested. Of the tested GLVs, the aldehydes, (3*Z*)-hexenal and (2*E*)-hexenal (Fig. 30c), exhibited the strongest closing activities. (2*E*)-hexenal was particularly potent, providing even greater levels of closure than ABA, the phytohormone best-known for regulating stomatal closure. (2*E*)-hexenal is a strong reactive electrophilic species, which could be why it displays such potent closing activity. Dose-dependent treatments resulted in the verification of (2*E*)-hexenal as a strong regulator of stomatal aperture, and highlighted that only 10 µM concentration resulting in strong closure of both WT and *lox10-3* mutant stomata (Fig. 30d). A concentration of 100 µM of (2*E*)-hexenal was able to further induce stomatal closure. Collectively, these results are similar to previous results in *Arabidopsis* (Savchenko et al., 2014), which showed (3*Z*)-hexenal, but not (3*Z*)-hexenol, was capable of closing stomata. Though (2*E*)-hexenal was not emitted in response to light-to-dark transitions, (3*Z*)-hexenal was highly emitted, suggesting that GLVs also help facilitate stomatal closure at the onset of darkness. However, further work looking at stomata closure in

WT and *lox10-3* mutants after light-to-dark transitions with GLV complementation is required in order to confirm this hypothesis.

These results show that ZmLOX10 is required for GLVs production in response to light-to-dark transitions, which leads to large transient increases of jasmonates and results in transcriptional reprograming of a large number of dark-regulated genes, especially those involved in JA-mediated signaling. Collectively, this phenomenon results in strong priming against FAW that lasts for up to 24 h, until the next dark-induced release of GLVs. This system of daily priming results in the perpetual protection of maize against insect herbivory. GLVs emitted at this time may also serve as a homing beacon for FAW moths (Rojas et al., 2018), which are primarily active after dark (Sparks, 1979), or insect predators of FAW (Allman and Baldwin, 2010). This should be investigated in future works. Additionally, I have shown that dark-emitted GLVs can also help facilitate stomatal closure, but do not play a role in maintaining circadian rhythm. This work represents the first instance in which biological implications of light-to-dark GLV emissions have been described, and prompts further questions regarding the existence of this phenomenon under natural growth conditions. The precise mechanisms behind this phenomenon still remain unknown. It is also possible that insect priming and stomata closure, while consequences of light-to-dark GLV emissions, are not its main evolutionary driving forces. This phenomenon may be a result of plant-wide shade avoidance responses, in which JA is known to play a critical role (Robson et al., 2010; Leone et al., 2014). The role of GLVs in shade avoidance responses has yet to be determined, although VOC emissions are thought to play a role in this process (Pierik

and de Wit, 2013). Establishing whether this phenomenon exists under natural light conditions, the extent of its impact on plants, and mechanisms behind this process should be the focus of future studies. Regardless, the results of this study have widespread application to those performing laboratory-based plant experiments, particularly plant-insect assays, and emphasizes the selection of experimental timepoints in relation to light-dark cycles.

CHAPTER VI

SUMMARY

As sessile organisms, plants must directly face numerous biotic and abiotic stresses. In order to cope with these stresses, plants have evolved a volatile-mediated communication system with themselves and other organisms. Volatile communication is crucial for plants to anticipate stresses and pre-emptively raise defenses against them. These volatiles are collectively termed volatile organic compounds (VOC), and are comprised of many different classes of volatiles, including those produced in the lipoxygenase (LOX) pathway. The LOX pathway produces many different oxygenated lipids, or oxylipins, from polyunsaturated fatty acids. Some of these molecules represent well-characterized volatile signals, such as methyl jasmonates (MeJA) and green leaf volatiles (GLV), a group of C_6 volatiles produced in the hydroperoxide lyase branch (HPL) of the LOX pathway. Pentyl leaf volatiles (PLV), represent another group of highly emitted LOX-derived volatiles, although little is known regarding their biosynthesis or function. While much is known about GLVs, their role in plant-pathogen interactions remains understudied, as do the physiological impacts of their emission after light-to-dark transitions. The major goals of this study were to elucidate synthesis of PLVs, to characterize the role of GLVs in maize interactions with *Colletotrichum graminicola*, and to describe the physiological consequences of GLV release after maize light-to-dark transitions. Collectively, this study has provided important information regarding the synthesis and function of LOX-derived volatiles in maize.

I have provided pharmacological evidence to support the first detailed biosynthetic order of individual PLV molecular species, which are synthesized in the LOX branch of the LOX pathway. Many details regarding the PLV pathway were previously hypothesized, including the primary synthesis of (2*Z*)-pentenol and 1-penten-3-ol and their subsequent conversion to (2*Z*)-pentenal and 1-penten-3-one (Gardner et al., 1996). New and unexpected intricacies were also established, such as the reduction of unsaturated PLV alcohols to saturated alcohols and bi-directional interconversion between aldehydes and alcohols. Using maize genetic knockouts, this study also made it clear that ZmLOX10 is responsible for the synthesis of a majority of PLVs in maize. Experiments utilizing transgenic lines of *Arabidopsis* also suggest that ZmLOX6 is exclusively capable of synthesizing PLVs *in planta*. Because of its inability to oxygenate lipids, transgenic ZmLOX6 largely relies on substrate produced by the GLV-producing LOX isoform of *Arabidopsis*, AtLOX2. This strongly implies that ZmLOX6 relies on ZmLOX10 in maize, as ZmLOX10 is the predominant 13-LOX and sole GLV-producing LOX isoform of maize. Using the jasmonic acid (JA)-deficient double *op7op8* mutants, I revealed that JA signaling is important for both GLV and PLV synthesis in maize. Additionally, I revealed a popular method of volatile analysis in plants, freeze-thawing, results in drastically altered volatile profiles that do not reflect true volatile emissions. This problem stems from the fact that freeze-thawing seemingly destroys alcohol dehydrogenase (ADH) and acetyl transferases (CHAT) and that volatiles seem to be synthesized *de novo* after freeze-thawing has taken place.

Regarding the role of GLVs in plant-pathogen interactions, GLVs are thought to induce resistance to pathogens, but almost all studies have focused on plant interactions with necrotrophic pathogens. Utilizing GLV- and JA-deficient mutants of maize, *lox10-3* and *opr7-5opr8-2* mutants respectively, this study has shown that GLVs promote susceptibility of maize to two major forms of disease, anthracnose leaf blight (ALB) and anthracnose stalk rot (ASR), caused by the hemi-biotrophic fungus, *C. graminicola*. Both leaves and stalks of these mutants possessed high levels of salicylic acid (SA) and displayed significantly diminished levels of JA, or no JA at all, at the earliest points of infection. At these timepoints, *C. graminicola* still exhibits a biotrophic phase of growth, when SA-mediated defenses are the most effective. Treating *lox10-3* and *opr7-5opr8-2* mutants with GLVs prior to infection revealed that GLV-mediated susceptibility was achieved through induction of JA, as *lox10-3*, but not *opr7-5opr8-2* mutant susceptibility, was restored. Additionally, exogenous treatment of *lox10-3* and *opr7-5opr8-2* mutants with MeJA prior to infection resulted in restoration of WT-like susceptibility. Conversely, methyl salicylate treatment did not induce further resistance in these mutants, but did induce mutant-like resistance in WT plants. GLV treatment of *lox10-3* mutants during the necrotrophic phase of growth also restored susceptibility, however MeJA treatment did not. These results show that GLVs prime maize for susceptibility to ALB and ASR by inducing JA, which in turn results in suppression of SA-mediated defense, and promote disease progression during the necrotrophic phase of growth by *C. graminicola* through non-JA dependent mechanisms.

In order to pre-emptively prepare for defense against imminent stresses, plants respond to certain VOC cues by transcriptionally and metabolically reprograming defense responses, resulting in more rapid and robust defense responses upon encountering those stresses. This is referred to as 'priming'. GLVs are well-known agents of priming, which causes preemptive raising or lowering of defenses, as seen in maize interactions with *C. graminicola*. These volatiles are known to be emitted in high amounts after light-to-dark transitions, but the physiological significance of this process had yet to be investigated. Once again, utilizing *lox10-3* mutants and complementation with exogenous GLVs, this study revealed that light-to-dark emitted GLVs result in a strong and rapid increase of jasmonates, and that these metabolites collectively induce a large number of genes. This ultimately results in significant, long-lasting priming against *Spodoptera frugiperda*, commonly known as fall armyworm (FAW). FAW feeding and weight gain was significantly impaired by short-lived daily GLV treatments of normally susceptible *lox10-3* mutants at the onset of darkness, despite being allowed to feed for extended periods of time, 16 h or a week respectively. GLVs were also shown to be able to restore the increased stomatal apertures of *lox10-3* mutants, with (3*Z*)-hexenal and (2*E*)-hexenal exhibiting the most potent activity. This had broad implications regarding the role of GLVs in drought stress tolerance and nightly closure of stomata. Though GLVs are released at the onset of darkness in a daily, cyclical manner, they do not appear to regulate the circadian clock, with *lox10-3* mutants largely retaining normal expression patterns of important circadian clock oscillators. These results demonstrate

that light-to-dark GLV emissions have a profound effect on priming against insect herbivory, and suggest they facilitate nightly stomatal closure.

Collectively, these results expand upon the known functions of GLVs in plants, and provide important insight into the biosynthesis of PLVs in maize, which despite their widespread emission, remain poorly understood. Importantly, this study has shown that volatile analysis of freeze-thawed plant material, a popular method of volatile analysis, results in distorted profiles and should not be used. This study also provided important evidence supporting a more complex role of GLVs in plant-pathogen interactions, revealing that they retain the ability to induce either resistance or susceptibility depending on the particular pathosystem. Additionally, through the use of genetic mutants and pharmacological treatments, this study also established clearly defined roles of JA and SA in maize interactions with *C. graminicola,* with SA serving as a major defense hormone against this pathogen and JA being an antagonist of SA, promoting disease progression. Lastly, this study showed that GLV emissions upon light-to-dark transitions result in significant, long-term priming to FAW, which has widespread implications for those performing laboratory-based plant assays, especially those that utilize insects.

REFERENCES

Acosta, I.F., Laparra, H., Romero, S.P., Schmelz, E., Hamberg, M., Mottinger, J.P., Moreno, M.A. and Dellaporta, S.L. 2009. tasselseed1 is a lipoxygenase affecting jasmonic acid signaling in sex determination of maize. *Science,* 323 (5911), 262-265.

Albarouki, E., & Deising, H. B. 2013. Infection structure-specific reductive iron assimilation is required for cell wall integrity and full virulence of the maize pathogen *Colletotrichum graminicola*. *Molecular Plant-Microbe Interactions,* 26 (6), 695-708.

Allmann, S., & Baldwin, I. T. 2010. Insects betray themselves in nature to predators by rapid isomerization of green leaf volatiles. *Science,* 329 (5995), 1075-1078.

Ameye, M., Audenaert, K., De Zutter, N., Steppe, K., Van Meulebroek, L., Vanhaecke, L., De Vleesschauwer, D., Haesaert, G. and Smagghe, G., 2015. Priming of wheat with the green leaf volatile Z-3-hexenyl acetate enhances defense against *Fusarium graminearum* but boosts deoxynivalenol production. *Plant Physiology*, 167 (4), 1671-1684.

Ameye, M., Allmann, S., Verwaeren, J., Smagghe, G., Haesaert, G., Schuurink, R.C. and Audenaert, K., 2018. Green leaf volatile production by plants: a meta-analysis. *New Phytologist,* 220 (3), 666-683.

Ankala, A., Luthe, D.S., Williams, W.P. and Wilkinson, J.R., 2009. Integration of ethylene and jasmonic acid signaling pathways in the expression of maize defense protein Mir1-CP. *Molecular Plant-Microbe Interactions*, 22 (12), 1555-1564.

Andreou, A., & Feussner, I. 2009. Lipoxygenases–structure and reaction mechanism. *Phytochemistry*, 70 (13-14), 1504-1510.

Apostol, I., Heinstein, P. F., & Low, P. S. 1989. Rapid stimulation of an oxidative burst during elicitation of cultured plant cells: role in defense and signal transduction. *Plant Physiology,* 90 (1), 109-116.

Archbold, D. D., Hamilton-Kemp, T. R., Barth, M. M., & Langlois, B. E. 1997. Identifying natural volatile compounds that control gray mold (*Botrytis cinerea*) during postharvest storage of strawberry, blackberry, and grape. *Journal of Agricultural and Food Chemistry*, 45 (10), 4032-4037.

Arimura, G.I., Kost, C. and Boland, W., 2005. Herbivore-induced, indirect plant defences. *Biochimica et Biophysica Acta (BBA)-Molecular and Cell Biology of Lipids*, 1734 (2), 91-111.

Baldwin, I.T., Halitschke, R., Paschold, A., Von Dahl, C.C. and Preston, C.A., 2006. Volatile signaling in plant-plant interactions:" talking trees" in the genomics era. *Science*, 311 (5762), 812-815.

Balmer, D., de Papajewski, D. V., Planchamp, C., Glauser, G., & Mauch-Mani, B. 2013. Induced resistance in maize is based on organ-specific defence responses. *The Plant Journal*, 74 (2), 213-225.

Bancos, S., Szatmári, A.M., Castle, J., Kozma-Bognár, L., Shibata, K., Yokota, T., Bishop, G.J., Nagy, F. and Szekeres, M., 2006. Diurnal regulation of the brassinosteroid-biosynthetic CPD gene in *Arabidopsis*. *Plant Physiology*, 141 (1), 299-309.

Bate, N.J., Riley, J.C., Thompson, J.E. and Rothstein, S.J., 1998. Quantitative and qualitative differences in C6-volatile production from the lipoxygenase pathway in an alcohol dehydrogenase mutant of *Arabidopsis thaliana*. *Physiologia Plantarum*, 104 (1), 97-104.

Bate, N. J., & Rothstein, S. J. 1998. C6-volatiles derived from the lipoxygenase pathway induce a subset of defense-related genes. *The Plant Journal*, 16 (5), 561-569.

Bell, E., Creelman, R.A. and Mullet, J.E. 1995. A chloroplast lipoxygenase is required for wound-induced jasmonic acid accumulation in *Arabidopsis*. *Proceedings of the National Academy of Sciences*, 92 (19), 8675-8679.

Bergstrom, G. C., & Nicholson, R. L. 1999. The biology of corn anthracnose: knowledge to exploit for improved management. *Plant Disease*, 83 (7), 596-608.

Blázquez, M.A., Trénor, M. and Weigel, D., 2002. Independent control of gibberellin biosynthesis and flowering time by the circadian clock in *Arabidopsis*. *Plant Physiology*, 130 (4), 1770-1775.

Blée, E. 2002. Impact of phyto-oxylipins in plant defense. *Trends in Plant Science*, 7 (7), 315-322.

Borrego, E. J., & Kolomiets, M. V. 2016. Synthesis and functions of jasmonates in maize. *Plants*, 5 (4), 41.

Böttcher, C., & Pollmann, S. 2009. Plant oxylipins: Plant responses to 12-oxo-phytodienoic acid are governed by its specific structural and functional properties. *The FEBS Journal*, 276 (17), 4693-4704.

Brilli, F., Ruuskanen, T.M., Schnitzhofer, R., Müller, M., Breitenlechner, M., Bittner, V., Wohlfahrt, G., Loreto, F. and Hansel, A., 2011. Detection of plant volatiles after leaf wounding and darkening by proton transfer reaction "time-of-flight" mass spectrometry (PTR-TOF). *PLoS One*, 6 (5), e20419.

Caarls, L., Elberse, J., Awwanah, M., Ludwig, N.R., de Vries, M., Zeilmaker, T., Van Wees, S.C., Schuurink, R.C. and Van den Ackerveken, G. 2017. *Arabidopsis* JASMONATE-INDUCED OXYGENASES down-regulate plant immunity by hydroxylation and inactivation of the hormone jasmonic acid. *Proceedings of the National Academy of Sciences*, 114 (24), 6388-6393.

Chamberlain, K., Khan, Z.R., Pickett, J.A., Toshova, T. and Wadhams, L.J., 2006. Diel periodicity in the production of green leaf volatiles by wild and cultivated host plants of stemborer moths, *Chilo partellus* and *Busseola fusca*. *Journal of Chemical Ecology*, 32 (3), 565-577.

Chehab, E.W., Raman, G., Walley, J.W., Perea, J.V., Banu, G., Theg, S. and Dehesh, K. 2006. Rice HYDROPEROXIDE LYASES with unique expression patterns generate distinct aldehyde signatures in *Arabidopsis*. *Plant Physiology*, 141 (1), 121-134.

Chen, H., Gonzales-Vigil, E., Wilkerson, C.G. and Howe, G.A., 2007. Stability of plant defense proteins in the gut of insect herbivores. *Plant Physiology*, 143 (4), 1954-1967.

Chini, A., Monte, I., Zamarreño, A.M., Hamberg, M., Lassueur, S., Reymond, P., Weiss, S., Stintzi, A., Schaller, A., Porzel, A. and García-Mina, J.M. 2018. An OPR3-independent pathway uses 4, 5-didehydrojasmonate for jasmonate synthesis. *Nature Chemical Biology*, 14 (2), 171.

Choi, H.K., Song, G.C., Yi, H.S. and Ryu, C.M., 2014. Field evaluation of the bacterial volatile derivative 3-pentanol in priming for induced resistance in pepper. *Journal of Chemical Ecology*, *40* (8), 882-892.

Christensen, S.A., Nemchenko, A., Borrego, E., Murray, I., Sobhy, I.S., Bosak, L., DeBlasio, S., Erb, M., Robert, C.A., Vaughn, K.A. and Herrfurth, C. 2013. The maize lipoxygenase, Zm LOX 10, mediates green leaf volatile, jasmonate and herbivore-induced plant volatile production for defense against insect attack. *The Plant Journal*, 74 (1), 59-73.

Constantino, N.N., 2017. *Pathogen triggered plant volatiles induce systemic susceptibility in neighboring plants*. Doctoral Dissertation. Texas A&M University, College Station, TX.

Copolovici, L., Kännaste, A., Pazouki, L. and Niinemets, Ü., 2012. Emissions of green leaf volatiles and terpenoids from *Solanum lycopersicum* are quantitatively related to the severity of cold and heat shock treatments. *Journal of Plant Physiology*, 169 (7), 664-672.

Costa, J.M., Monnet, F., Jannaud, D., Leonhardt, N., Ksas, B., Reiter, I.M., Pantin, F. and Genty, B., 2015. Open all night long: the dark side of stomatal control. *Plant Physiology*, 167 (2), 289-294.

Croft, K.P., Juttner, F. and Slusarenko, A.J., 1993. Volatile products of the lipoxygenase pathway evolved from *Phaseolus vulgaris* (L.) leaves inoculated with *Pseudomonas syringae* pv *phaseolicola*. *Plant Physiology*, 101 (1), 13-24.

D'Auria, J.C., Pichersky, E., Schaub, A., Hansel, A. and Gershenzon, J., 2007. Characterization of a BAHD acyltransferase responsible for producing the green leaf volatile (Z)-3-hexen-1-yl acetate in *Arabidopsis thaliana*. *The Plant Journal*, 49 (2), 194-207.

Dave, A., & Graham, I. A. 2012. Oxylipin signaling: a distinct role for the jasmonic acid precursor cis-(+)-12-oxo-phytodienoic acid (cis-OPDA). *Frontiers in Plant Science*, 3, 42.

Dave, A., Hernández, M.L., He, Z., Andriotis, V.M., Vaistij, F.E., Larson, T.R. and Graham, I.A. 2011. 12-Oxo-phytodienoic acid accumulation during seed development represses seed germination in *Arabidopsis*. *The Plant Cell*, 23 (2), 583-599.

Day, R., Abrahams, P., Bateman, M., Beale, T., Clottey, V., Cock, M., Colmenarez, Y., Corniani, N., Early, R., Godwin, J. and Gomez, J., 2017. Fall armyworm: impacts and implications for Africa. *Outlooks on Pest Management*, 28 (5), 196-201.

Dean, R., Van Kan, J.A., Pretorius, Z.A., Hammond-Kosack, K.E., Di Pietro, A., Spanu, P.D., Rudd, J.J., Dickman, M., Kahmann, R., Ellis, J. and Foster, G.D. 2012. The Top 10 fungal pathogens in molecular plant pathology. *Molecular Plant Pathology*, 13 (4), 414-430.

Duan, H., Huang, M.Y., Palacio, K. and Schuler, M.A., 2005. Variations in CYP74B2 (hydroperoxide lyase) gene expression differentially affect hexenal signaling in the

Columbia and Landsberg erecta ecotypes of *Arabidopsis*. *Plant Physiology*, 139 (3), 1529-1544.

Engelberth, J., Alborn, H. T., Schmelz, E. A., & Tumlinson, J. H. 2004. Airborne signals prime plants against insect herbivore attack. *Proceedings of the National Academy of Sciences*, 101 (6), 1781-1785.

Engelberth, J., Seidl-Adams, I., Schultz, J. C., & Tumlinson, J. H. 2007. Insect elicitors and exposure to green leafy volatiles differentially upregulate major octadecanoids and transcripts of 12-oxo phytodienoic acid reductases in *Zea mays*. *Molecular Plant-Microbe Interactions*, 20 (6), 707-716.

Engelberth, J. (2011). Selective inhibition of jasmonic acid accumulation by a small α, β-unsaturated carbonyl and phenidone reveals different modes of octadecanoid signalling activation in response to insect elicitors and green leaf volatiles in *Zea mays*. *BMC Research Notes*, 4 (1), 377.

Engelberth, J., Contreras, C. F., Dalvi, C., Li, T., & Engelberth, M. 2013. Early transcriptome analyses of Z-3-hexenol-treated *Zea mays* revealed distinct transcriptional networks and anti-herbivore defense potential of green leaf volatiles. *PLoS One*, 8 (10), e77465.

Fall, R., Karl, T., Hansel, A., Jordan, A. and Lindinger, W., 1999. Volatile organic compounds emitted after leaf wounding: On-line analysis by proton-transfer-reaction mass spectrometry. *Journal of Geophysical Research: Atmospheres*, 104 (D13), 15963-15974.

Fall, R., Karl, T., Jordan, A. and Lindinger, W., 2001. Biogenic C5 VOCs: release from leaves after freeze–thaw wounding and occurrence in air at a high mountain observatory. *Atmospheric Environment*, 35 (22), 3905-3916.

Farag, M.A. and Pare, P.W., 2002. C6-Green leaf volatiles trigger local and systemic VOC emissions in tomato. *Phytochemistry*, 61 (5), 545-554.

Farag, M. A., Fokar, M., Abd, H., Zhang, H., Allen, R. D., & Pare, P. W. 2005. (Z)-3-Hexenol induces defense genes and downstream metabolites in maize. *Planta*, 220 (6), 900-909.

Farmer, E. E., & Ryan, C. A. 1990. Interplant communication: airborne methyl jasmonate induces synthesis of proteinase inhibitors in plant leaves. *Proceedings of the National Academy of Sciences*, 87 (19), 7713-7716.

Felton, G.W., Bi, J.L., Summers, C.B., Mueller, A.J. and Duffey, S.S., 1994. Potential role of lipoxygenases in defense against insect herbivory. *Journal of Chemical Ecology*, 20 (3), 651-666.

Feussner, I., & Wasternack, C. 2002. The lipoxygenase pathway. *Annual Review of Plant Biology*, 53 (1), 275-297.

Fonseca, S., Chico, J. M., & Solano, R. 2009. The jasmonate pathway: the ligand, the receptor and the core signalling module. *Current Opinion in Plant Biology*, 12 (5), 539-547.

Franco, F.P., Moura, D.S., Vivanco, J.M. and Silva-Filho, M.C., 2017. Plant–insect–pathogen interactions: a naturally complex ménage à trois. *Current Opinion in Plant Biology*, 37, 54-60.

Froehlich, J.E., Itoh, A. and Howe, G.A., 2001. Tomato allene oxide synthase and fatty acid hydroperoxide lyase, two cytochrome P450s involved in oxylipin metabolism, are targeted to different membranes of chloroplast envelope. *Plant Physiology*, 125 (1), 306-317.

Frost, C. J., Mescher, M. C., Dervinis, C., Davis, J. M., Carlson, J. E., & De Moraes, C. M. 2008. Priming defense genes and metabolites in hybrid poplar by the green leaf volatile cis-3-hexenyl acetate. *New Phytologist*, 180 (3), 722-734.

Gangappa, S.N. and Chattopadhyay, S., 2010. MYC2, a bHLH transcription factor, modulates the adult phenotype of SPA1. *Plant Signaling & Behavior*, 5 (12), 1650-1652.

Gao, X., Shim, W.B., Göbel, C., Kunze, S., Feussner, I., Meeley, R., Balint-Kurti, P. and Kolomiets, M. 2007. Disruption of a maize 9-lipoxygenase results in increased resistance to fungal pathogens and reduced levels of contamination with mycotoxin fumonisin. *Molecular Plant-Microbe Interactions*, 20 (8), 922-933.

Gao, X., Stumpe, M., Feussner, I. and Kolomiets, M., 2008. A novel plastidial lipoxygenase of maize (*Zea mays*) ZmLOX6 encodes for a fatty acid hydroperoxide lyase and is uniquely regulated by phytohormones and pathogen infection. *Planta*, 227 (2), 491-503.

Gardner, H.W. and Grove, M.J., 1998. Soybean lipoxygenase-1 oxidizes 3Z-nonenal: a route to 4S-hydroperoxy-2E-nonenal and related products. *Plant Physiology*, 116 (4), 1359-1366.

Gardner, H.W., Grove, M.J. and Salch, Y.P., 1996. Enzymic pathway to ethyl vinyl ketone and 2-pentenal in soybean preparations. *Journal of Agricultural and Food Chemistry*, 44 (3), 882-886.

Gardner, H.W., 1991. Recent investigations into the lipoxygenase pathway of plants. *Biochimica et Biophysica Acta (BBA)/Lipids and Lipid Metabolism*, 1084 (3), 221-239.

Glazebrook, J. 2005. Contrasting mechanisms of defense against biotrophic and necrotrophic pathogens. *Annual Review of Phytopathology*, 43, 205-227.

Galliard, T. and Matthew, J.A., 1975. Enzymic reactions of fatty acid hydroperoxides in extracts of potato tuber. I. Comparison 9D-and 13L-hydroperoxy-octadecadienoic acids as substrates for the formation of a divinyl ether derivative. *Biochimica et Biophysica Acta*, 398 (1), 1-9.

Goodfriend, T.L., Ball, D.L. and Gardner, H.W., 2002. An oxidized derivative of linoleic acid affects aldosterone secretion by adrenal cells in vitro. *Prostaglandins, Leukotrienes and Essential Fatty Acids*, 67 (2-3), 163-167.

Goodspeed, D., Chehab, E.W., Min-Venditti, A., Braam, J. and Covington, M.F., 2012. *Arabidopsis* synchronizes jasmonate-mediated defense with insect circadian behavior. *Proceedings of the National Academy of Sciences*, 109 (12), 4674-4677.

Gorman, Z., Christensen, S.A., Yan, Y., He, Y., Borrego, E. and Kolomiets, M.V., 2020. Green leaf volatiles and jasmonic acid enhance susceptibility to anthracnose diseases caused by *Colletotrichum graminicola* in maize. *Molecular Plant Pathology*, 21 (5), 702-715.

Gouinguené, S., Pickett, J.A., Wadhams, L.J., Birkett, M.A. and Turlings, T.C., 2005. Antennal electrophysiological responses of three parasitic wasps to caterpillar-induced volatiles from maize (*Zea mays mays*), cotton (*Gossypium herbaceum*), and cowpea (*Vigna unguiculata*). *Journal of Chemical Ecology*, 31 (5), 1023-1038.

Graus, M., Schnitzler, J.P., Hansel, A., Cojocariu, C., Rennenberg, H., Wisthaler, A. and Kreuzwieser, J., 2004. Transient release of oxygenated volatile organic compounds during light-dark transitions in grey poplar leaves. *Plant Physiology*, 135 (4), 1967-1975.

Grunseich, J.M., Thompson, M.N., Hay, A.A., Gorman, Z., Kolomiets, M.V., Eubanks, M.D. and Helms, A.M., 2020. Risky roots and careful herbivores: Sustained herbivory by a root-feeding herbivore attenuates indirect plant defences. *Functional Ecology*. 34 (9), pp.1779-1789.

Halitschke, R., Ziegler, J., Keinänen, M. and Baldwin, I.T., 2004. Silencing of hydroperoxide lyase and allene oxide synthase reveals substrate and defense signaling crosstalk in Nicotiana attenuata. *The Plant Journal*, 40 (1), 35-46.

Hatanaka, A., 1993. The biogeneration of green odour by green leaves. *Phytochemistry*, 34 (5), 1201-1218.

Hamilton-Kemp, T. R., McCracken, C. T., Loughrin, J. H., Andersen, R. A., & Hildebrand, D. F. 1992. Effects of some natural volatile compounds on the pathogenic fungi *Alternaria alternata* and *Botrytis cinerea*. *Journal of Chemical Ecology*, 18 (7), 1083-1091.

Hanano, S., Domagalska, M.A., Nagy, F. and Davis, S.J., 2006. Multiple phytohormones influence distinct parameters of the plant circadian clock. *Genes to Cells*, 11 (12), 1381-1392.

He, Y., Borrego, E.J., Gorman, Z., Huang, P.C. and Kolomiets, M.V., 2020. Relative contribution of LOX10, green leaf volatiles and JA to wound-induced local and systemic oxylipin and hormone signature in *Zea mays* (maize). *Phytochemistry*, 174, 112334.

Heiden, A.C., Kobel, K., Langebartels, C., Schuh-Thomas, G. and Wildt, J., 2003. Emissions of oxygenated volatile organic compounds from plants Part I: Emissions from lipoxygenase activity. *Journal of Atmospheric Chemistry*, 45 (2), 143-172.

Hirao, T., Okazawa, A., Harada, K., Kobayashi, A., Muranaka, T., & Hirata, K. 2012. Green leaf volatiles enhance methyl jasmonate response in *Arabidopsis*. *Journal of Bioscience and Bioengineering*, 114 (5), 540-545.

Hoopes, G.M., Hamilton, J.P., Wood, J.C., Esteban, E., Pasha, A., Vaillancourt, B., Provart, N.J. and Buell, C.R., 2019. An updated gene atlas for maize reveals organ-specific and stress-induced genes. *The Plant Journal*, 97 (6), 1154-1167.

Howe, G. A., & Jander, G. 2008. Plant immunity to insect herbivores. *Annual. Rev. Plant Biology*, 59, 41-66.

Howe, G. A., & Schilmiller, A. L. 2002. Oxylipin metabolism in response to stress. *Current Opinion in Plant Biology*, 5 (3), 230-236.

Huang, F., Qureshi, J.A., Meagher Jr, R.L., Reisig, D.D., Head, G.P., Andow, D.A., Ni, X., Kerns, D., Buntin, G.D., Niu, Y. and Yang, F., 2014. Cry1F resistance in fall

armyworm Spodoptera frugiperda: single gene versus pyramided Bt maize. *PloS One*, 9 (11), e112958.

Jardine, K., Barron-Gafford, G.A., Norman, J.P., Abrell, L., Monson, R.K., Meyers, K.T., Pavao-Zuckerman, M., Dontsova, K., Kleist, E., Werner, C. and Huxman, T.E., 2012. Green leaf volatiles and oxygenated metabolite emission bursts from mesquite branches following light–dark transitions. *Photosynthesis Research*, 113 (1-3), 321-333.

Joo, Y., Schuman, M.C., Goldberg, J.K., Wissgott, A., Kim, S.G. and Baldwin, I.T., 2019. Herbivory elicits changes in green leaf volatile production via jasmonate signaling and the circadian clock. *Plant, Cell & Environment*, 42 (3), 972-982.

Kallenbach, M., Gilardoni, P.A., Allmann, S., Baldwin, I.T. and Bonaventure, G., 2011. C12 derivatives of the hydroperoxide lyase pathway are produced by product recycling through lipoxygenase-2 in Nicotiana attenuata leaves. *New Phytologist*, 191 (4), 1054-1068.

Kazan, K. and Manners, J.M., 2013. MYC2: the master in action. *Molecular Plant*, 6 (3), 686-703.

Kihara, H., Tanaka, M., Yamato, K.T., Horibata, A., Yamada, A., Kita, S., Ishizaki, K., Kajikawa, M., Fukuzawa, H., Kohchi, T. and Akakabe, Y., 2014. Arachidonic acid-dependent carbon-eight volatile synthesis from wounded liverwort (*Marchantia polymorpha*). *Phytochemistry*, 107, 42-49.

Kishimoto, K., Matsui, K., Ozawa, R., & Takabayashi, J. 2006. Components of C6-aldehyde-induced resistance in *Arabidopsis* thaliana against a necrotrophic fungal pathogen, *Botrytis cinerea*. *Plant Science*, 170 (4), 715-723.

Kishimoto, K., Matsui, K., Ozawa, R., & Takabayashi, J. 2008. Direct fungicidal activities of C6-aldehydes are important constituents for defense responses in *Arabidopsis* against *Botrytis cinerea*. *Phytochemistry*, 69 (11), 2127-2132.

Keller, N.P., Bergstrom, G.C. and Carruthers, R.I. 1986. Potential yield reductions in maize associated with an anthracnose/European corn borer pest complex in New York. *Phytopathology*, 76, 586-589.

Kessler, A. and Baldwin, I.T., 2001. Defensive function of herbivore-induced plant volatile emissions in nature. *Science*, 291 (5511), 2141-2144.

Kramell, R., Miersch, O., Atzorn, R., Parthier, B., & Wasternack, C. 2000. Octadecanoid-derived alteration of gene expression and the “oxylipin signature” in stressed barley leaves. Implications for different signaling pathways. *Plant Physiology*, 123 (1), 177-188.

Kunishima, M., Yamauchi, Y., Mizutani, M., Kuse, M., Takikawa, H. and Sugimoto, Y., 2016. Identification of (Z)-3:(E)-2-hexenal isomerases essential to the production of the leaf aldehyde in plants. *Journal of Biological Chemistry*, 291 (27), 14023-14033.

Leone, M., Keller, M.M., Cerrudo, I. and Ballaré, C.L., 2014. To grow or defend? Low red: far-red ratios reduce jasmonate sensitivity in *Arabidopsis* seedlings by promoting DELLA degradation and increasing JAZ10 stability. *New Phytologist*, 204 (2), 355-367.

Li, L., Zhao, Y., McCaig, B.C., Wingerd, B.A., Wang, J., Whalon, M.E., Pichersky, E. and Howe, G.A., 2004. The tomato homolog of CORONATINE-INSENSITIVE1 is required for the maternal control of seed maturation, jasmonate-signaled defense responses, and glandular trichome development. *The Plant Cell*, 16, 126-143.

Livak, K. J., & Schmittgen, T. D. 2001. Analysis of relative gene expression data using real-time quantitative PCR and the $2^{-\Delta\Delta CT}$ method. *Methods*, 25 (4), 402-408.

López-Gresa, M.P., Payá, C., Ozáez, M., Rodrigo, I., Conejero, V., Klee, H., Bellés, J.M. and Lisón, P., 2018. A new role for green leaf volatile esters in tomato stomatal defense against *Pseudomonas syringe* pv. *tomato*. *Frontiers in Plant Science*, 9, 1855.

Loreto, F., Barta, C., Brilli, F. and Nogues, I., 2006. On the induction of volatile organic compound emissions by plants as consequence of wounding or fluctuations of light and temperature. *Plant, Cell & Environment*, 29 (9), 1820-1828.

Majeran, W., Cai, Y., Sun, Q., & van Wijk, K. J. 2005. Functional differentiation of bundle sheath and mesophyll maize chloroplasts determined by comparative proteomics. *The Plant Cell*, 17 (11), 3111-3140.

Major, R. T., Marchini, P., & Sproston, T. 1960. Isolation from Ginkgo biloba L. of an inhibitor of fungus growth. *J. Biol. Chem*, 235 (11), 3298-3299.

Matsui, K., Sugimoto, K., Mano, J. I., Ozawa, R., & Takabayashi, J. 2012. Differential metabolisms of green leaf volatiles in injured and intact parts of a wounded leaf meet distinct ecophysiological requirements. *PLoS One*, 7 (4), e36433.

Mellersh, D. G., Foulds, I. V., Higgins, V. J., & Heath, M. C. 2002. H2O2 plays different roles in determining penetration failure in three diverse plant–fungal interactions. *The Plant Journal*, 29 (3), 257-268.

Mims, C. W., & Vaillancourt, L. J. 2002. Ultrastructural characterization of infection and colonization of maize leaves by *Colletotrichum graminicola*, and by a *C. graminicola* pathogenicity mutant. *Phytopathology*, 92 (7), 803-812.

Mohanty, A., Luo, A., DeBlasio, S., Ling, X., Yang, Y., Tuthill, D.E., Williams, K.E., Hill, D., Zadrozny, T., Chan, A. and Sylvester, A.W. 2009. Advancing cell biology and functional genomics in maize using fluorescent protein-tagged lines. *Plant Physiology*, 149 (2), 601-605.

Mochizuki, S., Sugimoto, K., Koeduka, T. and Matsui, K. 2016. *Arabidopsis* lipoxygenase 2 is essential for formation of green leaf volatiles and five-carbon volatiles. *FEBS Letters*, 590 (7), 1017-1027.

Moon, J.H., Watanabe, N., Ijima, Y., Yagi, A. and Sakata, K., 1996. cis-and trans-Linalool 3, 7-oxides and methyl salicylate glycosides and (Z)-3-hexenyl β-D-glucopyranoside as aroma precursors from tea leaves for oolong tea. *Bioscience, Biotechnology, and Biochemistry*, 60 (11), 1815-1819.

Mukhtarova, L. S., Brühlmann, F., Hamberg, M., Khairutdinov, B. I., & Grechkin, A. N. 2018. Plant hydroperoxide-cleaving enzymes (CYP74 family) function as hemiacetal synthases: Structural proof of hemiacetals by NMR spectroscopy. *Biochimica et Biophysica Acta (BBA)-Molecular and Cell Biology of Lipids*.1863 (10), 1316-1322

Müller, M., & Munné-Bosch, S. 2011. Rapid and sensitive hormonal profiling of complex plant samples by liquid chromatography coupled to electrospray ionization tandem mass spectrometry. *Plant Methods*, 7 (1), 37.

Nakamura, S., & Hatanaka, A. 2002. Green-leaf-derived C6-aroma compounds with potent antibacterial action that act on both gram-negative and gram-positive bacteria. *Journal of Agricultural and Food Chemistry*, 50 (26), 7639-7644.

Nemchenko, A., Kunze, S., Feussner, I., & Kolomiets, M. 2006. Duplicate maize 13-lipoxygenase genes are differentially regulated by circadian rhythm, cold stress, wounding, pathogen infection, and hormonal treatments. *Journal of Experimental Botany*, 57 (14), 3767-3779.

Nyambura, M.C., Matsui, K. and Kumamaru, T., 2011. Establishment of an efficient screening system to isolate rice mutants deficient in green leaf volatile formation. *Journal of Plant Interactions*, 6 (2-3), 185-186.

O'Connell, R. J., Bailey, J. A., & Richmond, D. V. 1985. Cytology and physiology of infection of *Phaseolus vulgaris* by *Colletotrichum lindemuthianum*. *Physiological Plant Pathology*, 27 (1), 75-98.

Oestreich D. 2005. Biotechnology: Where is it coming from and where is it going. *Proc. 60th Annual Corn and Sorghum Res.* Conf. American Seed Trade Association, Washington, DC.

Oliw, E.H. and Hamberg, M., 2019. Biosynthesis of Jasmonates from Linoleic Acid by the Fungus *Fusarium oxysporum*. Evidence for a Novel Allene Oxide Cyclase. *Lipids*, 54 (9), 543-556.

Patkar, R. N., Benke, P. I., Qu, Z., Chen, Y. Y. C., Yang, F., Swarup, S., & Naqvi, N. I. 2015. A fungal monooxygenase-derived jasmonate attenuates host innate immunity. *Nature Chemical Biology*, 11 (9), 733.

Wenda-Piesik, A., Piesik, D., Ligor, T. and Buszewski, B., 2010. Volatile organic compounds (VOCs) from cereal plants infested with crown rot: their identity and their capacity for inducing production of VOCs in uninfested plants. *International Journal of Pest Management*, 56 (4), 377-383.

Ponzio, C., Gols, R., Pieterse, C. M., & Dicke, M. 2013. Ecological and phytohormonal aspects of plant volatile emission in response to single and dual infestations with herbivores and phytopathogens. *Functional Ecology*, 27 (3), 587-598.

Prost, I., Dhondt, S., Rothe, G., Vicente, J., Rodriguez, M. J., Kift, N., ... & Castresana, C. 2005. Evaluation of the antimicrobial activities of plant oxylipins supports their involvement in defense against pathogens. *Plant Physiology*, 139 (4), 1902-1913.

Reinbothe, C., Springer, A., Samol, I., & Reinbothe, S. 2009. Plant oxylipins: role of jasmonic acid during programmed cell death, defence and leaf senescence. *The FEBS Journal*, 276 (17), 4666-4681.

Ribot, C., Zimmerli, C., Farmer, E. E., Reymond, P., & Poirier, Y. 2008. Induction of the *Arabidopsis* PHO1; H10 gene by 12-oxo-phytodienoic acid but not jasmonic acid via a CORONATINE INSENSITIVE1-dependent pathway. *Plant Physiology*, 147 (2), 696-706.

Robson, F., Okamoto, H., Patrick, E., Harris, S.R., Wasternack, C., Brearley, C. and Turner, J.G., 2010. Jasmonate and phytochrome A signaling in *Arabidopsis* wound and shade responses are integrated through JAZ1 stability. *The Plant Cell*, 22 (4), 1143-1160.

Rodriguez-Saona, C., Crafts-Brandner, S. J., ParÉ, P. W., & Henneberry, T. J. 2001. Exogenous methyl jasmonate induces volatile emissions in cotton plants. *Journal of Chemical Ecology*, 27 (4), 679-695.

Rojas, J.C., Kolomiets, M.V. and Bernal, J.S., 2018. Nonsensical choices? Fall armyworm moths choose seemingly best or worst hosts for their larvae, but neonate larvae make their own choices. *Plos One*, 13 (5), 0197628.

Salas, J.J., García-González, D.L. and Aparicio, R., 2006. Volatile compound biosynthesis by green leaves from an *Arabidopsis thaliana* hydroperoxide lyase knockout mutant. *Journal of Agricultural and Food Chemistry*, 54 (21), 8199-8205.

Salch, Y.P., Grove, M.J., Takamura, H. and Gardner, H.W., 1995. Characterization of a C-5, 13-cleaving enzyme of 13 (S)-hydroperoxide of linolenic acid by soybean seed. *Plant Physiology*, 108 (3), 1211-1218.

Savchenko, T. and Dehesh, K., 2014. Drought stress modulates oxylipin signature by eliciting 12-OPDA as a potent regulator of stomatal aperture. *Plant Signaling & Behavior*, 9 (4), 1151-60.

Savchenko, T., Yanykin, D., Khorobrykh, A., Terentyev, V., Klimov, V. and Dehesh, K., 2017. The hydroperoxide lyase branch of the oxylipin pathway protects against photoinhibition of photosynthesis. *Planta*, 245 (6), 1179-1192.

Scala, A., Mirabella, R., Mugo, C., Matsui, K., Haring, M. A., & Schuurink, R. C. 2013. (E)-2-hexenal promotes susceptibility to *Pseudomonas syringae* by activating jasmonic acid pathways in *Arabidopsis*. *Frontiers in Plant Science*, 4, 74.

Schmelz, E.A., Engelberth, J., Tumlinson, J.H., Block, A. and Alborn, H.T., 2004. The use of vapor phase extraction in metabolic profiling of phytohormones and other metabolites. *The Plant Journal*, 39 (5), 790-808.

Schneider, C. A., Rasband, W. S., & Eliceiri, K. W. 2012. NIH Image to ImageJ: 25 years of image analysis. *Nature Methods*, 9 (7), 671.

Sena Jr, D.G., Pinto, F.A.C., Queiroz, D.M. and Viana, P.A., 2003. Fall armyworm damaged maize plant identification using digital images. *Biosystems Engineering*, 85 (4), 449-454.

Shen, J., Tieman, D., Jones, J.B., Taylor, M.G., Schmelz, E., Huffaker, A., Bies, D., Chen, K. and Klee, H.J. 2014. A 13-lipoxygenase, TomloxC, is essential for synthesis of C5 flavour volatiles in tomato. *Journal of Experimental Botany*, 65 (2), 419-428.

Shin, J., Heidrich, K., Sanchez-Villarreal, A., Parker, J.E. and Davis, S.J., 2012. TIME FOR COFFEE represses accumulation of the MYC2 transcription factor to provide time-of-day regulation of jasmonate signaling in *Arabidopsis*. *The Plant Cell*, 24 (6), 2470-2482.

Shiojiri, K., Kishimoto, K., Ozawa, R., Kugimiya, S., Urashimo, S., Arimura, G., Horiuchi, J., Nishioka, T., Matsui, K. and Takabayashi, J. 2006. Changing green leaf volatile biosynthesis in plants: an approach for improving plant resistance against both herbivores and pathogens. *Proceedings of the National Academy of Sciences*, 103 (45), 16672-16676.

Shivaji, R., Camas, A., Ankala, A., Engelberth, J., Tumlinson, J.H., Williams, W.P., Wilkinson, J.R. and Luthe, D.S., 2010. Plants on constant alert: elevated levels of jasmonic acid and jasmonate-induced transcripts in caterpillar-resistant maize. *Journal of Chemical Ecology*, 36 (2), 179-191.

Song, G.C., Choi, H.K. and Ryu, C.M., 2015. Gaseous 3-pentanol primes plant immunity against a bacterial speck pathogen, *Pseudomonas syringae* pv. *tomato* via salicylic acid and jasmonic acid-dependent signaling pathways in *Arabidopsis*. *Frontiers in Plant Science*, 6, 821.

Sparks, A.N., 1979. Fall Armyworm Symposium: A review of the biology of the fall armyworm. *Florida Entomologist*, 82-87.

Speirs, J., Lee, E., Holt, K., Yong-Duk, K., Scott, N.S., Loveys, B. and Schuch, W., 1998. Genetic manipulation of alcohol dehydrogenase levels in ripening tomato fruit affects the balance of some flavor aldehydes and alcohols. *Plant Physiology*, 117 (3), 1047-1058.

Spyropoulou, E.A., Dekker, H.L., Steemers, L., van Maarseveen, J.H., de Koster, C.G., Haring, M.A., Schuurink, R.C. and Allmann, S., 2017. Identification and characterization of (3Z):(2E)-hexenal isomerases from cucumber. *Frontiers in Plant Science*, 8, 1342.

Staswick, P. E., & Tiryaki, I. 2004. The oxylipin signal jasmonic acid is activated by an enzyme that conjugates it to isoleucine in *Arabidopsis*. *The Plant Cell*, 16 (8), 2117-2127.

Stintzi, A., Weber, H., Reymond, P., & Farmer, E. E. 2001. Plant defense in the absence of jasmonic acid: the role of cyclopentenones. *Proceedings of the National Academy of Sciences*, 98 (22), 12837-12842.

Sugimoto, K., Matsui, K., Iijima, Y., Akakabe, Y., Muramoto, S., Ozawa, R., Uefune, M., Sasaki, R., Alamgir, K.M., Akitake, S. and Nobuke, T., 2014. Intake and transformation to a glycoside of (Z)-3-hexenol from infested neighbors reveals a mode of plant odor reception and defense. *Proceedings of the National Academy of Sciences*, 111 (19), 7144-7149.

Taki, N., Sasaki-Sekimoto, Y., Obayashi, T., Kikuta, A., Kobayashi, K., Ainai, T., Yagi, K., Sakurai, N., Suzuki, H., Masuda, T. and Takamiya, K.I. 2005. 12-oxo-phytodienoic acid triggers expression of a distinct set of genes and plays a role in wound-induced gene expression in *Arabidopsis*. *Plant Physiology*, 139 (3), 1268-1283.

Tanaka, T., Ikeda, A., Shiojiri, K., Ozawa, R., Shiki, K., Nagai-Kunihiro, N., Fujita, K., Sugimoto, K., Yamato, K.T., Dohra, H. and Ohnishi, T., 2018. Identification of a hexenal reductase that modulates the composition of green leaf volatiles. *Plant Physiology*, 178 (2), 552-564.

Thain, S.C., Vandenbussche, F., Laarhoven, L.J., Dowson-Day, M.J., Wang, Z.Y., Tobin, E.M., Harren, F.J., Millar, A.J. and Van Der Straeten, D., 2004. Circadian rhythms of ethylene emission in *Arabidopsis*. *Plant Physiology*, 136 (3), 3751-3761.

Thomma, B. P., Eggermont, K., Penninckx, I. A., Mauch-Mani, B., Vogelsang, R., Cammue, B. P., & Broekaert, W. F. 1998. Separate jasmonate-dependent and salicylate-dependent defense-response pathways in *Arabidopsis* are essential for resistance to distinct microbial pathogens. *Proceedings of the National Academy of Sciences*, 95 (25), 15107-15111.

Timilsena, B. P, Seidl-Adams, I. and Tumlinson, J.H., 2020. Herbivore-specific plant volatiles prime neighboring plants for nonspecific defense responses. *Plant, Cell & Environment*, 43 (3), 787-800.

Tolley, J. P., Nagashima, Y., Gorman, Z., Kolomiets, M. V., & Koiwa, H. 2018. Isoform-specific subcellular localization of Zea mays lipoxygenases and oxo-phytodienoate reductase 2. *Plant Gene*, 13, 36-41.

Tolley, J. P., 2020. *Subcellular Localization and Characterization of Zea Mays 9-LOX Isoforms*. Master Thesis. Texas A&M University, College Station, TX.

Ton, J., D'Alessandro, M., Jourdie, V., Jakab, G., Karlen, D., Held, M., Mauch-Mani, B. and Turlings, T.C., 2007. Priming by airborne signals boosts direct and indirect resistance in maize. *The Plant Journal*, 49 (1), 16-26.

Tong, X., Qi, J., Zhu, X., Mao, B., Zeng, L., Wang, B., Li, Q., Zhou, G., Xu, X., Lou, Y. and He, Z. 2012. The rice hydroperoxide lyase OsHPL3 functions in defense responses by modulating the oxylipin pathway. *The Plant Journal*, 71 (5), 763-775.

Tsukada, K., Takahashi, K., & Nabeta, K. 2010. Biosynthesis of jasmonic acid in a plant pathogenic fungus, Lasiodiplodia theobromae. *Phytochemistry*, 71 (17-18), 2019-2023.

Turlings, T. C., Loughrin, J. H., Mccall, P. J., Röse, U. S., Lewis, W. J., & Tumlinson, J. H. 1995. How caterpillar-damaged plants protect themselves by attracting parasitic wasps. *Proceedings of the National Academy of Sciences*, 92 (10), 4169-4174.

Turlings, T.C. and Erb, M., 2018. Tritrophic interactions mediated by herbivore-induced plant volatiles: mechanisms, ecological relevance, and application potential. *Annual Review of Entomology*, 63, 433-452.

Van Doan, C., Züst, T., Maurer, C., Zhang, X., Machado, R.A., Mateo, P., Ye, M., Schimmel, B.C., Glauser, G. and Robert, C.A., 2020. Tissue-specific volatile-mediated defense regulation in maize leaves and roots. *BioRxiv*.

Van Tol, R.W., Bruck, D.J., Griepink, F.C. and De Kogel, W.J., 2012. Field attraction of the vine weevil Otiorhynchus sulcatus to kairomones. *Journal of Economic Entomology*, 105 (1), 169-175.

Vancanneyt, G., Sanz, C., Farmaki, T., Paneque, M., Ortego, F., Castañera, P. and Sánchez-Serrano, J.J., 2001. Hydroperoxide lyase depletion in transgenic potato plants leads to an increase in aphid performance. *Proceedings of the National Academy of Sciences*, 98 (14), 8139-8144.

Vargas, W.A., Martín, J.M.S., Rech, G.E., Rivera, L.P., Benito, E.P., Díaz-Mínguez, J.M., Thon, M.R. and Sukno, S.A. 2012. Plant defense mechanisms are activated during biotrophic and necrotrophic development of *Colletotricum graminicola* in maize. *Plant Physiology*, 158 (3), 1342-1358.

Venard, C. and Vaillancourt, L.. 2007. Penetration and colonization of unwounded maize tissues by the maize anthracnose pathogen *Colletotrichum graminicola* and the related nonpathogen *C. sublineolum*. *Mycologia*, 99, 368-377.

Vick, B. A., & Zimmerman, D. C. 1983. The biosynthesis of jasmonic acid: a physiological role for plant lipoxygenase. *Biochemical and Biophysical Research Communications*, 111 (2), 470-477.

Vliegenthart, J.F.G., de Groot, J.J.M.C., Veldink, G.A., Boldingh, J., Wever, R. and Van Gelder, B.F., 1975. Demonstration by EPR spectroscopy of the functional role of iron in soybean lipoxygenase-1. *Biochimica et Biophysica Acta*, 377, 71-79.

Wang, K.D., Borrego, E.J., Kenerley, C.M. and Kolomiets, M.V., 2020a. Oxylipins other than jasmonic acid are xylem-resident signals regulating systemic resistance induced by *Trichoderma virens* in maize. *The Plant Cell*, 32, 166-185.

Wang, K.D., Gorman, Z., Huang, P.C., Kenerley, C.M. and Kolomiets, M.V., 2020. *Trichoderma virens* colonization of maize roots triggers rapid accumulation of 12-oxophytodienoate and two $_{\gamma}$-ketols in leaves as priming agents of induced systemic resistance. *Plant Signaling & Behavior*, 15 (9), 1792187.

Wasternack, C., & Strnad, M. 2018. Jasmonates: news on occurrence, biosynthesis, metabolism and action of an ancient group of signaling compounds. *International Journal of Molecular Sciences*, 19 (9), 2539.

Wenda-Piesik, A., 2011. Volatile organic compound emissions by winter wheat plants (Triticum aestivum L.) under Fusarium spp. Infestation and various abiotic conditions. *Polish Journal of Environmental Studies*, 20 (5), 1335-1342.

Wharton, P. S., Julian, A. M., & O'Connell, R. J. 2001. Ultrastructure of the infection of Sorghum bicolor by Colletotrichum sublineolum. *Phytopathology*, 91 (2), 149-158.

Yamauchi, Y., Kunishima, M., Mizutani, M., & Sugimoto, Y. 2015. Reactive short-chain leaf volatiles act as powerful inducers of abiotic stress-related gene expression. *Scientific Reports*, 5, 8030.

Yan, J., Li, S., Gu, M., Yao, R., Li, Y., Chen, J., Yang, M., Tong, J., Xiao, *et al.* 2016. Endogenous bioactive jasmonate is composed of a set of (+)-7-iso-JA-amino acid conjugates. *Plant Physiology*, 172 (4), 2154-2164.

Yan, Y., Christensen, S., Isakeit, T., Engelberth, J., Meeley, R., Hayward, A., Emery, R.N. and Kolomiets, M.V. 2012. Disruption of OPR7 and OPR8 reveals the versatile functions of jasmonic acid in maize development and defense. *The Plant Cell*, 24 (4), 1420-1436.

Zeringue, H. J., & McCormick, S. P. 1989. Relationships between cotton leaf-derived volatiles and growth of *Aspergillus flavus*. *Journal of the American Oil Chemists' Society*, 66 (4), 581-585.

Zoeller, M., Stingl, N., Krischke, M., Fekete, A., Waller, F., Berger, S. and Mueller, M.J., 2012. Lipid profiling of the *Arabidopsis* hypersensitive response reveals specific lipid peroxidation and fragmentation processes: biogenesis of pimelic and azelaic acid. *Plant Physiology*, 160 (1), 365-378.